SELF REINFORCEMENT OF POLY(ETHYLENE TEREPHTHALATE) AND POLYETHYLENE BLENDS

A THESIS SUBMITTED TO
THE GRADUATE SCHOOL OF NATURAL AND APPLIED SCIENCES
OF
MIDDLE EAST TECHNICAL UNIVERSITY

BY

CEREN KURTULUŞ

IN PARTIAL FULFILLMENT OF THE REQUIREMENTS
FOR
THE DEGREE OF MASTER OF SCIENCE
IN
CHEMICAL ENGINEERING

APRIL 2007

Approval of the Graduate School of Natural and Applied Sciences

Prof. Dr. Canan Özgen
Director

I certify that this thesis satisfies all the requirements as a thesis for the degree of Master of Science.

Prof. Dr. Nurcan BAÇ
Head of Department

This is to certify that we have read this thesis and that in our opinion it is fully adequate, in scope and quality, as a thesis for the degree of Master of Science.

Prof.Dr. Nurcan BAÇ
Co-Supervisor

Assoc. Prof. Dr. Göknur Bayram
Supervisor

Examining Committee Members

Prof.Dr. Leyla ARAS	(METU, CHEM)	_____
Assoc. Prof. Dr.Göknur Bayram	(METU, CHE)	_____
Prof.Dr. Nurcan BAÇ	(METU, CHE)	_____
Prof.Dr. Ülkü Yılmazer	(METU, CHE)	_____
Prof.Dr. Cevdet Kaynak	(METU, METE)	_____

,

I hereby to declare that all information in this document has been obtained and presented in accordance with academic rules and ethical conduct. I also declare that, as required by these rules and conduct, I have fully cited and referenced all material and results that are not original to this work.

Name, Last Name: Ceren KURTULUŞ

Signature:

ABSTRACT

SELF REINFORCEMENT OF POLY(ETHYLENE TEREPHTHALATE) AND POLYETHYLENE BLENDS

Kurtuluş, Ceren
M.S., Department of Chemical Engineering
Supervisor : Assoc. Prof. Dr. Göknur BAYRAM
Co-supervisor: Prof. Dr. Nurcan BAÇ

April 2007, 130 pages

In this study, 20/80 (weight %) Poly(ethylene terephthalate) (PET) /High Density Polyethylene (HDPE) Microfibrillar Reinforced Composites (MFC) were prepared by using high density polyethylene (HDPE) as the matrix material, poly(ethylene terephthalate) (PET) as the reinforcing component. Ethylene n-butyl acrylate-glycidyl methacrylate (E-nBA-GMA) and ethylene methyl acrylate (E-MA) as the compatibilizers in 1, 5, and 10 wt. %.

The objective of this study is to produce MFCs based on PET and HDPE via extrusion-drawing-injection method and to characterize as extruded, as drawn and injection molded materials in terms of morphologies, and

mechanical and thermal properties. In addition, the effect of compatibilizer type and content on properties of PET-HDPE composites was studied. For comparison purposes, conventional PET-HDPE composites with and without compatibilizer were prepared. Also, the effect of screw speed and drawing speed on the morphologies and mechanical and thermal properties were investigated. The effect of low and high injection temperature molding on morphologies were also observed.

SEM analyses showed that, extruded blends became oriented after drawing. The fibrillar structure was preserved after injection molding. High injection molding temperature destroyed the structure of PET microfibers. In addition, it was also observed that the adhesion between HDPE and PET improved with the addition of the compatibilizers.

Tensile strength and tensile modulus values of PET/HDPE MFCs increased with increasing drawing speed. Increasing the screw speed resulted in a slight decrease in tensile strength values. Addition of the compatibilizers to the system decreased tensile strength and tensile modulus values. Results of impact tests designated that the impact strength of the materials with and without MFC structure increased with the increasing amounts of E-nBA-GMA.

DSC analyses pointed out that, melting temperatures of HDPE and PET phase did not change significantly with increasing drawing speed or with the addition of the compatibilizer. As the drawing speed increased from 2.7 m/min to 6.2 m/min, degree of crystallinity of the drawn samples of the PET phase increased.

Key words: Poly(ethylene terephthalate), polyethylene, compatibilizer, morphology, mechanical properties

ÖZ

POLİ(ETİLEN TEREFTALAT) VE POLİETİLEN KARIŞIMLARININ KENDİLİĞİNDEN GÜÇLENDİRİLMESİ

Kurtuluş, Ceren
Yüksek Lisans, Kimya Mühendisliği Bölümü
Tez Yöneticisi : Doç. Dr. Göknur Bayram
Ortak Tez Yöneticisi: Prof. Dr. Nurcan Baç

Nisan 2007, 130 sayfa

Bu çalışmada, 20/80 (% ağr.) Poli(etilen tereftalat) (PET)/Yüksek yoğunluklu polietilen (YYPE) Mikrolifsel Güçlendirilmiş Kompozitler (MGK) hazırlanmasında, matrix bileşen olarak YYPE, güçlendirici bileşen olarak PET, uyumlaştırıcı olarak da % 1, 5 ve 10 oranlarında etilen n-bütil akrilat-glisidil metakrilat (E-nBA-GMA) ve etilen metakrilat (E-MA) kullanılarak hazırlanmıştır.

Bu çalışmanın amacı, ekstrüksiyon-çekme-enjeksiyon kalıplama yöntemiyle PET/YYPE MGKları üretmek ve ekstrüde edilmiş, çekilmiş ve enjeksiyonlanmış malzemeleri morfolojik, mekanik ve termal özellikler

açısından karakterize etmektir. Bunun yanında, uyumlaştırıcı tipi ve miktarının (% ağr.) PET/YYPE kompozitlerinin özellikleri üzerine etkileri de araştırılmıştır. Karşılaştırma amaçlı olarak, ekstrüde edilmiş PET/YYPE kompozitleri, uyumlaştırıcılı ve uyumlaştırıcı kullanılmadan hazırlanmıştır. Ayrıca, vida hızının ve çekme hızının morfolojiler, mekaniksel ve termal özellikler üzerine etkileri incelenmiştir. Bununla birlikte yüksek ve düşük enjeksiyonlama sıcaklıklarının morfoloji üzerindeki etkileri değerlendirilmiştir.

.

SEM analizleri, ekstrüde edilmiş örneklerin çekme işleminden sonra yöneltilmiş olduklarını göstermiştir. Lifsel yapı, enjeksiyonlamadan sonra da korunmuştur. Yüksek enjeksiyonlama sıcaklığı, PET mikroliflerinin yapısını bozmuştur. Bunun yanında, uyumlaştırıcıların eklenmesiyle PET ve YYPE arasındaki yapışmanın da arttığı gözlenmiştir.

PET/YYPE MGKlarının gerilme dayanımı ve gerilme modülleri, artan çekme hızıyla artmıştır. Vida hızındaki artış, çekme dayanımının bir miktar azalmasına sebep olmuştur. Uyumlaştırıcıların sisteme eklenmesi gerilme dayanımı ve modüllerini düşürmüştür. Darbe dayanımı analizleri, MGK yapısına sahip olan ve olmayan malzemelerin darbe dayanımı değerlerinin, artan E-nBA-GMA miktarıyla arttığı göstermiştir.

DSC analizleri YYPE ve PET fazlarının erime sıcaklıklarının çekme hızıyla ve uyumlaştırıcı eklenmesiyle önemli ölçüde değişmediğini göstermiştir. Çekme hızı 2.7 m/dak'dan 6.2 m/dak'ya çıkarıldığında, çekilmiş malzemelerin PET fazının kristallenme derecesi artmıştır.

Anahtar kelimeler: poli(etilen tereftalat), polietilen, uyumlaştırıcı, morfoloji, mekaniksel özellikler

To family, my husband, and my son ARIN KAAN...

ACKNOWLEDGEMENTS

I would like to express my deepest gratitude to my supervisor Assoc. Prof. Dr. Göknur Bayram and co-supervisor Prof. Dr. Nurcan Baç for their guidance, advice, criticism, encouragements and insight throughout the research and writing of this thesis.

I am very thankful to my husband Volkan Kurtuluş for his unlimited love, patience and encouragement till the end of my study. I would also like to thank to my sisters Figen & Gökçen Çamlıyurt for their special care, understanding and for their faith in me. At every step of my life they were just beside me with their endless love.

I thank especially to Mihrican Açıkgöz from Chemical Engineering Department for the DSC analyses, Cengiz Tan from Metallurgical and Materials Engineering department for the SEM analyses.

!

Many thanks to my friends Güralp Özkoç, Işıl IŞIK, Sertan Yeşil, Mert Kılınç, Miray Mert, Saniye Yayla, and Özcan Köysüren for their friendship and helping me a lot during my thesis. I would also like to thank Assist. Prof. Dr. Bahadır Körbahti, not only for being my friend, but also for his invaluable guidance and enlightening suggestions.

Finally, my deepest gratidute is to my parents Filiz & Erdoğan Çamlıyurt, who are the greatest parents that a daughter may have. I am dedicating this work to them, whose love and support always encouraged me.

TABLE OF CONTENTS

LIST OF TABLES

TABLE

LIST OF FIGURES

FIGURE

CHAPTER 1

INTRODUCTION

Composites are defined as materials consisting of two or more distinct components with recognizable interfaces or interphases [1]. An important characteristic feature of common composites is that they are prepared via a controlled combining process of the different components. Blending of two polymers is also a common approach to the creation of polymeric materials with new or improved properties. However, it usually results in immiscibility, so that often a third component, i.e., a compatibilizer such as a block copolymer, must be added to obtain a more uniform phase distribution.

Blending polyolefins (HDPE, LDPE, PP, etc.) with general engineering plastics is a major route to improve the mechanical properties and heat resistance of the blend components. In engineering applications, polyolefins have to be reinforced to meet the demands on stiffness and strength. Numerous studies have been done concerning the reinforcement of polyolefins with different types of fibers. Over the last few decades, glass or carbon fiber reinforced composites have found widespread application as injection-molded composites in the automobile and other technical industries. Despite their benefits, processing and fabrication of these composites present some technical difficulties: the presence of solid fibers during processing increases the viscosity of the molten plastic and produces wear on the processing equipment. Also in the view of recyclability, glass fibers

can cause environmental problems, both in mechanical recycling and thermal recycling (incineration). In recent years, several attempts have been made to use liquid crystalline polymers (LCPs), instead of the conventional fiber reinforced systems. The main advantage of these polymers is that, they can be processed in the melt state and they are capable of forming highly oriented crystalline structures when subjected to shear above their melting temperature. This highly oriented nature of LCP produces highly anisotropic physical property and makes LCP quite attractive as a potential dispersed phase reinforcing material. Besides, the advantages of LCP/Thermoplastic composites include [2]:

1. Easy manufacturing
2. Low-processing viscosity adaptable to extrusion, injection molding, and other processing techniques
3. Low energy consumption and high-production efficiency
4. Very low abrasion of processing machinery
5. Significant improvement in some mechanical properties of the composite caused by a small quantity of LCP (not higher than 20 wt %)

LCPs also have some disadvantages [3]:
1. They are generally immiscible with other thermoplastics and form a two phase structure
2. They are expensive
3. The application of the self reinforcing approach on a commercial scale requires a well defined set of processing parameters.

The concept of *self reinforcement,* i.e. reinforcing a polymer with its own morphological entities such as fibrils, crystallites or fibers, is an important method for improving the mechanical characteristics of many polymers [4]. The reinforcing elements grow in the amorphous matrix during crystallization process. A property of these systems is that they contain only one

constituent, in contrast to the more common types of composites. An interesting approach has been started recently which is based on the self reinforcement of polyolefins and their blending with a polycondensate phase [5-8]. This new type of polymer-polymer composite meets the basic requirements for polymer blends and composites. Unlike the classical macrocomposites (the glass or carbon fiber-reinforced ones) or “LCP” composites, this new group of polymer composites is reinforced by polymer fibrils of flexible macromolecules and is called “Microfibrillar reinforced composites” (MFC) [9]. In order to create microfibrils, first, melt blending with extrusion of the two immiscible polymers takes place. This is followed by the fibrillization step which is the drawing of the extrudate with orientation of the two phases. Lastly, in the isotropization step, injection molding takes place at a temperature between the melting temperatures of the two polymer partners. While during the second step the two polymers are converted into an oriented state, the third step results in melting of the lower melting component and its transformation into an isotropic matrix, reinforced with the microfibrils of the higher melting component.

This study aims to produce microfibrillar composite materials based on poly(ethylene terephthalate) (PET) and high density polyethylene (HDPE). These polymers were selected because of their commercial importance for large-scale production of packaging materials (bottles, films, containers, etc.) and were prepared by using extrusion-drawing-injection molding method. The other objective of this study is to characterize the composites as extruded, as drawn and injection molded materials in terms of morphologies and mechanical and thermal properties. In addition, the effect of compatibilizers on properties of PET/HDPE composites is studied. For comparison purposes, conventional PET/HDPE composites with and without compatibilizer were prepared. Also, the effects of screw speed and drawing speed on the morphologies and mechanical and thermal properties were

investigated. The effects of low and high injection molding temperature on the morphologies were also observed.

Mechanical characterizations of the MFCs were performed by tensile and impact tests. Thermal and morphological characterizations of the samples were done by using a differential scanning calorimeter (DSC) and a scanning electron microscope (SEM), respectively. Besides, microfiber diameters of the as drawn samples and PET particle size of the as extruded samples were measured from the SEM micrographs.

Lastly, the type of compatibilizers, ethylene n-butylacrylate glycidyl-methacrylate (E-nBA-GMA) and ethylene methacrylate (E-MA) and their content (wt. %) were studied to determine their effects on final properties of the composites.

CHAPTER 2

BACKGROUND INFORMATION

2.1 Polymer Blends

The blending of two or more polymers has become an increasingly important technique for improving the cost/performance ratio of commercial plastics. For example, blending may be used to reduce the cost of an expensive engineering thermoplastic, to improve the processability of a high-temperature or heat-sensitive thermoplastic, or to improve impact resistance.

Commercial blends may be homogeneous or phase-separated [10]. Generally, they exist as two separate phases. In this case, the morphology of the phases is of great importance. In the case of a miscible single phase blend, there is single T_g, which is dependent on the composition of the blend. Where two phases exist, the blend will exhibit two separate T_g values, one for each of the phases present. In the case where polymers can crystallize, the crystalline portions will exhibit a melting point (T_m), even in the case where the two polymers are a miscible blend.

Control of the morphology of these two-phase systems is critical to achieve the desired properties. However, most of the polymer pairs are thermodynamically immiscible and technologically incompatible; hence produce a multi-phase system during processing, which may damage the performance of the materials. Fortunately, owing to the deformable nature of

the dispersed phase in the immiscible blends, various morphologies can be generated in-situ such as fiber, ribbon, plate, etc. during processing some of which enhance the properties of the blends. As a result, the properties of the polymer blend depend on the type of polymers, the morphology of the blend, and the effects of processing parameters [11].

Polymer blends can be typically prepared in five techniques: melt blending, latex blending, partial block copolymerization, graft copolymerization, and synthesis of interpenetrating networks. Melt blending is a simple mechanical means of creating a homogeneous mixture of polymers. It could be performed in twin or single screw extruder, two-roll mill, or in an intensive mixer. In this study, a twin screw extruder was utilized to mix the blend components.

2.1.1 Microfibrillar Reinforced Composites (MFCs)

A new type of polymer-polymer composite, satisfying to a great extent the basic requirements of polymer blends and composites, and having reinforcing elements with sizes between those of fiber-reinforced and the "molecular" composites, was recently developed. Unlike the classical macrocomposites (e.g. fiber-reinforced ones) and the "molecular" composites (with single rod-like macromolecules as reinforcing elements such as LCPs), this new group is reinforced with polymer fibrils or, more frequently bundles of them, and is called "Microfibrillar reinforced composites (MFCs)" as mentioned above. They are developed on the basis of polymer blends [12].

The essential difference between the MFCs and the classical macrocomposites or LCP- based (molecular) composites is that MFCs are reinforced by microfibrils of flexible molecules. In contrast to the *in-situ*

composites where the microfibrils of LCP are also produced during processing, in case of MFC, a completely isotropic matrix is created during processing via special thermal treatment conditions. The important point is that in MFC systems the reinforcing elements grow in the amorphous matrix during the crystallization process.

2.1.1.1 Preparation of MFCs

MFCs are prepared from polymer blends of thermodynamically *immiscible* partners having different melting temperatures, T_m. In contrast to the common composites - the ones reinforced by discontinuous or continuous fibers - MFC cannot be manufactured by conventional blending of the two starting components, the matrix and the reinforcing material, since microfibrils are not available as a separate material. The essential stages of MFC preparation are as follows: (i) melt blending with extrusion, (ii) drawing with orientation of all components, and (iii) thermal treatment above the T_m of the lower-melting component but below the T_m of the higher-melting one. During the drawing step, the blend components are oriented and microfibrils are created *(fibrillization step).* In the subsequent processing, melting of the lower-melting component occurs *(isotropization step)* with preservation of the microfibrillar structure of the higher melting component. Technologically this transition to an MFC structure can take place during processing of the drawn blend via injection or compression molding. The essential requirement is that the processing window is not too close to the T_m of the microfibrils; otherwise they will melt and return into their spherical shape [11]. If the heat treatment temperature, T_a, is set below the melting point, T_m, of both components, the microfibrillar structure imparted by drawing is preserved and further improved as a result of physical processes, such as additional crystallization, minimization of defects in the crystalline regions, and relaxation of residual stresses in the amorphous regions. On the other hand, if T_a is set between

the melting temperatures of the two components, melting of the lower melting polymer takes place, thus forming an isotropic, relaxed matrix, while the microfibrillar regions, involving the component with the higher T_m, preserve their orientation and morphological characteristics. In the case of polycondensates, in addition to the isotropization during the thermal treatment, additional condensation and trans-reactions in the melt and solid state take place at the interface, resulting in a formation of a copolymeric interphase playing the role of a *self-compatibilizer.* The preparation steps for MFC are represented schematically in Figure 2.1.

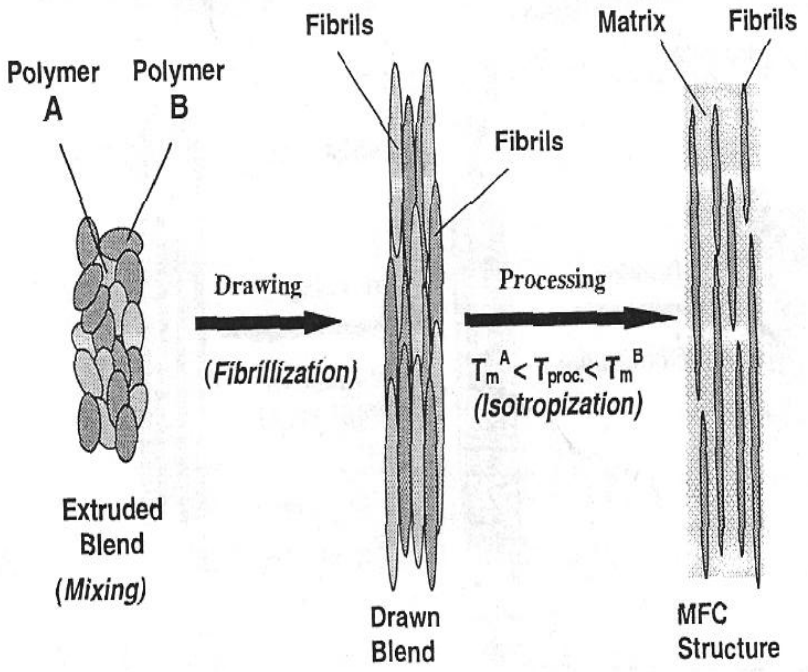

Figure 2.1 Preparation steps for MFC. (a) melt blending with extrusion, (b) drawing of the extrudate with orientation of the two phases (the fibrillization step), (c) thermal treatment at a temperature ($T_{proc.}$ is the injection molding temperature) between the melting points of two components at constant strain (isotropization step) [13]

The manufacturing of MFCs is schematically shown in Figure 2.2. For performing industrially relevant experiments, different polymer partners are melt blended and extruded which is followed by continuous drawing at the designed production line. These polymer partners are: Low density polyethylene (LDPE)/recycled PET (R-PET), high density polyethylene (HDPE)/R-PET, polypropylene (PP)/R-PET and poly(phenyl ether) (PPE)/different LCPs.

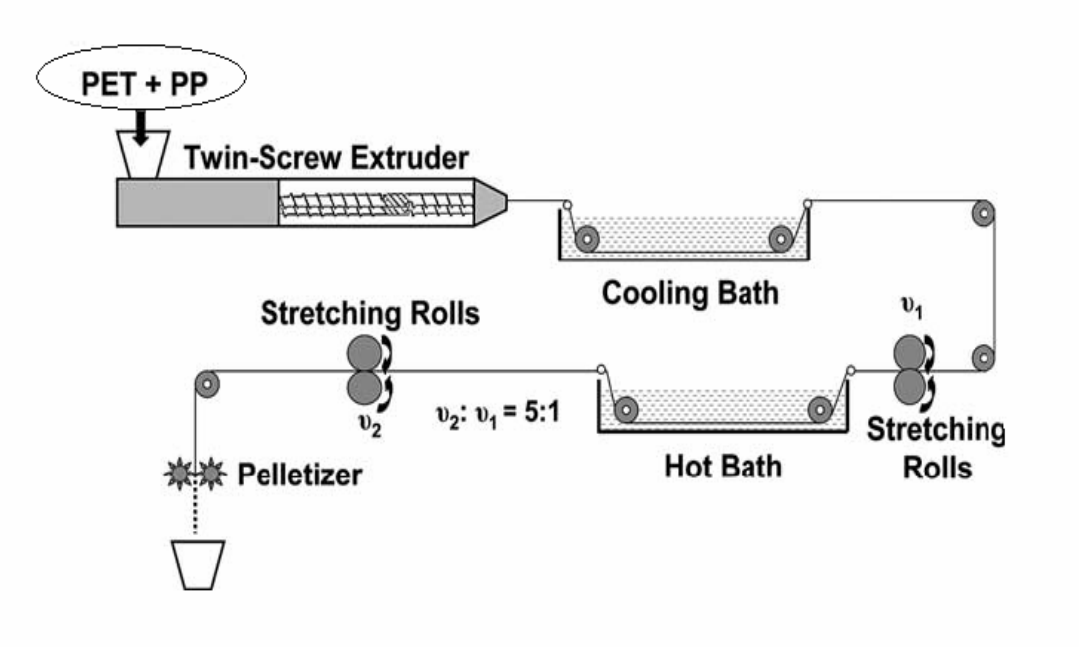

Figure 2.2 Schematic presentation of the industrial relevant extrusion and drawing [11]

2.1.1.2 Properties of MFCs

The MFC concept is a new and useful approach for processing of polymer blends and manufacturing of polymeric materials and articles with environmentally friendly properties so far no mineral reinforcement or additives are needed. Another characteristic feature of these materials is the

extremely homogeneous distribution of the reinforcement in the matrix polymer, which fact is of particular importance for the intensive studied nanocomposites nowadays. The problem dealing with the common nanocomposites regarding the fine and homogeneous dispersion of the reinforcing elements does not exist in the case of MFC approach, namely, the fine and homogeneous dispersion of the reinforcing component in the matrix starts from the very beginning as spheres, and later as micro- or nanofibrils. In addition, MFCs offer other potential advantages such as reduction in weight, increased processability, control liability of matrix crystallization and its susceptibility to aggressive agents; improved mechanical integrity and ability for recycling [14].

The properties of MFCs are quite promising. MFCs exhibit Young's moduli and tensile strengths, 30%-50% higher than the weight-average values of the components; they are comparable to those of short glass fiber-reinforced composites having the same matrix. Moreover, the ultimate strain and toughness of MFCs are much higher than those of corresponding glass fiber-reinforced systems [5,12].

2.1.1.3 Applications of MFCs

The manufacturing and processing of MFCs is successfully realized in commercial scale equipment. MFCs have some application opportunities in the car production, particularly in Europe, since they do not contain mineral reinforcement [14].

The MFC concept is also applied for manufacturing of *microplates* reinforced composites (MPC) via pressing of the non-drawn extrudate in order to transform the spheres into plates and subsequent processing for manufacturing of films or thin-walled containers. By selecting MPC partners

with mutually complementing barrier properties (e.g. PET/PE or PET/PP) it is possible to improve the properties of the conventional packaging materials consisting of a single polymer.

Applying again the MFC approach, *nanofibrils,* characterized by extremely homogeneous diameters (around 100 nm), are recently obtained and isolated as a single material. After compression molding of a drawn blend comprising nanofibrils and thus transforming the lower melting component in isotropic matrix a nanofibrils reinforced composite is obtained [14].

The isolation of nano- and microfibrils via selective dissolution of the second blend component offers potentials for their biomedical applications as scaffolds for the regenerative medicine or as carriers for controlled drug delivery as well as nanofilter materials.

The most recent development of the MFC is the loading of microfibrils with carbon nanotubes where a *double reinforcing effect* is realized which can be defined as “the reinforcement of the reinforcing material”. In addition, this approach allows one to obtain electro conductive polymeric materials where only a part of the material is loaded with carbon nanotubes. Films or injection molded containers of this material show good shielding properties [14].

2.2 Poly(ethylene terephthalate), PET

Poly(ethylene terephthalate), PET, is a typical member of the polyester family composed of repeated units of (-CH_2CH_2-OOC-C_6H_4-COO-) containing a phenyl group (C_6H_4). It is also called aromatic polyester. The chemical structure of PET is illustrated in Figure 2.3.

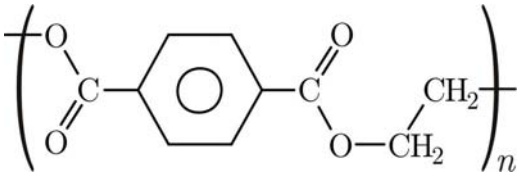

Figure 2.3 Chemical Structure of PET [15]

First introduced as a material for synthetic fibers in 1953, PET has progressively found new and interesting applications, in many cases without any competing alternative. In its most conventional applications in the textile industry, PET fibers can mimic cotton, wool or silk. PET films find widespread usage owing to their excellent electrical properties. Finally, the use of PET in the packaging industry, particularly for soft drinks is universal [16].

PET is a step-growth (condensation) polymer derived from terephthalic acid (PTA) or dimethyl terephthalate (DMT) and ethylene glycol (EG). Figures 2.4 and 2.5 represent the reactions of PET formations via acid route and ester interchange, respectively.

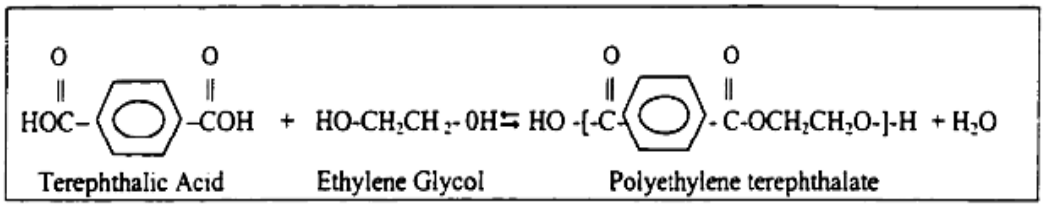

Figure 2.4 PET formation via acid route

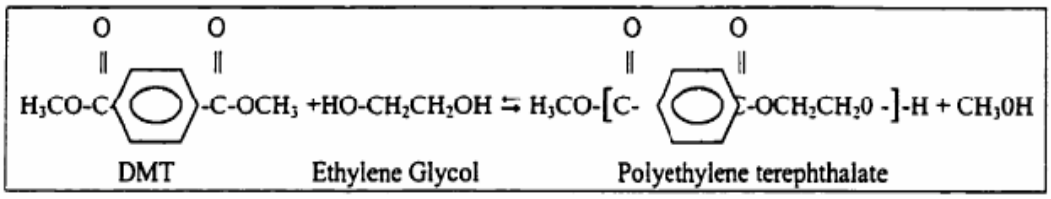

Figure 2.5 PET formation via ester interchange

2.3 Polyethylene, PE

Polyethylene (PE) is the highest-volume polymer in the world [17]. Its high toughness, ductility, excellent chemical resistance, low water vapor permeability, and very low water absorption, combined with the ease of processing, make PE of all different density grades an attractive choice for a variety of goods. PE is limited by its relatively low modulus, yield stress, and melting point. It is used to make containers, bottles, film, and pipes, among other things. It is an incredibly versatile polymer with almost limitless variety due to copolymerization potential. It has a wide density range and a molecular weight which ranges from very low (waxes have a MW of a few hundred) to very high as $6x10^6$ [1].

PE homopolymers are made up exclusively of carbon and hydrogen atoms. Chemical structure of PE is shown in Figure 2.6. Different grades of PE have markedly different thermal and mechanical properties. The density of a particular grade is governed by the morphology of the backbone; long, linear chains with very few side branches can assume a much more three-dimensionally compact, regular, crystalline structure. Commercially available grades are: very-low density PE (VLDPE), low-density PE (LDPE), linear low-density PE (LLDPE), high-density PE (HDPE) and ultra-high molecular weight PE (UHMWPE).

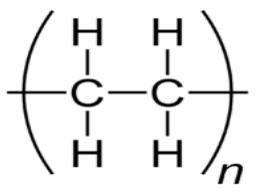

Figure 2.6 Chemical Structure of PE [15]

2.4 Compatibilizers

Many polymer pairs are immiscible and, therefore, phase-separation occurs during processing. The mechanical properties of these immiscible blends are often poor due to inadequate interfacial strength between the dispersed phase and matrix.

Compatibility is usually promoted by the presence of graft or block copolymers whose segments can give rise to physical and/or chemical interactions with the blend components, with the effect of reducing the interfacial tension and improving the phase dispersion and adhesion through interpenetration and entanglements at the polymer-polymer interface. The copolymers may be added separately (physical compatibilization) or formed *in situ* during melt-blending by using suitable polymers containing functional groups (e.g. carboxyl, anhydride, epoxy, etc.) capable of reacting with the other polymer component (reactive compatibilization) [18,19].

In previous studies, PET/HDPE blends have been compatibilized by addition of maleic anhydride grafted polyolefins [20], styrene-ethylene/butylene-styrene block copolymers (SEBS and SEBS-g-MA) [21], ethylene-acrylic acid copolymers (E-AA) [22], ethylene glycidyl-methacrylate (E-GMA)

copolymers and ethylene-ethyl acrylate glycidyl-methacrylate terpolymers (E-EA-GMA) [23].

In this study, PET and HDPE were used as the blend components. Compatibilizers such as ethylene n-butylacrylate glycidyl-methacrylate (E-nBA-GMA) and ethylene methylacrylate (E-MA) have been used to compatibilize PET/HDPE blends. During melt mixing of the blend components, *in situ* graft copolymers may be generated by reaction of the carboxyl or hydroxyl end-groups of PET with the reactive functionalities of the compatibilizer molecules. Potential reactions of E-nBA-GMA group of elastomer with the carboxyl and hydroxyl groups of PET are given in Figure 2.7.

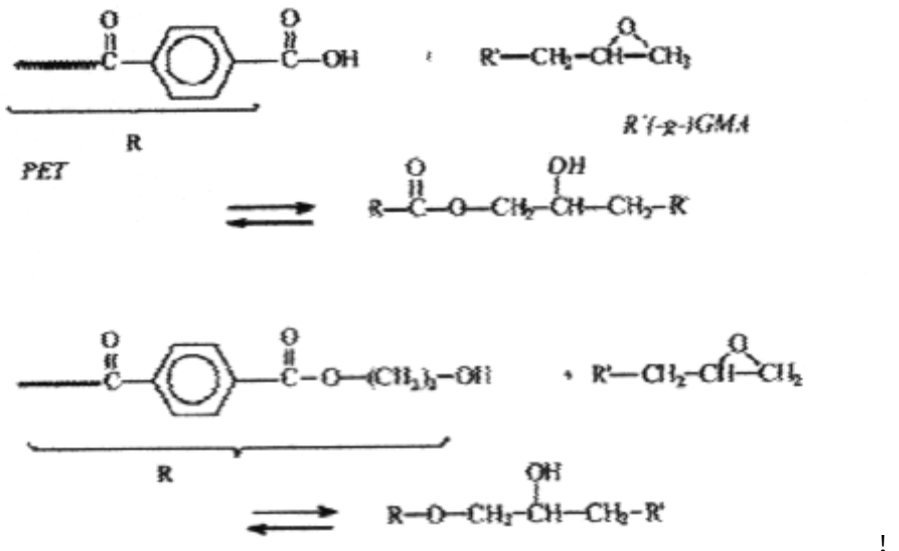

Figure 2.7 Chemical reaction schemes for epoxy and PET functional end groups [24]

2.5 Polymer Processing

Polymer processing is the technology of converting raw polymer, or compounds containing raw polymer, to articles of a desired shape. It may be classified in five broad categories: extrusion, molding, spinning, calendaring, and coating [25].

Only extrusion and injection molding processes are explained here, since they were used in this study.

2.5.1 Extrusion

The word “extrusion” is derived from the Latin words *ex* and *trudere* meaning, respectively, “out” and “to thrust” or “to push”. These words describe literally the process of extrusion, where a polymer melt is pushed across a melt die that continuously shapes the melt into the desired form. Polymer products that are “infinite” in one direction are manufactured by the extrusion process. These include wires, cables, rods, tubes, pipes, and a variety of profiles, which include filaments, films, and sheets that are products of great volume and importance [26].

During extrusion, the raw polymer in the form of particulate solids (pellets, powder, etc.) is gravitationally fed onto the screw through a hopper. The solids are conveyed forward, plasticated, homogenized, and pressurized along the screw. Thus a uniformly molten polymer is pumped or pushed across the die attached to the extruder “head”. The screw is rotated by electric motors through a gear reducer. The barrel is heated electrically or by a fluid heat exchanger system. Thermocouples placed in the metal barrel wall record and help to control barrel temperature settings. Sections of barrel, however, are often cooled to remove the excessive heat generated by viscous dissipation. The main operating variables are the frequency of screw

rotation and the barrel temperature profile. The main design variables are screw diameter and length- usually expressed as length-to-diameter ratio L/D. These determine to a large extent extruder throughput, polymer residence time in the extruder, and available barrel surface for heat transfer.

In addition to the shaping of parts by the extrusion process, extrusion is the most efficient and widely used process for melting plastic resin as part of the process of adding or mixing fillers, colorants, and other additives into the molten plastics. A cross section view of extrusion process can be seen in Figure 2.8.

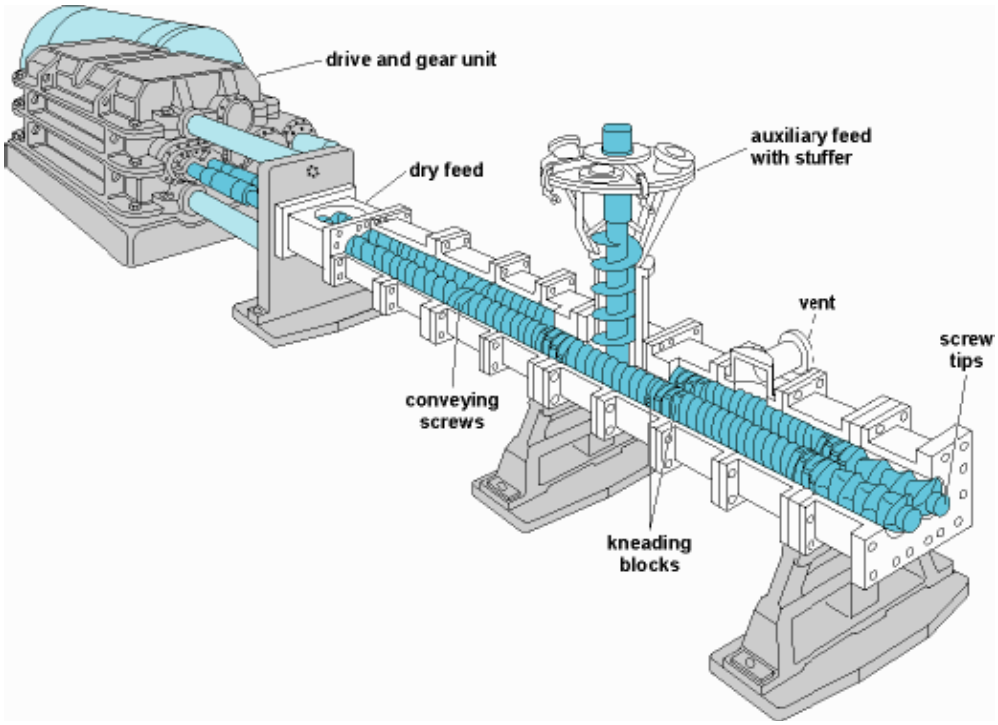

Figure 2.8 Cross section view of extrusion process [27]

The most common types of extruders are single-screw extruders and twin-screw extruders. Single screw extruders are relatively similar in design and function. All single-screw extruders convey the polymer to the die by means of drag flow. They provide high head pressures, uncontrolled shear, and a degree of mixing that relies on the screw design. In contrast, principles of operation, and applications of twin-screw extruders may vary widely. While the two screws are usually arranged side by side, the introduction of two screws produces different conveyance mechanisms, varied degrees of mixing, and controllable shear. The low head pressure generated by twin-screw extruders limits their use to processing of shear-sensitive materials, such as PVC, and to compounding [26]. A schematic of twin-screw extruder design patterns are shown in Figure 2.9.

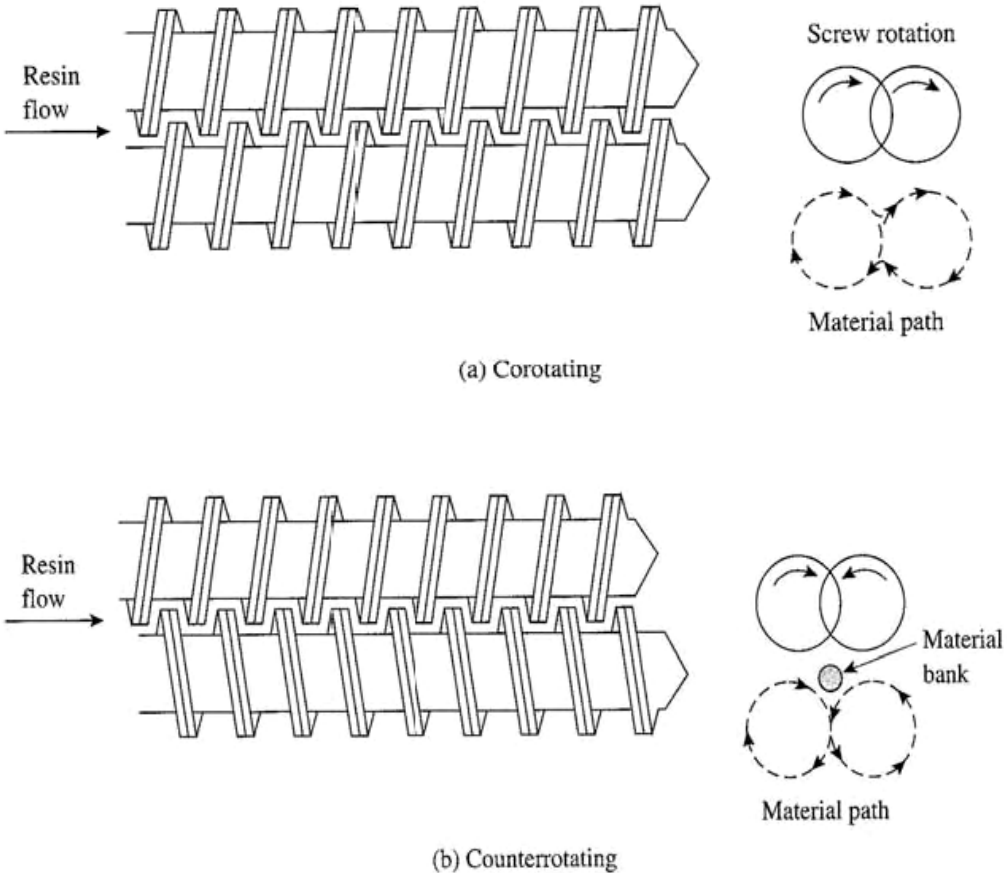

Figure 2.9 Twin-screw extruder design patterns [28]

2.5.2 Injection Molding

Injection molding is the process for producing identical articles from a hollow mold [26]. In addition to thermoplastic polymers, thermosetting polymers and elastomers are molded by this process. The polymer is preheated in a cylindrical chamber to a temperature at which it will flow and then is forced into a relatively cold, closed mold cavity which gives shape to the plastic. After sufficient time is given for the plastic part to solidify, the mold opens and the part is removed. Schematic presentation of injection molding machine is seen in Figure 2.10.

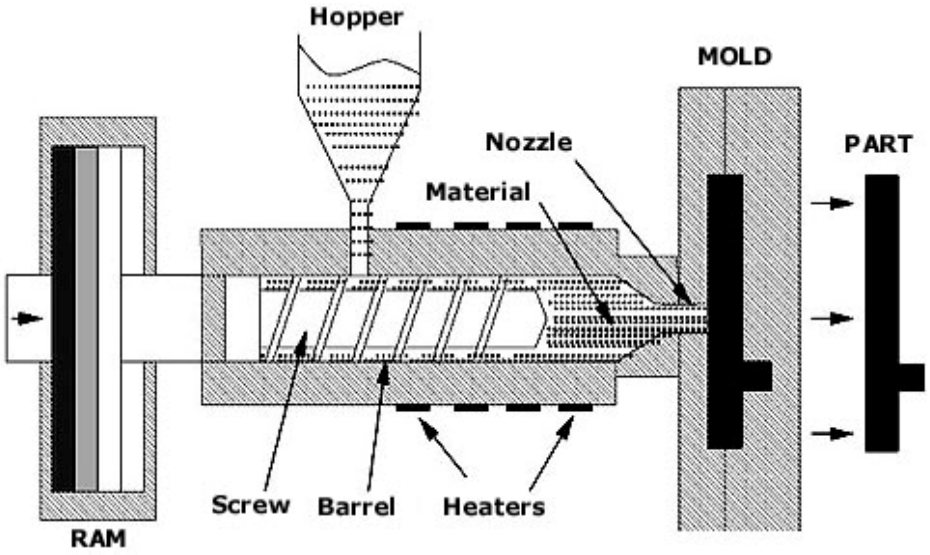

Figure 2.10 Schematic presentation of injection molding machine [29]

2.6 Polymer Characterization

Characterization techniques for polymers are categorized in terms of mechanical testing methods, thermal analysis, electron and optical microscopy, NMR techniques, chromatographic methods, spectroscopy, scattering and fluorescence techniques. As polymer blends become more popular in research and in application, many new characterization techniques specific for blends have been developed [27].

In the characterization part of this study, scanning electron microscopy observations, mechanical tests and differential scanning calorimetry analyses were performed.

2.6.1 Morphological Analyses

2.6.1.1 Scanning Electron Microscopy

Some of the structure elements are too small to examine by using optical light microscopy. In case of such circumstances, the electron microscope, which is capable of much higher magnifications, is employed.

Due to the great depth of focus, relatively simple image interpretation, and ease of sample preparation, SEM is the preferred technique for viewing specimen in detail at a resolution well exceeding that of the light microscope. The SEM images vividly display the three-dimensional characteristics of the object surface under examination [30].

In SEM analysis, the surface of the specimen is coated with a gold-platinum including solution with a sputter coater under vacuum firstly. This is due to make the specimen surface conductive in order to obtain electron reflection.

Then the specimen is placed into the SEM and the surface of the specimen is scanned with an electron beam, and the reflected (or back-scattered) beam of electrons is collected, and then displayed at the same scanning rate on a cathode ray tube. The image on the screen, which may be digitized, represents the surface features of the specimen. A schematic of SEM is schematically shown in Figure 2.11.

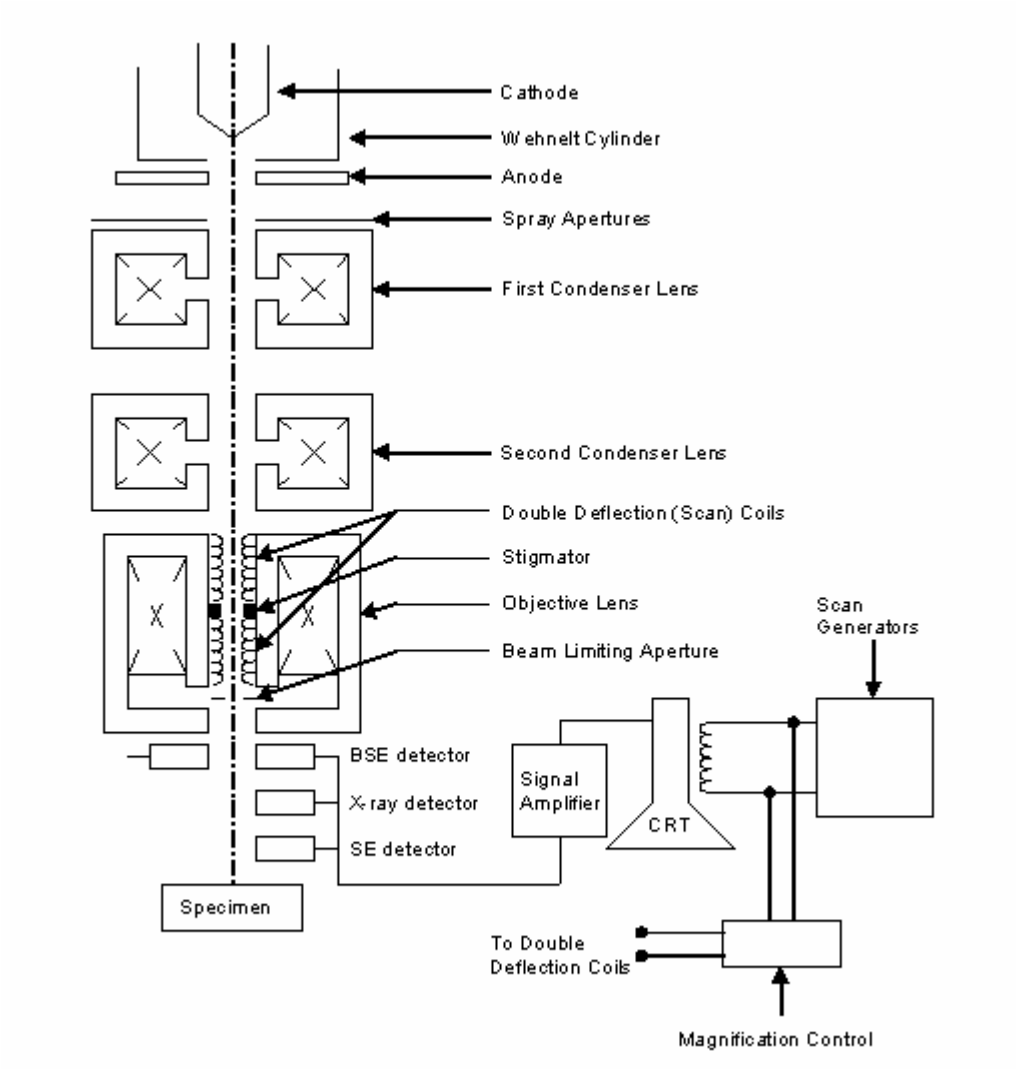

Figure 2.11 A schematic of Scanning Electron Microscope (SEM) [30]

2.6.2 Mechanical Properties

2.6.2.1 Tensile Test

Tensile testing of polymers usually means the recording of load-versus-elongation curves. Tensile properties, on the other hand, indicate characteristic stress and/or elongation values extracted from these curves [31].

Tensile tests are applied to observe the strength of produced material. Specifically designed specimens, usually dog bone shape, are gripped at their two ends and subjected to uniaxial loading at a constant rate. The change of force *F* is measured and recorded as a function of elongation ΔL during the test. The force and the elongation are transformed into stress σ and strain ε, and the results are reported in this form. The original cross section of the sample A_0 is used for the calculation of stress. Elongation is related to the original length of the gauge length of the specimen, L_0 to calculate strain. Engineering quantities are expressed as;

!

$$\sigma = F / A_0 \qquad (2.1)$$

$$\varepsilon = (L-L_0) / L_0 .100 = (\Delta L / L_0) . 100 \qquad (2.2)$$

where L is the length of the specimen after the test.

Tensile Modulus, (Young's Modulus), E, is the ratio between stress and strain at break which can be given in the following equation:

$$E = \sigma / \varepsilon \qquad (2.3)$$

The force on the specimen is measured and the test ends when the specimen breaks. Then a plot of stress versus strain (elongation), as shown in Figure 2.12 is prepared. The height of the curve when the sample breaks is the tensile strength, and the tensile modulus is the slope of the initial straight line. If the slope is steep, the sample has a high tensile modulus, which means it resists deformation. If the slope is gentle, then the sample has a low tensile modulus, which means it is easily deformed.

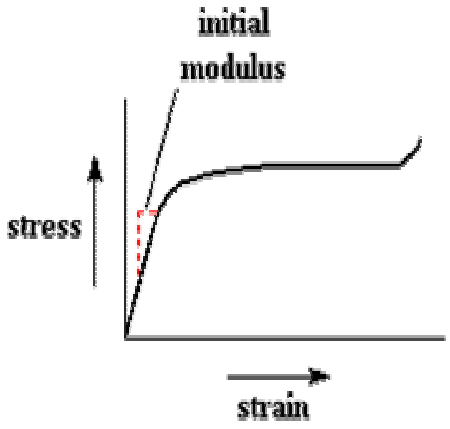

Figure 2.12 A plot of stress-strain curve [31]

2.6.2.2 Impact Test

Impact tests measure the energy required for failure when a standard specimen receives a rapid stress loading. The impact strength of a polymer can be measured employing a number of techniques including Izod and Charpy tests. In the Izod and Charpy impact tests a pendulum with a hammerlike weight strikes a specimen (a notched or unnotched bar), and the energy to break a specimen is determined from the loss in kinetic energy of the weight.

In high speed tensile tests and similar tests on unnotched specimens, the impact strength is defined in terms of the area under the stress-strain curve or as energy to break. For notched Charpy tests, impact strength is defined as:

$$\text{Impact strength} = \frac{\text{absorbed energy (J)}}{\text{the original cross-sectional area of the notch of the specimen } (m^2)} \quad (2.4)$$

2.6.3 Thermal Analyses

2.6.3.1 Differential Scanning Calorimetry

Differential scanning calorimetry (DSC) is a thermoanalytical technique in which the difference in the amount of heat required to increase the temperature of a sample and reference are measured as a function of temperature. Both the sample and reference are maintained very nearly the same temperature throughout the experiment. Generally, the temperature program for a DSC analysis is designed such that the sample holder temperature increases linearly as a function of time. The reference sample should have a well-defined heat capacity over the range of temperatures to be scanned. The basic principle underlying this technique is that, when the sample undergoes a physical transformation such as phase transitions, more or less heat will need to flow to it than the reference to maintain both at the same temperature. Whether more or less heat must flow to the sample depends on whether the process is exothermic or endothermic. By observing the difference in heat flow between the sample and reference, differential scanning calorimeters are able to measure the amount of energy absorbed or released during such transitions [32].

The sample (in a condensed form such as powder, liquid, or crystal) is generally placed in an aluminum sample pan, which is then placed in the sample cell. The reference consists of a matched empty aluminum sample pan that is placed in the reference cell of the instrument. The sample pans are designed to have a very high thermal conductivity. Sample weights generally range from 0.1 to 100 mg. The instrument cells are often airtight in order to shield the sample and the reference from external thermal perturbations. This also allows experiments to be performed under variable pressures and atmospheres. Figure 2.13 represents the drawing of Differential Scanning Calorimetry.

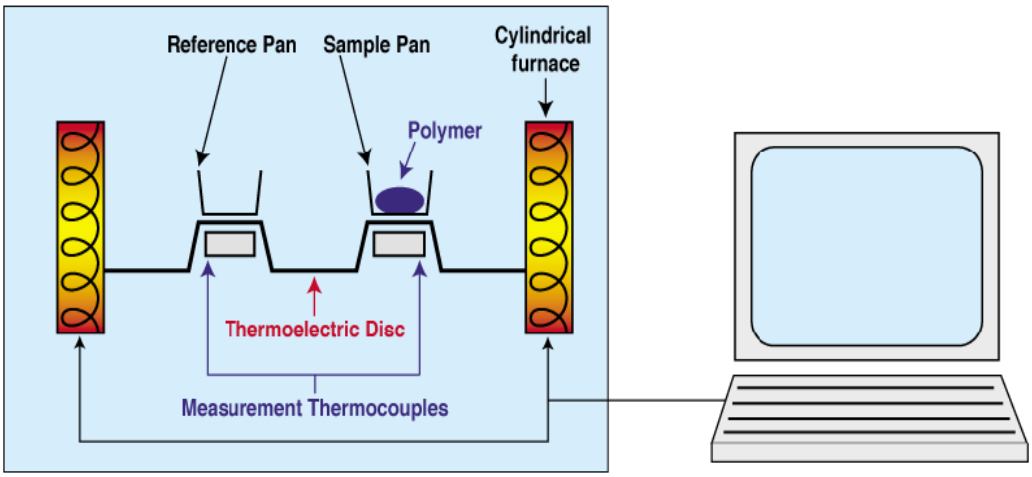

Figure 2.13 Representative drawing of Differential Scanning Calorimetry [32].

Glass transitions occur as the temperature of an amorphous solid is increased. A glass transition is characterized by a decrease in viscosity. These transitions appear as a step in the baseline of the recorded DSC

signal. This is due to the sample undergoing a change in heat capacity, but no formal phase change occurs.

As the temperature increases, an amorphous solid will become less viscous. At some point the molecules will obtain enough freedom of motion to spontaneously arrange themselves into a crystalline form. This is known as the crystallization temperature (T_c). This transition from amorphous solid to crystalline solid is an exothermic process, and results in a peak in the DSC signal. As the temperature increases the sample eventually reaches its melting temperature (T_m). The melting process results in an endothermic peak in the DSC curve. A schematic of DSC curve is shown in Figure 2.14.

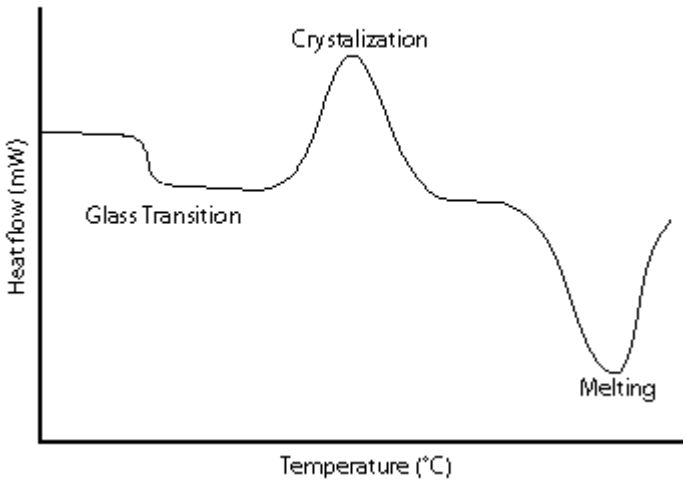

Figure 2.14 A schematic of DSC curve demonstrating the appearance of several common features [32]

The degree of crystallinity, X_c is one of the most important properties of semi-crystalline thermoplastics. The assesment of percent crystallinity of polymers can most easily be performed using DSC. The degree of crystallinity is defined as:

$$X_c = \left(\frac{\Delta H_m}{\Delta H^{\circ}_m \times w_{poly}} \right) \times 100 \qquad (2.5)$$

ΔH°_m (J/g)$\rightarrow$ Melting energy of the 100% crystalline structure

ΔH_m (J/g) $\rightarrow$ Melting energy

$X_C \rightarrow$ degree of crystallinity

$w_{poly} \rightarrow$ Polymer amount in the composite (wt.%)

2.7 Previous Studies

Friedrich et al. [11] studied MFC based blends from recycled PET, PP and a compatibilizer (E-GMA). The composites were prepared under industry-relevant conditions by melt-extrusion and cold-drawing. The PET/PP/E-GMA weight ratios were 40/60/0, 40/59/1, 40/57/3, 40/54/6, and 40/51/9. The extrusion was performed by using a twin screw extruder at a temperature profile of 260-270-260-245°C, and the screw speed of 30 rpm. A self designed take-up device was used for drawing the extrudate. Test materials were prepared by compression and injection molding at processing temperatures either below or above the melting temperatures of PET. In the characterization part, they performed SEM, WAXS and mechanical testing to the samples of as extruded, as drawn and injection molded MFC bars. They found out that extruded blends are isotropic, but become highly oriented

after drawing and they are converted into MFC structured composites during compression and injection molding. The flexural modulus and the flexural strength of the injection molded samples are by 50% higher than those of the pure PP. Both the flexural modulus and strength of the compression molded samples increased with an increase in E-GMA content.

Evstatiev et al. [3] studied structure-property relationships of injection molded microfibrillar reinforced PET/PA-6 blends with different weight ratios of the components. The blends were prepared by using a single-screw extruder. The temperature profile was 210-270-275-280-242°C. All blends were drawn in a tensile testing machine at room temperature to a draw ratio of about 4. Test materials were both processed by injection and compression molding. DSC, X-Ray (WAXS), SEM, Polarized Light Microscopy (PLM) and mechanical analysis were performed for characterization. Morphological studies of the injection molded samples showed that the fibrillar structure was basically preserved in the skin of the samples and the core region is composed of a small amount of randomly oriented fibrillar PET bundles, as well as a large amount of spherical PET domains in the PA-6 matrix. However, the SEM observations of the fracture surface of compression molded samples showed well extended PET fibrils in the PA-6 matrix. They found out that morphology strongly affected the tensile properties of the samples. The elastic modulus and strength of the injection molded MFC blends were increased by a factor of 2.5 and 1.7, respectively compared to the injection molded pure PA-6. In the case of compression molding, both modulus and strength were about four times higher than those of pure PA-6.

Sarkissova et al. [33] studied the design and characterization of microfibrillar reinforced composite materials based on PET/PA12 blends. MFCs were prepared by reactive melt-extrusion of PET and PA12 in the presence of a catalyst. The composites were produced by a series of processes: first extrusion in a twin screw extruder, then drawing in Instron testing machine at

a draw ratio of 3.8, and finally the isotropization of the lower melting PA12 phase, this step took place inside the Instron oven at fixed ends under controlled thermal conditions. In the characterization part, they performed DSC in order to study the crystallization and melting behavior, X-ray diffraction to analyze the chain orientation and the crystallization upon drawing and annealing, SEM to analyze the microstructure of the blends, and finally static and dynamic mechanical testing to measure the mechanical properties of the samples while they are subjected to a periodic stress. The modulus and tensile strength of MFCs were higher than pure PA12 and drawn pure PA12 samples.

Lin et al. [34] studied morphological development in melt extrusion of PET/PP microfibrillar composite. In this study, PET/PP blends of different compositions were extruded through a twin screw extruder. The extrudate was drawn in a solid state, either at room temperature or an elevated temperature to enhance the molecular orientation of PET fibers to give a microfibrillar composite. Basic extrusion setting was as follows: 160-220-270-270°C. The screw speed was 50 rpm and the drawing speed was 15 m/min. Effect of viscosity ratio, barrel temperature, die temperature, cooling medium, screw speed, and drawing speed on morphologies were studied. Three different screw speed (50, 100, and 150 rpm), five different drawing speed (10, 15, 20, 25, and 30 m/min), four different barrel temperature (260, 270, 280, and 290°C), three different die temperature (240, 260, and 290°C) and four different cooling media (air, water (at room temperature), ice water (0°C) and a mixture of nitrogen and acetone at -80°C) were used. They found out that, when the screw speed increased, the particle size and fiber diameter decreased; and with increase in drawing speed, the diameter of the PET fibers was reduced. Lower barrel temperature and die temperature produced smaller particle size and a large number of fibers. When the mixture of liquid nitrogen and acetone were used as a cooling media, smaller particle size was obtained.

Li et al. [35] studied the tensile properties of PET and PE in-situ microfiber reinforced composite. The MFC was prepared through slit die extrusion and hot stretching, followed by injection molding at the processing temperature of PE matrix, far below the melting temperature of PET in order to maintain the formed fibers. The extrusion temperature profile was: 190-250-275-280°C and the screw speed was 65 rpm. The extrudate was hot stretched by a take-up device with two pinching rolls to make the microfibers formation. The hot-stretching ratio was fixed at 25.6 for this study. Four different PET concentrations (10, 15, 20, and 25) were used to see the effect of composition. In order to observe the effect of high injection molding temperature, injection molding was conducted at the processing temperature of PET. They found out that, the mechanical properties of MFC at PET concentrations ranging from 10 to 25 wt % were improved greatly in comparison with the common PET/PE blend at the same compositions. The specimen with spherical particles of PET had much higher elongation at break than the one with PET microfibers.

Monticciolo et al. [36] reported a study on fibrillar morphology development of polyethylene/poly(butylene terephthalate) (PE/PBT) blends applying a two step process. During the extrusion step at 250°C, the fibrillar morphology of the PBT phase was elaborated. Then, in the second step, the PE/fibrillar PBT system was pelletized and extruded again at 180°C, preserving the PBT fibrils. The authors investigated further the correlation between fibrillar length, isotropy, and anisotropy of dispersed PBT fibrils and found that in the PE/PBT composites, the PBT fibrils are isotropically oriented; no data on the reinforcing effect of these fibrils was reported.

Li et al. [37] investigated the effect of microfiber reinforcement on morphologies of PET/PE systems. Composites were prepared through slit-die extrusion and hot-stretching and then molding by using injection molding technique. Composites were molded below the melting point of PET in order

to keep the fibers in the matrix. In the study, they changed the PET/PE weight percent and investigated the basic microfiber properties such as diameter, and diameter distribution. They concluded that with the increase of PET content, diameter of the fiber increased and diameter distribution widened, but minimum fiber diameter remained constant.

Quan et al. [38] examined the morphology and mechanical properties of poly (phenylene sulfide) (PPS)/isotactic polypropylene (iPP) in situ microfibrillar blends. The microfibrillar blend was prepared through a slit-die extrusion, hot stretching and water quenching process. Morphological observation indicated that the well-defined PPS microfibrils were achieved by the method used in this study. The morphological analysis showed that the minimum diameter of PPS phase was independent of PPS concentration. The tensile strength of the microfibrillar blend was higher than that of as extruded PPS/iPP blend and increased with stretching.

CHAPTER 3

EXPERIMENTAL

3.1 Materials

3.1.1 Poly(ethylene terephthalate), PET

Poly(ethylene terephthalate) (PET) was used as the reinforcing component in this study and obtained from AdvanSA Company, Adana, Turkey. PET pellets were in the amorphous form and, thus, they were transparent. It is synthesized by the esterification reaction between terephthalic acid (PTA) and ethylene glycol. Some properties of PET given by the producer are listed in Table 3.1.

Table 3.1 Some properties of PET given by the producer

Property	Value	Unit
Pellet size	1.5 ± 0.25	g/100 chips
iso-phthalic acid (IPA) content	1.5 ± 0.05	wt/wt %
Diethylene glycol (DEG) content	1.4 ± 0.10	wt/wt %
(COOH) content	40 ± 5	equiv./ton
Intrinsic Viscosity	0.61 ± 0.01	dl/g
DSC Amorhous Melting Point	255	ºC
DSC Crystallization Melting Point	245	ºC
Crystallization Heat of Fusion	45	kJ/kg

3.1.2 High Density Polyethylene, HDPE

High Density Polyethylene (HDPE) (PETILEN YY S 0464) was used as the matrix and purchased from PETKIM. It is a high density polyethylene and it is mainly used for blow molding applications such as large-sized containers for chemicals, drums for kerosene, large-sized toys. Its properties are given in Table 3.2.

Table 3.2 Manufacturer data of HDPE

PROPERTY	UNIT	VALUE	TEST METHOD
Melt Flow Rate (MFR) (2160 g, 190°C)	g/10 min	0.25-0.45	ASTM D-1238, TS-1675
Density, 23°C	g/cm^3	0.962-0.966	ASTM D-1505, TS-1818
Non Newtonian Index	-	38	ASTM D-3835
Color, WI	-	88	ASTM E-313
Tensile Strength - Yield - Break - Elongation At Break	 MPa MPa %	 26.5 36.8 1115	ASTM D-638, TS-1398 ASTM D-638, TS-1398 ASTM D-638, TS-1398
Stiffness	MPa	966	ASTM D-747
Izod Impact Strength	kgcm/cm	60	ASTM D-256, TS-1005
Environmental Stress Cracking Resistance (F50)	hour	15	ASTM D-1693

3.1.3 Compatibilizers

In this study, ethylene n-butylacrylate glycidyl-methacrylate (E-nBA-GMA, C_1) (Elvaloy PTW), which is a reactive functional terpolymer, and ethylene methacrylate (E-MA) (Elvaloy 1224 AC, C_2), which is a non-reactive polar copolymer were used as compatibilizers. These were procured from Dupont Chemicals Company, USA. They are in the form of pellets and solid at room temperature. Their properties are given in Tables 3.3 and 3.4. Also, their chemical structures are presented in Figures 3.1 and 3.2, respectively.

Table 3.3 Properties of Elvaloy PTW

Property	Values
Content	Ethylene (63 wt. %) Glycidyl Methacrylate (6 wt. %) Acrylate (31 wt. %)
Melt Flow Rate	12 g/10 min
Tensile Strength	5.2 MPa
Elongation at break	950 %
Hardness (Shore A)	73
Melting Point	72 °C
Glass Transition Temperature	-55 °C

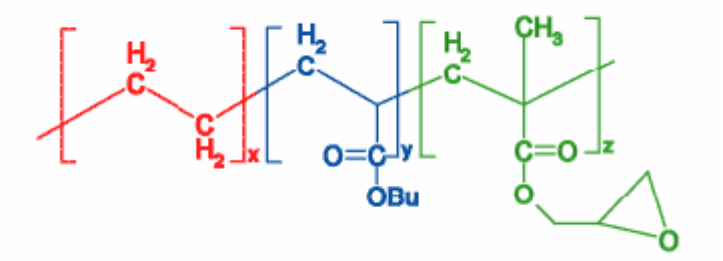

Figure 3.1 Chemical structure of E-nBA-GMA [40]

Table 3.4 Properties of Elvaloy 1224 AC

Property	Values
Content	Methacrylate (24 wt. %)
Melt Flow Index	2 g/10 min
Tensile Strength	12 MPa
Elongation at break	846 %
Density	944 kg/m^3
Hardness (Shore A)	78
Melting Point	91 °C

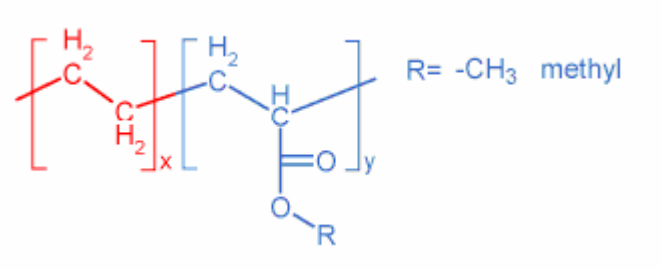

Figure 3.2 Chemical structure of E-MA [40]

3.1.3.1 Elvaloy PTW

Elvaloy PTW is a reactive functional ethylene terpolymer containing epoxy functionality that is a good toughener for polyester polymers [41]. It has several outstanding features. These include:

- Excellent adhesion to polyester because of its epoxy functionality.
- Good low temperature properties due to its T_g of -55°C.

The principle of action in reactive functional copolymers is to react at the interface to create "in-situ" a grafted block copolymer by reaction between functional groups of the different polymers. The functionalized copolymer is miscible with the matrix and can react with functional groups of the dispersed phase. Figure 3.3 illustrates the mechanism of action of reactive functional copolymer.

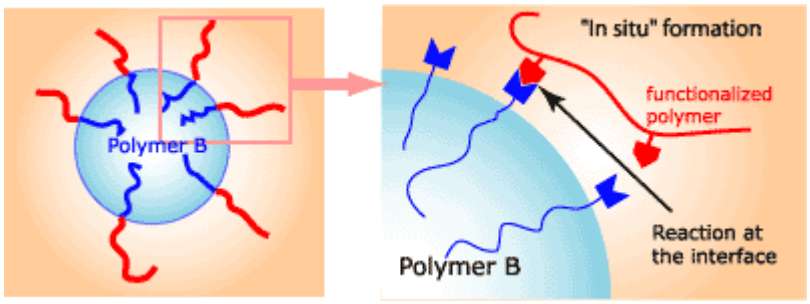

Figure 3.3 The mechanism of action of reactive functional copolymer [42]

Elvaloy PTW contains glycidyl-methacrylate (GMA) and provides excellent adhesion. It also contains n-butylacrylate (nBA) which provides very good low temperature properties. It is typically compounded with polyester in a twin screw extruder with the process temperature set by the melt temperature of the polyester.

3.1.3.2 Elvaloy® 1224 AC

Elvaloy 1224 AC is a non-reactive polar copolymer of ethylene and methyl acrylate (E-MA) [41].

The concept in non reactive polar copolymers is to reduce interfacial tension and increase the adhesion by creation of a specific polar interaction like hydrogen bonding or Van der Waals forces. The compatibilizer has to be compatible with one phase (generally nonpolar) and has to create specific interactions with the other phase. Figure 3.4 illustrates the mechanism of action of non-reactive polar copolymer.

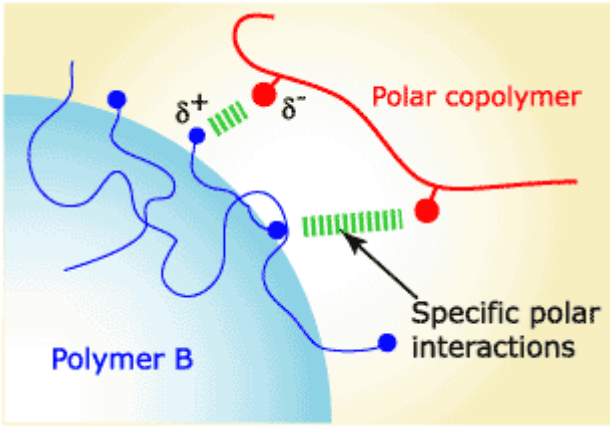

Figure 3.4 The mechanism of action of non-reactive polar copolymer [42]

Elvaloy 1224 AC is suitable for extrusion, coextrusion, compounding and injection molding. It offers excellent sealing properties and high filler acceptance. It can be recommended for parts requiring flexibility, stress cracking resistance and softness.

3.2 Preparation of Materials

3.2.1 Twin Screw Extrusion

In this study, a Thermo Prism TSE 16 TC co-rotating twin screw extruder was used for the preparation of the blends and composites. Twin-screw operates according to the “starve-feeding” principle, which means that the elements of screw are not fully filled through the whole screw. This is why the shear rate differs in each region depending on the fill ratio of the screw elements. The specifications of the extruder are given in Table 3.5.

Table 3.5 Specifications of the Twin Screw Extruder

PROPERTY	
Model	Thermo Prism TSE 16 TC
Type	Twin Screw
Screw Type	Corotating
Twin Bore Diameter	16 mm
Screw Diameter	15.6 mm
Maximum Screw Speed	500 rpm
Barrel Length	384 mm (24 D)
Die Length	16 mm (1 D)
Maximum Torque	12 Nm

Temperatures were adjusted using the temperature controllers on the control panel. The extrusion temperature profile was: 190-250-275-275-280ºC and the feed rate was constant at 10 g/min. Three different screw speeds (60, 120, and 180 rpm) were used throughout the experiments. A photograph of the twin screw extruder for melt blending is shown in Figure 3.5.

Figure 3.5 Photograph of the twin screw extruder for melt blending

3.2.2 Drawing

Drawing was performed by using a self-designed take-up device which is simply a motor-bobbin system. The experimental set-up for extrusion-drawing-injection molding operation is illustrated in Figure 3.6. The bobbin was attached to the motor and the drawing speed was adjusted by using the speed controller. Some preliminary experiments were carried out in order to determine the speed range of the device. For this purpose, PET was roughly mixed with HDPE in 20/80 wt.% and extruded and subsequently drawn at room temperature (~20ºC) at different drawing speeds starting from the

minimum (1.9 m/min) to the maximum (6.7 m/min) where the extrudate could resist without pulling out. Finally, three different drawing speeds (see in Appendix A) were determined where an increasing trend was observed on the draw ratio versus drawing speed graphs. The drawing speed values were calculated by multiplying the perimeter of the bobbin by the radial velocity of the motor.

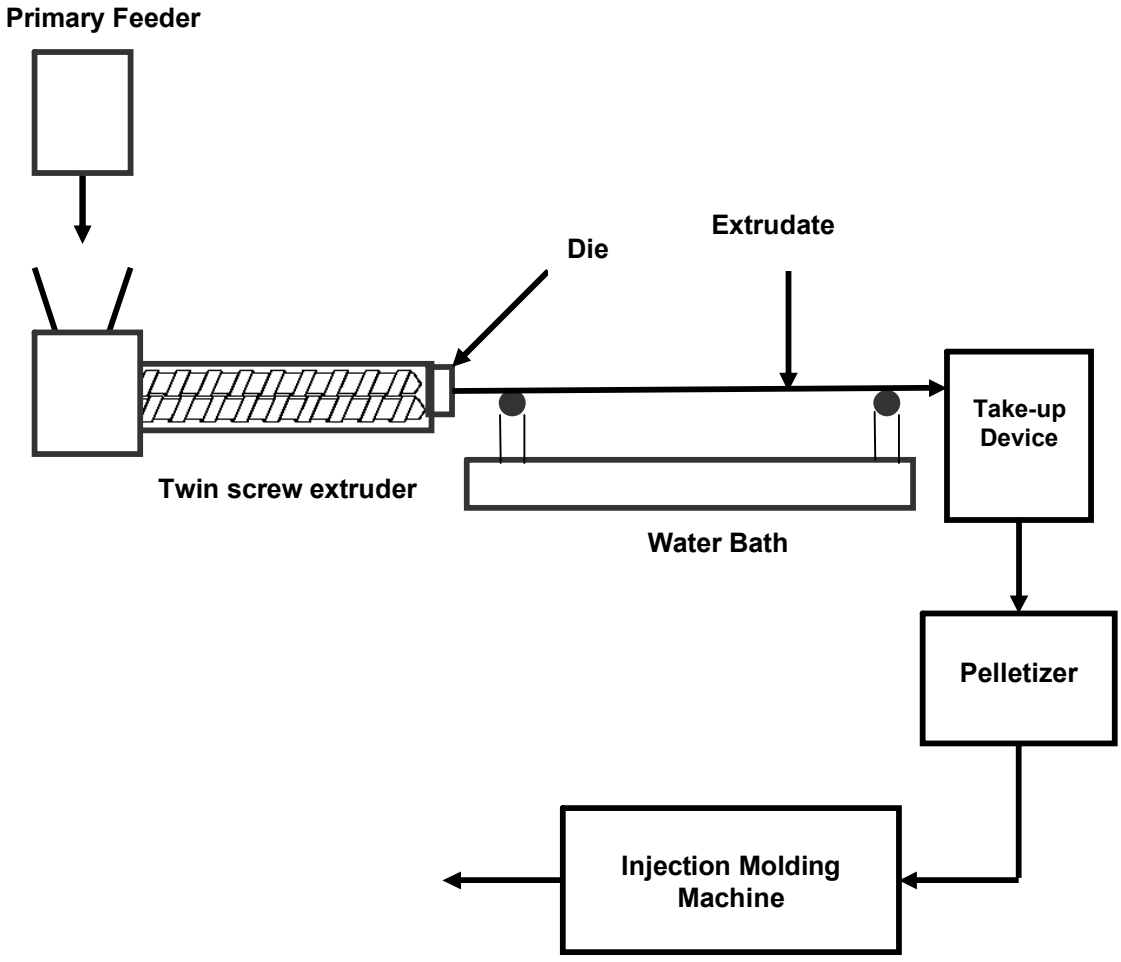

Figure 3.6 Experimental set-up for extrusion-drawing-injection molding method

.2.3. Injection Molding

A laboratory scale injection molding machine (DSM Xplore 12 mL) shown in Figure 3.7 was used to mold specimens.

!

!

Figure 3.7 Injection molding machine

Molding parameters given in Table 3.6 were kept constant throughout the process. In order to observe the effect of injection molding temperature on morphologies of the materials, two processing temperatures were selected. Low refers to the processing temperature which is far below the melting point of PET but above that of HDPE. High refers to the processing temperature which is higher than the melting temperature of PET.

Table 3.6 Molding parameters for injection molding

Injection molding parameters	Unit	Value
Mold temperature	°C	30
Melting temperature (low)	°C	205
Melting temperature (high)	°C	280
Hold time	min	4

Injection molding pressure was 15 bar and kept constant throughout the experiments.

Water was used as a coolant for the mold temperature controller, which was connected to the mold in order to maintain a constant and specific mold temperature.

3.2.4 Experimental Procedure

In this study, prior to mixing, PET and the compatibilizer pellets were dried in a vacuum oven according to the conditions given in Table 3.7. The materials were also dried before injection molding at 80°C for 4 hrs.

Table 3.7 Drying temperature and time for the materials used in the study

Material	Drying Temperature, °C	Duration, hr
PET	120	12
HDPE	60	4
E-nBA-GMA	40	4
E-MA	40	4

Some preliminary experiments were carried out in order to determine the appropriate PET/HDPE composition, extrusion conditions and injection molding parameters. Four different PET/HDPE compositions (5, 10, 15 and 20 wt% PET) were studied at the beginning and according to the morphological analysis results, a constant composition, 20%PET-80%HDPE was chosen and focused on throughout the study. Processing temperatures from hopper to die were: 190-250-275-275-280ºC as shown in Figure 3.8. Four different sets were performed during experimental studies. In the first set, MFCs based on PET/HDPE were prepared. The dried PET pellets were mixed with HDPE pellets in a constant weight ratio of 20/80. The extrusion of the mixture was performed by using a co-rotating twin-screw extruder as mentioned earlier.

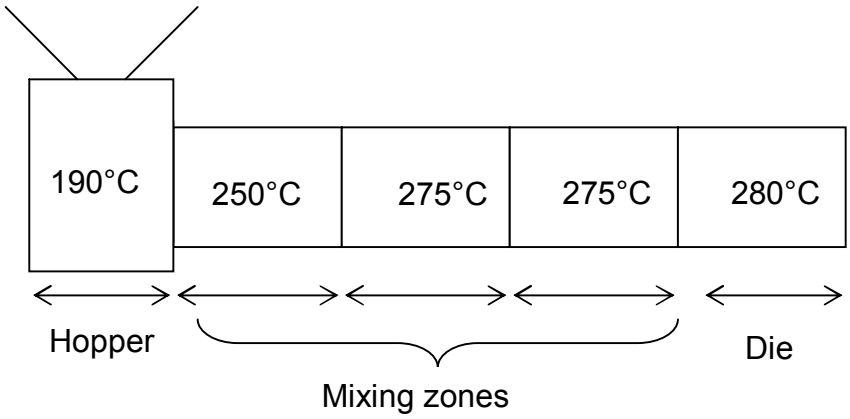

Figure 3.8 Processing temperatures of hopper, die, and mixing zones.

In the first part of the study, three different screw speeds (60, 120, and 180 rpm) were applied to observe their effects on final properties of composites. The feed rate was kept constant at 10 g/min throughout the study. The temperature profile was: 190-250-275-275-280°C from hopper to die. The

extrudate was drawn at room temperature (~20ºC) by using a self designed take-up device. Different draw ratios (diameter of the extrudate to the diameter of drawn sample at the take-up device) were obtained by adjusting the speed of the device. As a result of the preliminary experiments, three different drawing speeds (2.7, 4.7, and 6.2 m/min) were determined. After drawing was carried out, the as drawn samples were manually pelletized. The pellets obtained were dried under vacuum at 80°C for 4 hrs. Then they were injection molded into dumbbell specimens. To avoid the fracture of PET microfibers during injection molding, the processing temperature was selected as 205ºC which is far below the melting point of PET. For comparison, injection molding of the MFC was conducted at the processing temperature of PET which was selected as 280ºC. At this temperature, it could be expected that the PET microfibers would be destroyed and melted again to form spherical shape since the processing temperature was higher than the melting temperature of PET.

In the second set of experiments, as extruded PET/HDPE composites without microfibers were prepared for comparison purposes. First, the mixture of PET and HDPE was melt blended in a twin-screw extruder with the same temperature profile as in the first set of experiments. The blends were extruded and no drawing was applied. Subsequently the extrudate was pelletized and dried under vacuum at 80°C for 4 hrs before injection molding. The molding temperature was selected as 205ºC which is the processing temperature of HDPE.

In the third set, in order to produce MFCs, the dried PET pellets were mixed with HDPE and compatibilizer pellets, the MFCs of PET/HDPE/E-nBA-GMA and PET/HDPE/E-MA were prepared in the following weight ratios: 20/79/1; 20/75/5 and 20/70/10. After the morphological and mechanical analysis results of the first two sets of experiments, 60 rpm screw speed and 6.2 m/min drawing speed were selected as constant parameters for the third and

fourth sets. The same process temperature profile was used through the third set extrusion. After drawing the extrudate at room temperature (~20ºC) with 6.2 m/min drawing speed, the as-drawn extrudate was manually pelletized, dried and injection molded at the same conditions of the second set.

In the fourth set, common PET/HDPE/compatibilizer composites without microfibers were prepared for comparison. For this aim, the dried PET pellets were mixed with HDPE and compatibilizer pellets in the following weight ratios: 20/79/1; 20/75/5 and 20/70/10. The same extrusion, drying and injection molding conditions were applied as in the second set of experiment.

For comparison purposes, pure HDPE and PET were also extruded at the same temperature profile. No drawing was applied. The extrudate was pelletized and injection molded at the same conditions as in the second set. The flowchart of general experimental procedure is shown in Figure 3.9.

3.3 Characterization Experiments

In order to observe the effects of screw speed, drawing speed, high and low injection molding temperature, and compatibilizer type/content on the properties of as extruded, as drawn and injection molded MFC samples, the materials were characterized in terms of morphologies and mechanical and thermal properties.

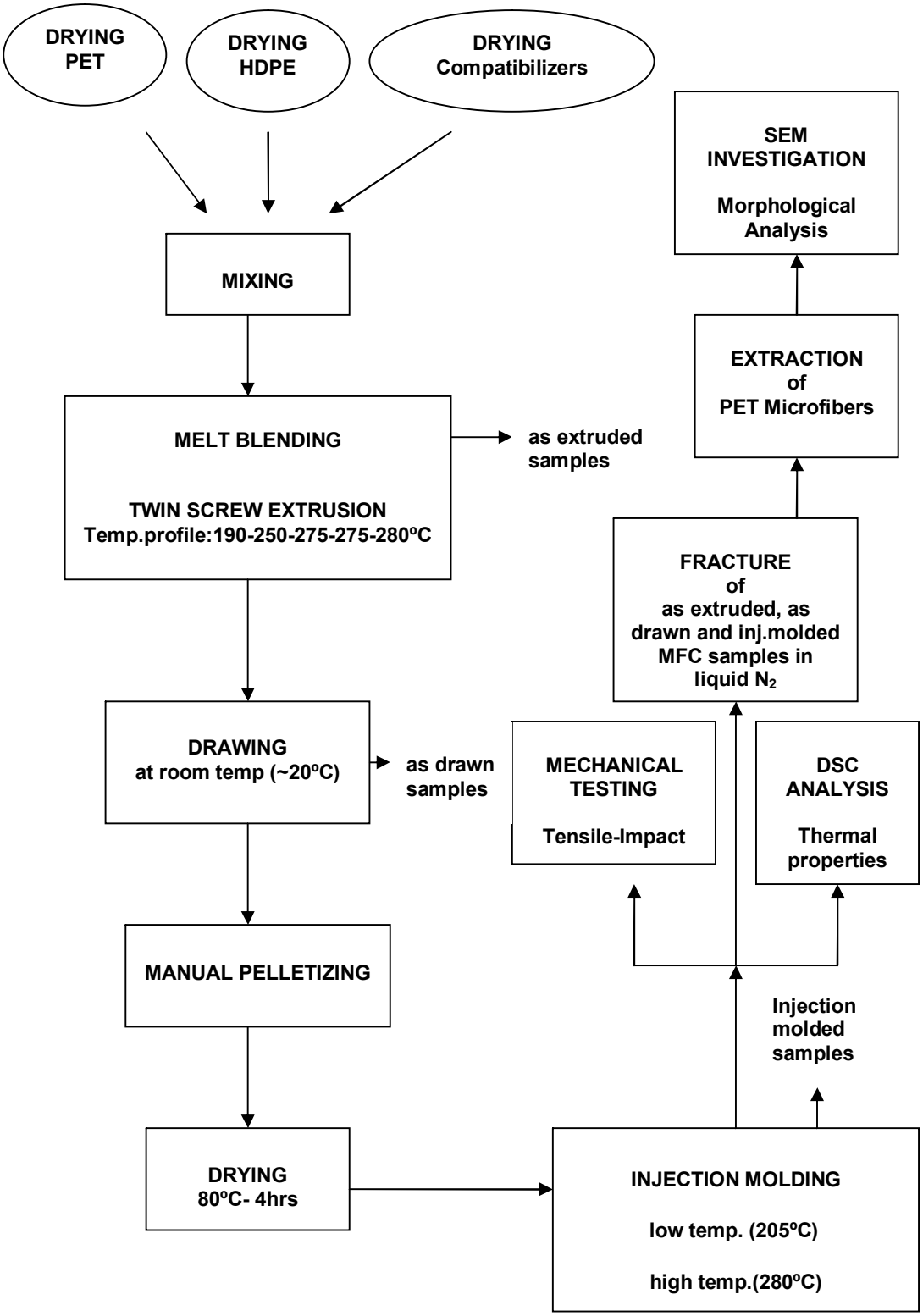

Figure 3.9 Flowchart of general experimental procedure

3.3.1 Morphological Analyses

3.3.1.1 Scanning Electron Microscopy (SEM) Analyses

In morphology observation, samples from the various processing stages (as extruded, as drawn and injection molded) were used. The materials were frozen in liquid nitrogen, then quickly taken out and broken into two pieces by using a hammer, to make surfaces for SEM observation. In order to clearly examine the morphology of the reinforcing PET microfibers, some samples were immersed in hot xylene (110ºC) for 30 mins to etch away HDPE matrix.

The fracture surfaces of the samples were investigated by using a low voltage SEM (JEOL JSM-6400). The surfaces were coated with a thin layer of gold to prevent arcing.

Several micrographs of fracture surfaces were taken for samples at various magnifications. The diameters of the PET microfibers within the as drawn samples and the diameters of the PET spheres and ellipsoids within the as extruded samples were measured from these micrographs. Several micrographs were obtained for the samples and approximately 20 PET microfibers were taken into account for diameter measurements. The diameters were measured manually by using vernier calipers.

3.3.2 Mechanical Tests

3.3.2.1 Tensile Tests

All tensile tests were performed at room temperature. After stress versus strain diagrams of the measurements were obtained, tensile strength, tensile modulus and elongation at break values were calculated. For each sample,

average results of at least five measurements with standard deviations were reported and the error bars were drawn according to the standard deviations. Tensile tests were performed by using a Lloyd 5K Universal Testing Machine according to ISO 527 standard on the samples with dimensions specified and illustrated in Figure 3.10 and Table 3.8, respectively. The crosshead speed of the machine was set at the rate of 2 mm/min, which was calculated considering the specimen gauge length of 20 mm and strain rate of 0.1 min^{-1}. The specimen was pulled at this constant rate of extension until the center of the specimen fails. Tensile strain was recorded as a function of the stress required to stretch the sample.

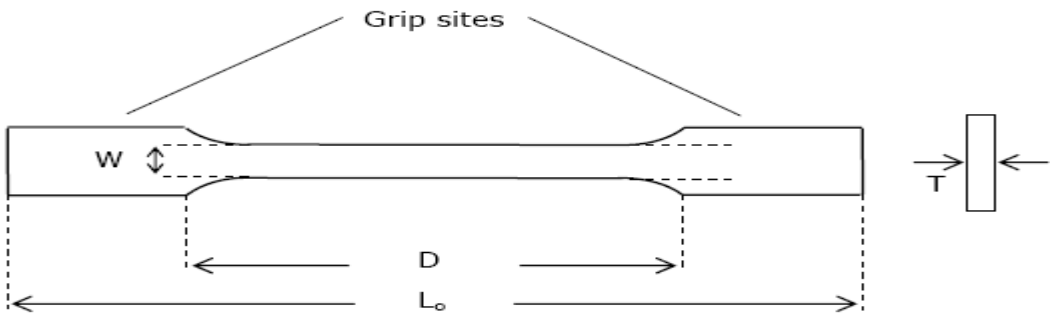

Figure 3.10 Tensile Test Specimen

Table 3.8 Dimensions of tensile test specimen

Symbol, Term	Dimension (mm)
D - distance between grips	50
L_0- overall length	75
T- Thickness	2
W- width of narrow section	4
Gauge length	20

3.3.2.2 Impact Tests

Charpy impact tests were carried out by using a CEAST RESIL IMPACTOR, based on ISO 179. Its photograph is shown in Figure 3.11.

Samples with dimensions 80 x 10 x 4 mm were used and a 2 mm notch was formed on one side of the specimen. Dimensions of the impact test sample are illustrated in Figure 3.12. During the test, the specimen was located in a position in which the 7.5 J pendulum strikes the specimen from the unnotched side.

Figure 3.11 Impact Testing Machine

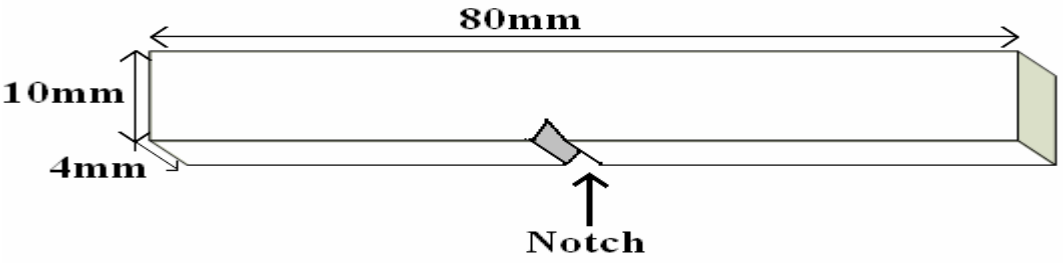

Figure 3.12 Impact test specimen

3.3.3 Thermal Analyses

3.3.3.1 Differential Scanning Calorimetry (DSC) Analyses

DSC measurements on the samples were performed by using a General V4.1.C DuPont 2000. 10 mg of sample was cut from the center of the as extruded, as drawn or injection molded materials. Two heating runs were performed during DSC Analyses. They were first heated at a rate of 10ºC/min to a temperature of 300ºC (1st run), then cooled to 30ºC and re-heated to 300ºC (2nd run) under nitrogen atmosphere. Melting temperatures (T_m) and melting enthalpy (ΔH_m) were recorded. The degree of crystallinity, X_c, of each polymer component was calculated from the ratio of the observed melting enthalpy (ΔH_m) on the 1st run to the melting enthalpy of 100% crystalline polymer (ΔH^0_m) which are 138 J/g for PET [43], and 293 J/g for HDPE [44].

CHAPTER 4

RESULTS AND DISCUSSION

4.1 Morphological Analyses

4.1.1 Scanning Electron Microscopy Observations

In order to observe the morphologies of as extruded, as drawn and injection molded MFC samples, SEM analyses were performed.

Figure 4.1 shows the fracture surface of PET/HDPE (20/80 wt.%) as extruded sample processed at 60 rpm. Drawing was not applied to this material. It can clearly be seen that the extrusion of the PET/HDPE resulted in an incompatible blend morphology. Dispersed PET phase is in the shape of spheres or ellipsoids which are distributed in HDPE matrix. The average PET domain size is determined as approximately 4.5 μm. Some voids, so called cavitation, are seen on the observed surface; this is because some PET particles responsible for these voids are left on the other part of the fracture surface. As expected, this cavitation of particles supports the lack of interfacial reactions.

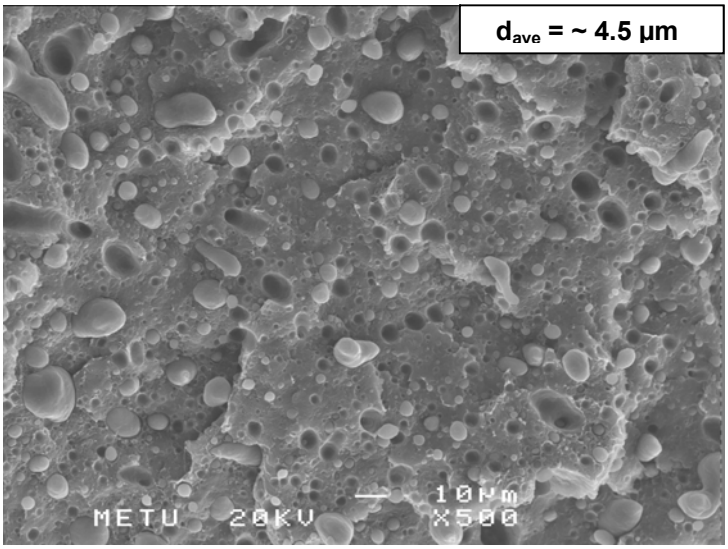

Figure 4.1 SEM micrograph of PET/HDPE as extruded sample processed at 60 rpm without drawing.

4.1.1.1 Effect of drawing speed and screw speed on the morphologies of as-drawn and injection molded MFC samples

During extrusion of PET/HDPE (20/80 wt%), under shear and drawing conditions, the dispersed PET phase domains as seen in Figure 4.1 deform and orient along the flowing direction. Initially, they are present in the form of spherical particles with larger size. Then, these spherical particles break up, deform and generate smaller domains. With the increase in screw speed (resulting in high shear) and drawing speed, the spherical or ellipsoidal particles deform into fibers and fiberlike structures as seen in Figures 4.2 and 4.3.

To observe clearly the morphology of the PET microfibers, the HDPE matrix was etched away by hot xylene.

Figure 4.2 shows the SEM micrographs of the PET/HDPE as drawn samples processed at 60 rpm with drawing speed of 2.7 m/min, 4.7 m/min and 6.2 m/min, respectively.

As seen from the SEM micrographs in Figure 4.2, drawing of the extrudate results in the formation of PET microfibers. Apparently in Figure 4.2c, well-defined microfibers were formed. The size and amount of the PET microfiber are non-uniform through the thickness of the extrudate and are also affected by the drawing speed. The minimum, maximum and average PET Microfiber of the samples at different screw speeds, drawing speeds and compatibilizer type/content are shown in Table B. As the drawing speed increases, the microfiber diameter decreases from 4.3 μm to 1.3 μm and a more fibrous morphology is observed. The diameter of the microfibers has an important consequence for the mechanical performance of MFC. Because of the increase of the aspect ratio of the reinforcing microfibers, an improvement in mechanical properties can be expected [45, 46]. Unfortunately, since there exists hardly any microfiber within the viewfield, it is not easy to get accurate aspect ratio of the microfibers, though it is a crucial factor to characterize the fibrous structure. But in spite of this, when the SEM micrographs of the samples drawn with 2.7 m/min (Figure 4.2 a) and 6.2 m/min (Figure 4.2 c) are taken into consideration, due to the decrease in microfiber diameter, an increase in mechanical properties is observed as will be seen in further parts of the study.

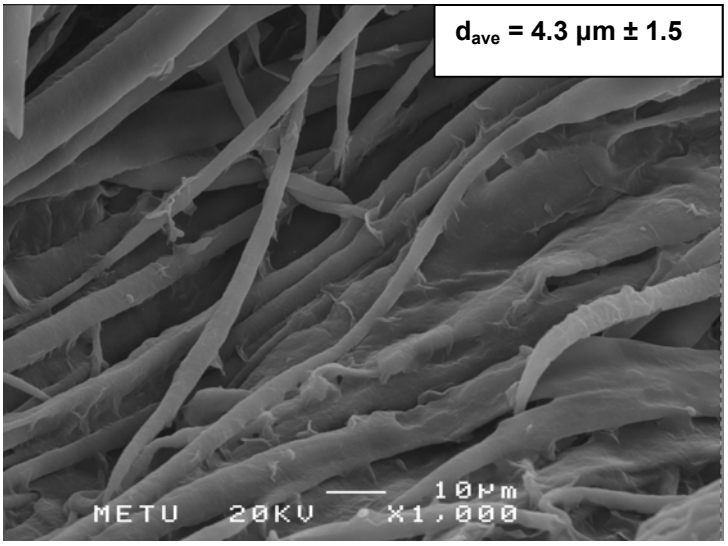

(a) 2.7 m/min (X1000)

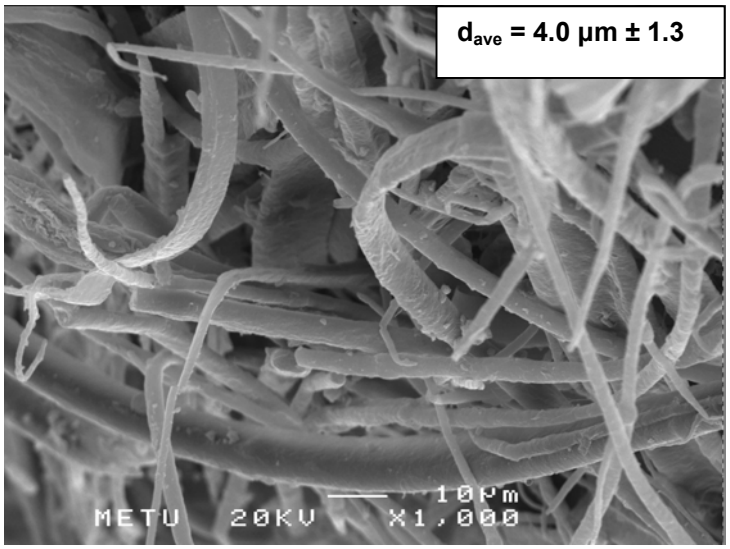

(b) 4.7 m/min (X1000)

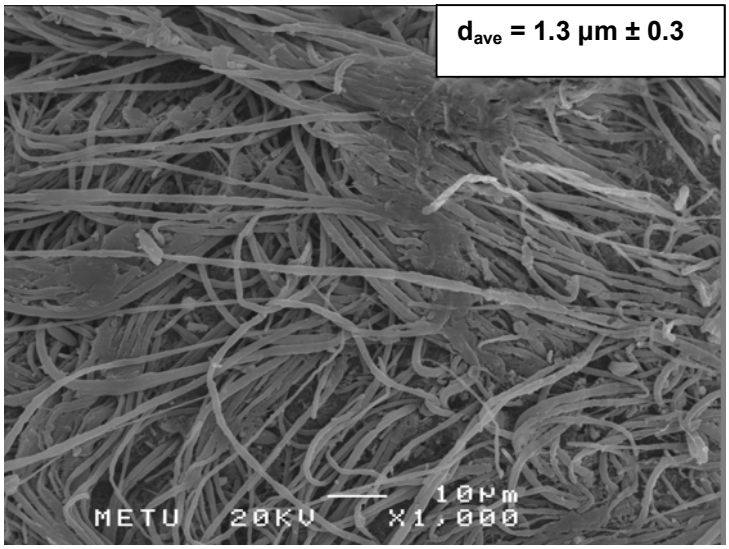

(c) 6.2 m/min (X1000)

Figure 4.2 SEM micrographs of as drawn PET/HDPE blend processed at 60 rpm and drawn with (a) 2.7 m/min (b) 4.7 m/min (c) 6.2 m/min after extraction of HDPE fraction with hot xylene.

Figure 4.3 shows the SEM micrographs of the PET/HDPE as drawn samples processed at 120 rpm and drawn at 2.7 m/min, 4.7 m/min and 6.2 m/min, respectively.

As the screw speed increases from 60 rpm (Figure 4.2b) to 120 rpm (Figure 4.3b), the domain size of the dispersed PET phase decreases as a result of a possible increase in shear and the promoted dispersive mixing. It can be observed from these figures that the diameter and amount of PET microfibers decrease with increasing screw speed.

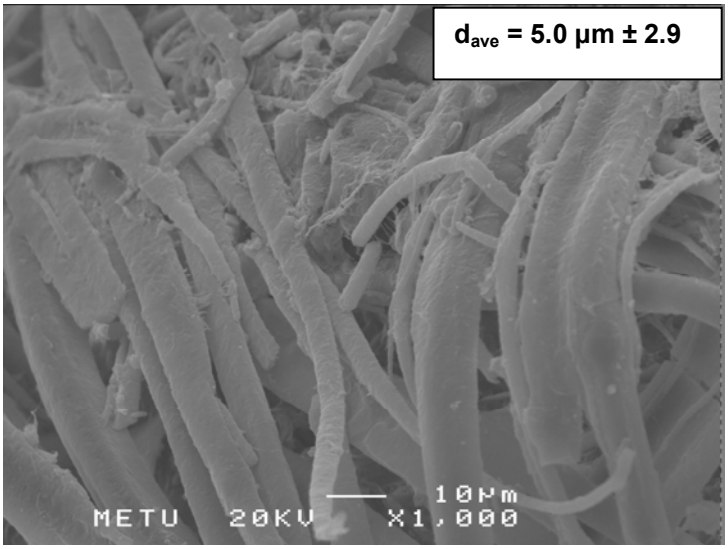

(a) 2.7 m/min (X1000)

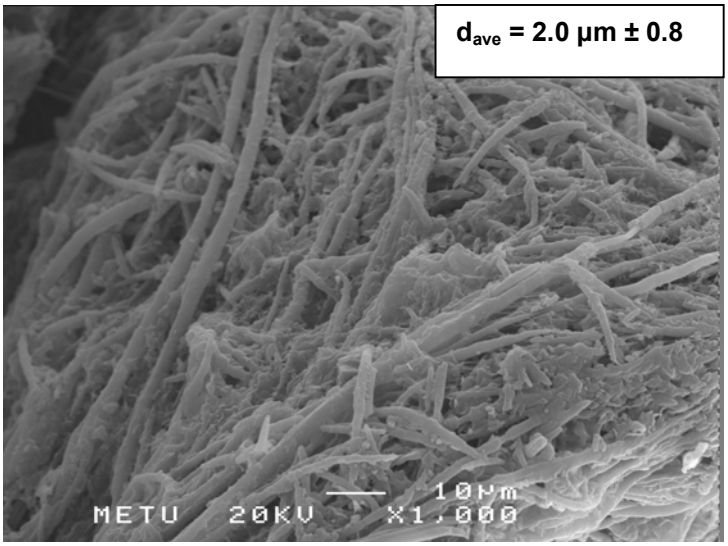

(b) 4.7 m/min (X1000)

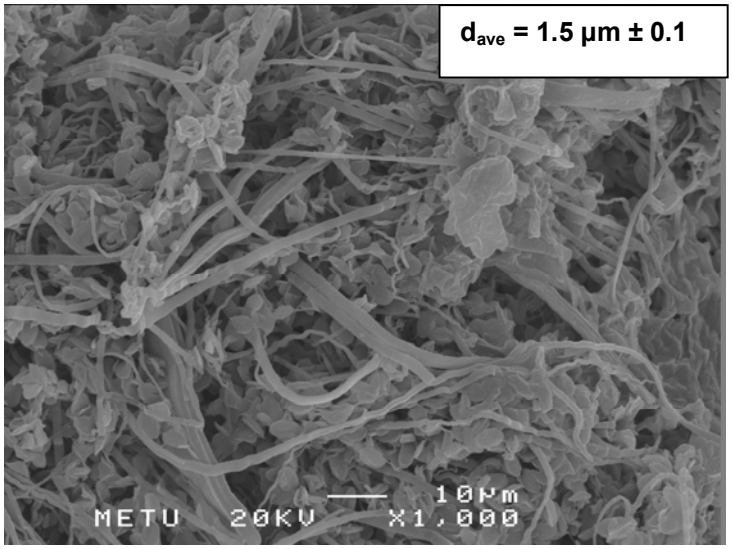

(c) 6.2 m/min (X1000)

Figure 4.3 SEM micrographs of the PET/HDPE as drawn samples processed at 120 rpm at (a) 2.7 m/min, (b) 4.7 m/min and (c) 6.2 m/min after extraction of HDPE fraction with xylene.

Figure 4.4 shows the SEM micrographs of the PET/HDPE as drawn samples processed at 180 rpm and with drawing speeds of 2.7 m/min, 4.7 m/min and 6.2 m/min, respectively. When Figures 4.2, 4.3 and 4.4 are compared, it is observed that the domain size of the dispersed PET phase decreases with an increasing screw speed. In some micrographs, non-fibrillar structures are also observed together with the microfibers. Etching treatment is performed at ~110ºC. At this temperature HDPE is about to reach melting temperature which is around 140ºC. The HDPE phase dissolves in the presence of xylene and at the same time some of the HDPE leaves the structure and attaches to the other parts of the structure. As a result of these physical changes, these non-fibrillar structures may be observed. It can also be

concluded that they may be formed as a result of the incomplete solvent (xylene) etching which block the microfibers in the system generated during drawing. The presence of these non-observable microfibers is also supported with the mechanical tests which can be seen in further parts of the thesis.

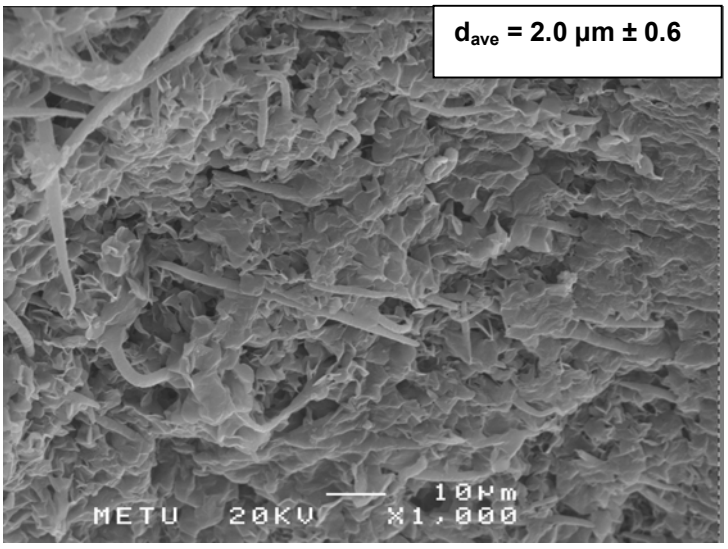

(a) 2.7 m/min (X1000)

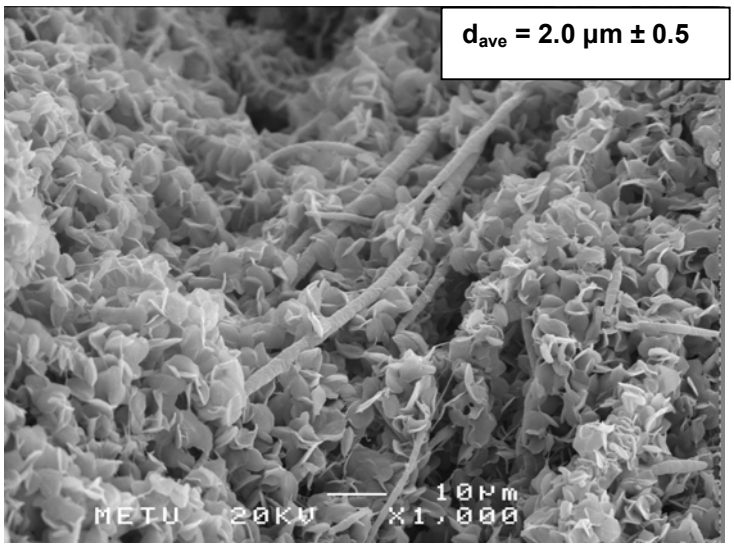

(b) 4.7 m/min (X1000)

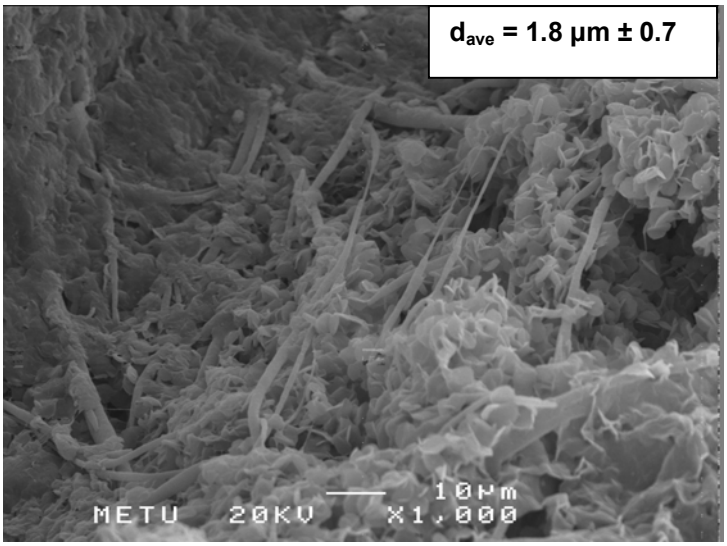

(c) 6.2 m/min (X1000)

Figure 4.4 SEM micrographs of the PET/HDPE as drawn samples processed at 180 rpm at (a) 2.7 m/min, (b) 4.7 m/min and (c) 6.2 m/min after extraction of HDPE fraction with hot xylene.

When Figures 4.2, 4.3 and 4.4 are compared, an important conclusion can be drawn: the most fibrous morphology is observed in the microfibers processed at 60 rpm and drawn with 6.2 m/min drawing speed. For the samples processed at 60 rpm, the domain size of the dispersed PET particles is larger when compared to the ones processed at 120 and 180 rpm. Because the shear stress applied by the rotating screws is lower at 60 rpm, which means that the breakage of dispersed PET particles into smaller ones does not take place as in the case of higher screw speeds (120 and 180 rpm). This observation is important for the mechanical behavior of the MFCs. As can be seen from the mechanical test results in further sections (Figures 4.14 and 4.15), the tensile strength and tensile modulus values of the samples processed at 60 rpm and drawn with 6.2 m/min are the highest among the others.

In the isotropization step of MFC preparation, melting of the lower melting component (HDPE) and its transformation into isotropic matrix reinforced with the microfibers of the higher melting component (PET) take place during injection molding [2]. Figure 4.5 shows the SEM micrograph of injection molded sample processed at 60 rpm and drawn with 6.2 m/min and molded at 205ºC which is the processing temperature of HDPE. It can clearly be observed that PET microfibers preserved their fibrillar structure but they are not aligned in the initial drawing direction, they appear to be dispersed randomly. The maximum processing temperature was set up to 205ºC, but under high shear and high pressure conditions during injection molding, the melt temperature could be even higher than the set temperature. Due to the velocity pattern in the barrel, it can be assumed that the PET microfibers do not maintain their straight shape, but rather tend to shrink and coil to some degree. This may be the reason why a complete orientation can not be observed.

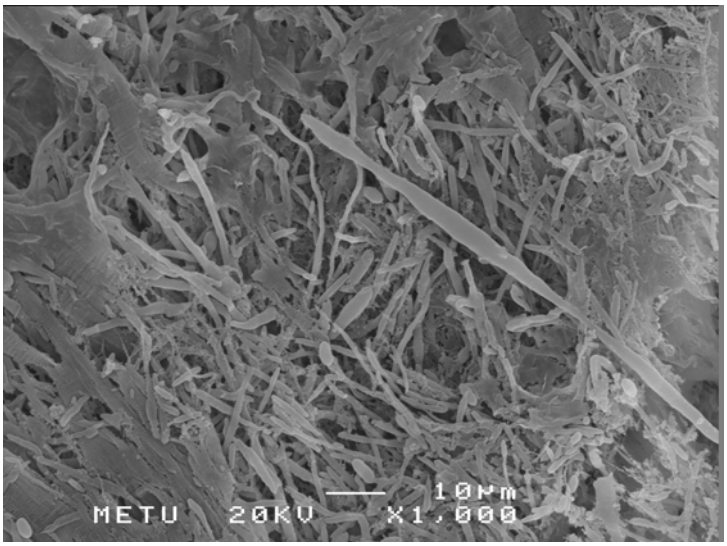

Figure 4.5 SEM micrograph of fracture surface of injection molded (at 205ºC) MFC sample processed at 60 rpm and drawn with 6.2 m/min after extraction of HDPE fraction with hot xylene.

The morphology of the injection molded samples processed at different screw speeds can also be observed in Figure 4.6. In these micrographs, the HDPE fraction is not extracted for better observation. The difference between etched (Figure 4.5) and unetched (Figure 4.6) systems is that, the fiber ends are more clearly seen. It can be said that, most of the microfibers are broken during the fracture, and only their ends can be seen. Some of them are pulled out (debonded) from HDPE matrix. Therefore, some voids are also observed. This can be explained by the fact that the PET/HDPE interface is weak because of the incompatibility of the two polymers.

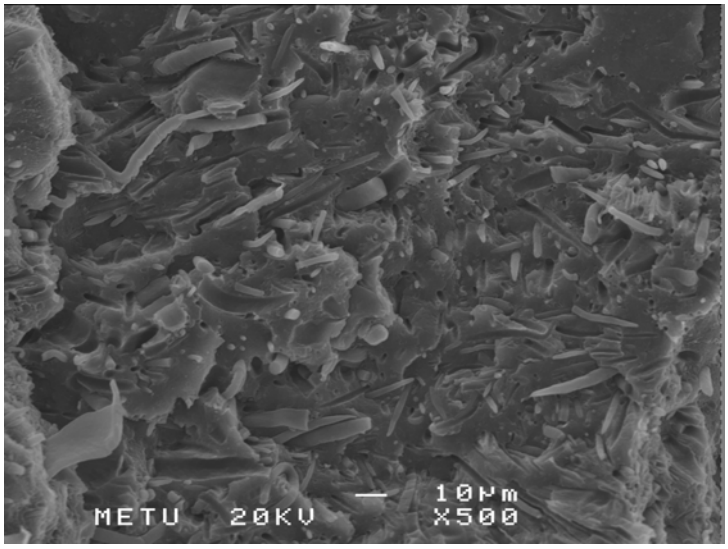

(a) 60 rpm – 6.2 m/min (X500)

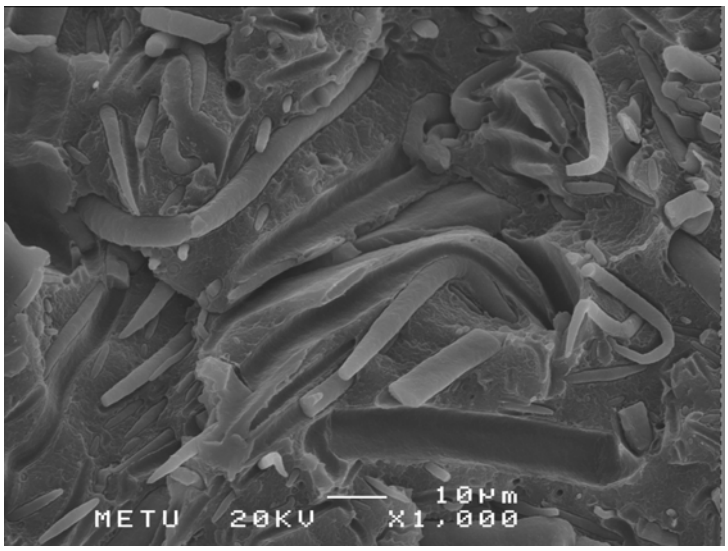

(a) 60 rpm – 6.2 m/min (X1000)

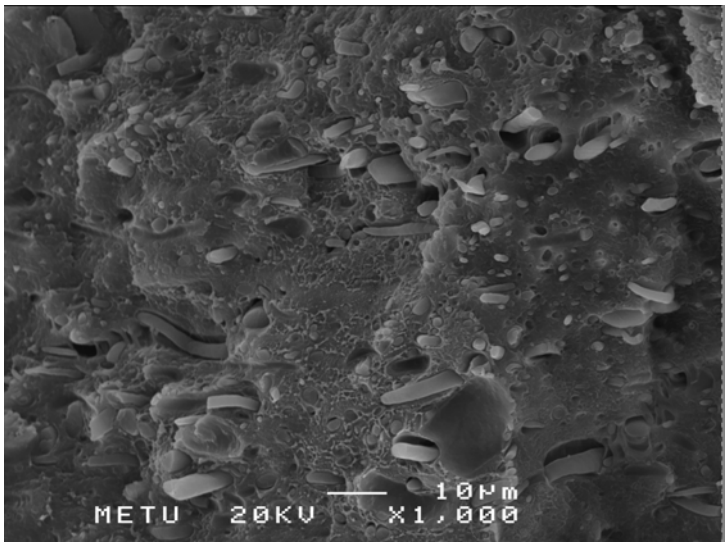

(b) 120 rpm – 6.2 m/min (x1000)

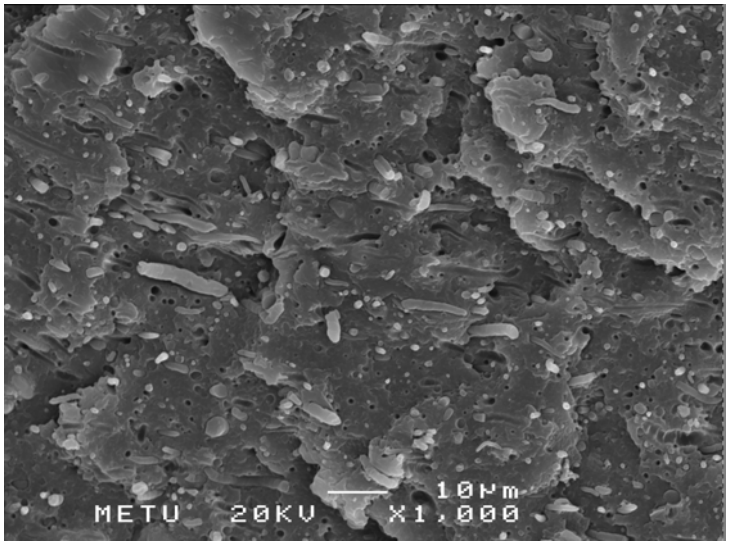

(c) 180 rpm – 6.2 m/min (x1000)

Figure 4.6 SEM micrographs of fracture surfaces of injection molded MFC samples processed at (a) 60 rpm (b) 120 rpm (c) 180 rpm and drawn with 6.2 m/min (No extraction of HDPE fraction with hot xylene).

4.1.1.2 Effect of injection molding temperature on the morphology of MFC samples

To study the effect of injection molding temperature, the MFC sapmle is injection molded at 205ºC and 280ºC. A low temperature of 205ºC is used in order to keep microfibers from being destroyed through injection molding processing. The effect of injection molding temperature on the morphology of MFC is presented in Figures 4.6 and 4.7. The samples are fractured in liquid nitrogen and this time the surfaces are not etched for clear observation. Obviously, low temperature molding (205ºC) maintains the PET microfibers as seen in Figure 4.6a. However, high temperature injection molding (at processing temperature of PET, 280ºC) destroys the microfibers. They are melted again and formed spherical particles as shown in Figure 4.7.

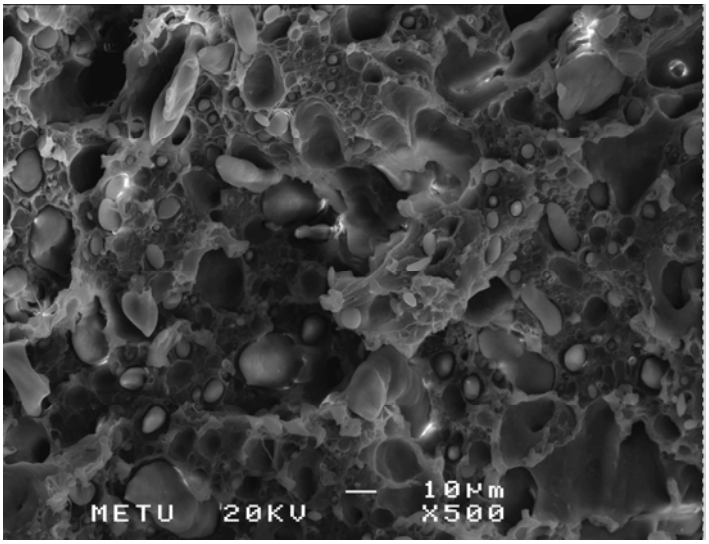

Figure 4.7 SEM micrograph of injection molded MFC sample processed at 60 rpm and drawn with 6.2 m/min and injection molded at 280ºC. HDPE phase was not extracted by hot xylene.

4.1.1.3 Effect of compatibilizer type and content on the morphologies of as extruded, as drawn and injection molded MFC samples

All the MFC samples which are as extruded, as drawn and injection molded were processed at 60 rpm and drawn with a speed of 6.2 m/min for the compatibilization experiments.

4.1.1.3.a Effect of E-nBA-GMA content on the morphologies of as extruded, as drawn and injection molded MFC samples

Figure 4.8 illustrates the micrographs of as extruded PET/HDPE samples compatibilized with different amounts of E-nBA-GMA (C_1). As mentioned earlier, C_1, is a reactive functional terpolymer. When 1% C_1 is initially added, the average particle diameter is reduced from ~ 4.5 μm (Figure 4.1) to ~ 4.0

μm (Figure 4.8a). The reason for this decrease may be due to the possible reactions that may occur between hydroxyl and carboxyl functional groups of PET and epoxy functional group of C_1. When its content increases to 5% and to 10%, the surface becomes more homogeneous. The possibility of the reactions increases with the increasing amount of the compatibilizer, so the surface becomes finely dispersed. It is even impossible to obtain an accurate average particle diameter from the observed magnifications.

When Figure 4.1 is compared with Figures 4.8b and 4.8c, the effect of E-nBA-GMA becomes more apparent. In Figure 4.1, the dispersed PET phase is in the shape of spheres and ellipsoids which are distributed in the HDPE matrix whereas in Figures 4.8b and 4.8c, the PET phase and HDPE tend to be miscible phases, in the presence of 5 and 10% compatibilizer.

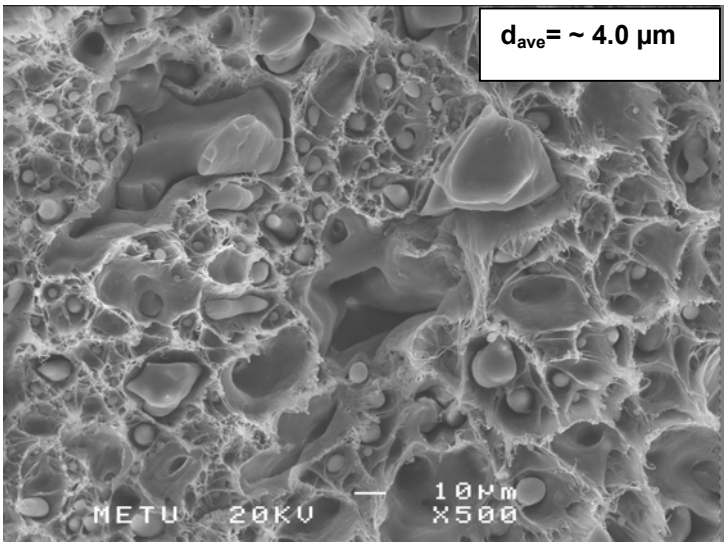

(a) 1% E-nBA-GMA

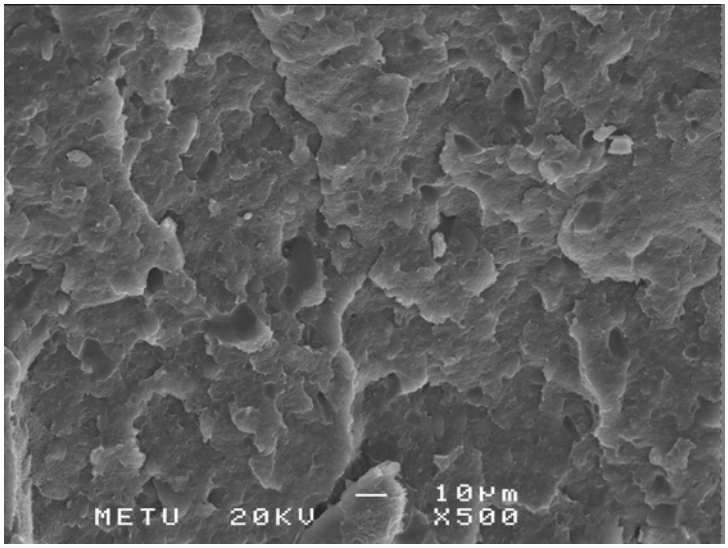

(b) 5% E-nBA-GMA

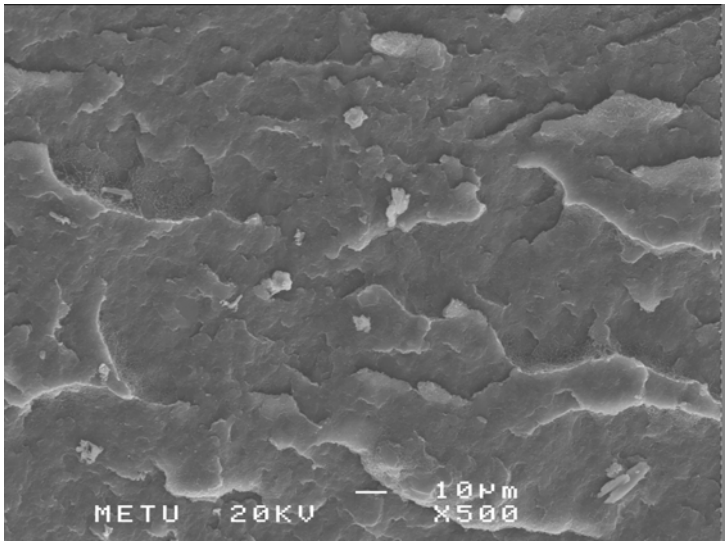

(c) 10% E-nBA-GMA

Figure 4.8 SEM micrographs of fracture surfaces of as extruded (a) PET/HDPE/C_1 (20/79/1), (b) PET/HDPE/C_1 (20/75/5), (c) PET/HDPE/C_1 (20/70/10) (C_1 refers to E-nBA-GMA)

Figure 4.9 shows the micrographs of as drawn samples compatibilized with different contents of C_1. When Figures 4.2 and 4.9 are compared, it can be seen that, with the addition of C_1, the average PET microfiber diameter of the samples processed at 60 rpm and drawn with 6.2 m/min decreased from ~ 1.3 μm to ~ 0.9 μm. This is the possible result of the reactions taking place between PET and the compatibilizer. It is also observed that, the microfibers, which are obtained in the blends without compatibilizer, are longer than those obtained in the blends with C_1. This can be explained with the way of formation of microfibers. Prior to drawing, PET phase appears to be spherical or ellipsoidal particles (droplets) in HDPE matrix. With the process of drawing, the matrix HDPE melt is elongated and simultaneously transfers stress to the droplets. Under such stress, these droplets are also elongated, they become thinner but longer. When they begin to contact each other, due to the coalescence, they build up microfibers comprising many starting spheres. In the blends with C_1, this process is impossible because with the influence of E-nBA-GMA, a thin shell is formed around each PET sphere which does not allow their coalescence during drawing [11].

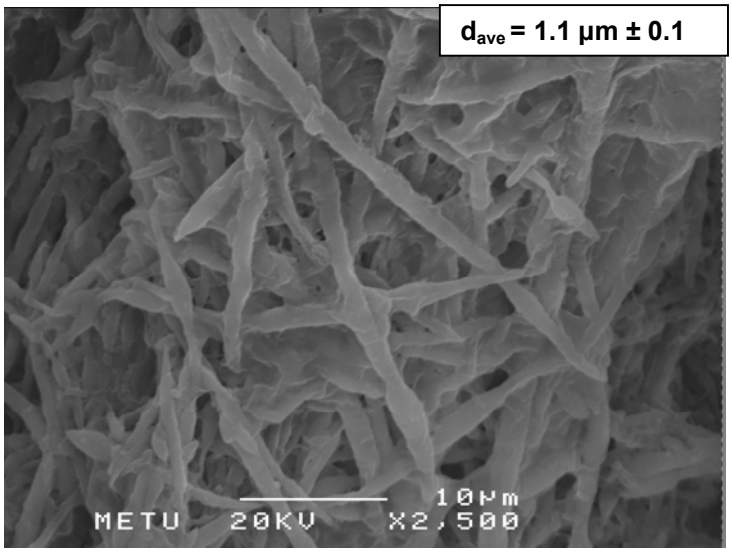

(a) 1% E-nBA-GMA

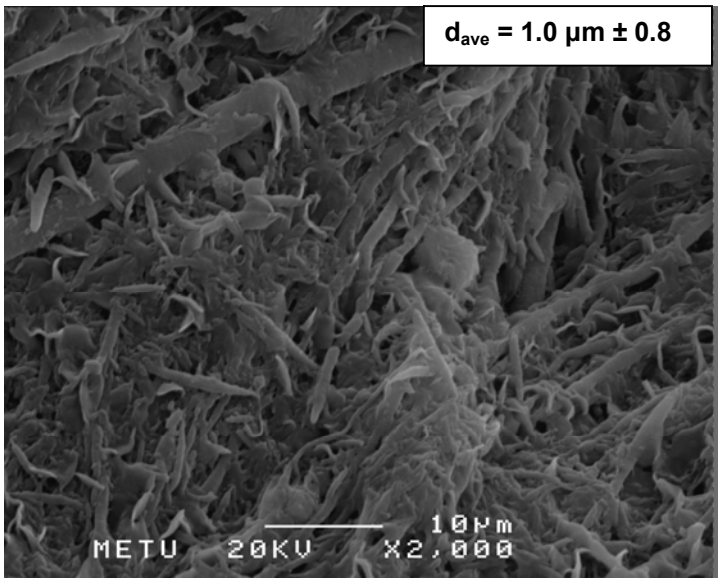

(b) 5% E-nBA-GMA

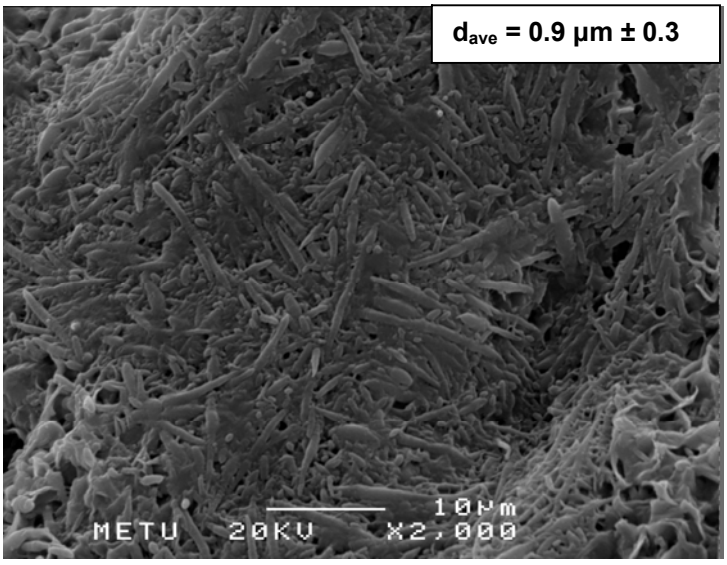

(c) 10% E-nBA-GMA

Figure 4.9 SEM micrographs of fracture surfaces of as drawn samples after extraction of HDPE fraction with hot xylene (a) PET/HDPE/C_1 (20/79/1), (b) PET/HDPE/C_1 (20/75/5), (c) PET/HDPE/C_1 (20/70/10) (C_1 refers to E-nBA-GMA)

Figure 4.10 represents the micrographs of injection molded samples compatibilized with 1% C_1. The fibrillar morphology is preserved together with a non-fibrillar lamellar structure which is the possible result of the incomplete solvent etching as mentioned earlier. There are possibly more microfibers in the system, but these non-fibrillar formations do not allow to be observed clearly. The maximum processing temperature is set to 205ºC, but under shear and high pressure conditions during injection molding, the melt temperature can be even higher than 205ºC. So, PET microfibers do not maintain their straight shape, but rather tend to coil as seen in the figure.

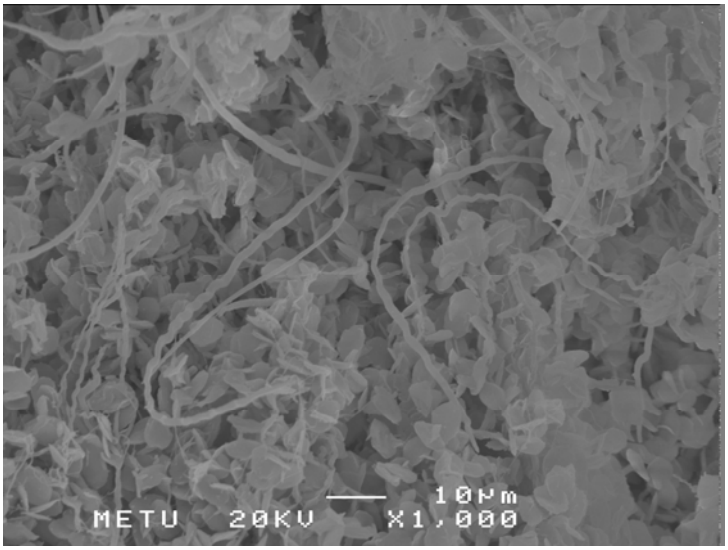

Figure 4.10 SEM micrograph of injection molded PET/HDPE/C_1 (20/79/1) MFC sample after extraction of the HDPE fraction with hot xylene. (C_1 refers to E-nBA-GMA)

4.1.1.3.b Effect of E-MA content on the morphologies of as extruded, as drawn and injection molded MFC samples

Figure 4.11 shows the fracture surfaces of as extruded samples compatibilized with different contents of E-MA (C_2). These micrographs show dispersion of PET spheres and ellipsoids in the HDPE matrix. The average particle diameter of the as extruded samples compatibilized with C_2 is similar to those without compatibilizer. With the initial addition of C_2, the average particle diameter is ~ 4.5 μm and with the further addition, it decreased to ~ 4.3 μm and finally to ~ 4.1 μm at 10 % E-MA.

When the average particle diameters of the samples compatibilized with C_1 and C_2 are compared, it can be seen that, C_1 caused a higher amount of decrease. The reason is possibly caused from the difference in the type of copolymers. Since C_2 is considered to be a non-reactive copolymer compared to C_1, its compatibilization efficiency is expected to be far less than that of C_1 which is a reactive functional terpolymer. This conclusion is also supported with the mechanical test results as seen in further parts of the thesis. When Figures 4.8 and 4.11 are compared, the effect of compatibilizer type can be clearly observed. The micrographs of 4.8b and 4.8c represent single phase morphology, whereas micrographs of Figure 4.11 represent a dispersion of PET spheres and ellipsoids in the HDPE matrix.

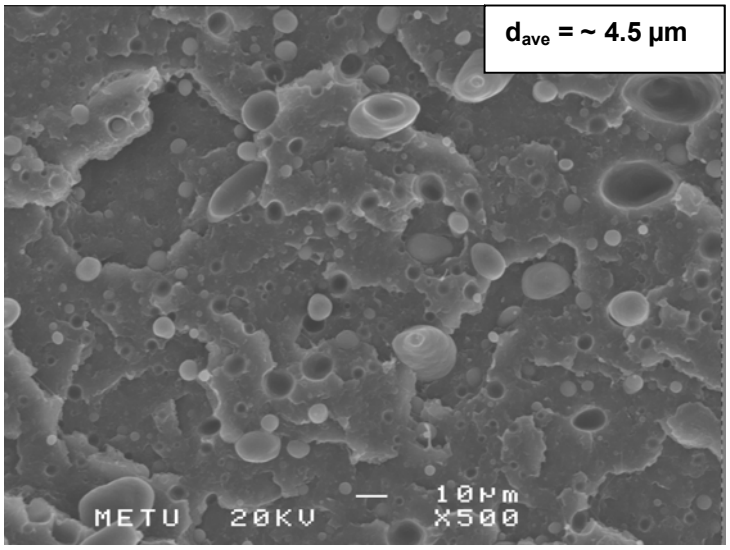

(a) 1% E-MA

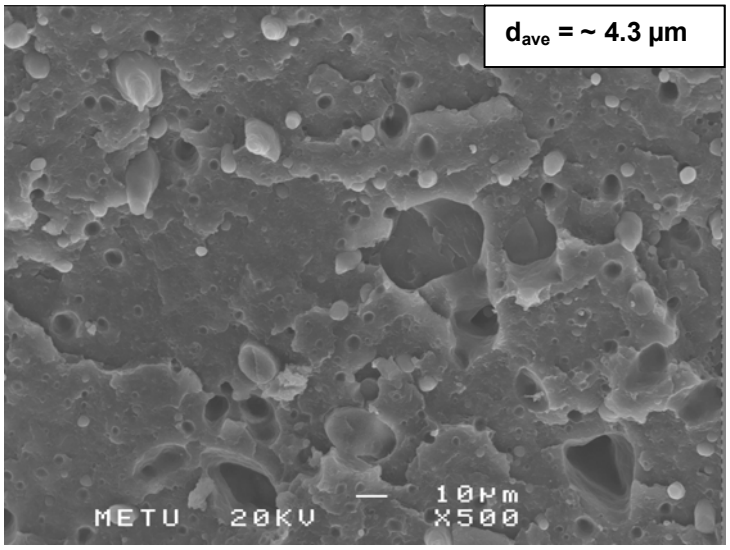

(b) 5% E-MA

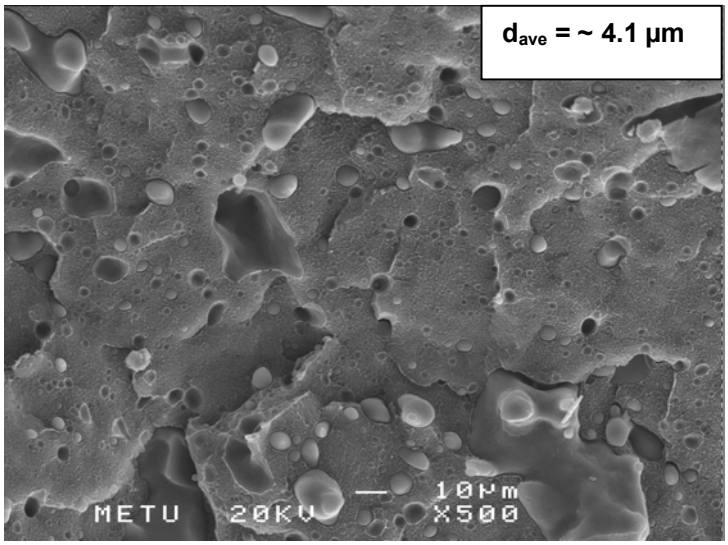

(c) 10% E-MA

Figure 4.11 SEM micrographs of fracture surfaces of as extruded (a) PET/HDPE/C_2 (20/79/1), (b) PET/HDPE/C_2 (20/75/5), (c) PET/HDPE/C_2 (20/70/10) (C_2 refers to E-MA)

Figure 4.12 illustrates the micrographs of drawn samples compatibilized with different contents of C_2. As seen from the figure, the samples compatibilized with C_2 do not possess shorter microfibers as in the case of the samples compatibilized with C_1. Since C_2 is a non-reactive polar copolymer, it is not expected for C_2 to form a thin shell around PET particles. So, with the process of drawing, the matrix HDPE melt is elongated and simultaneously transfers stress to the spherical or ellipsoidal particles (droplets). Under such stress, these droplets are also elongated, they become thinner but longer. When they begin to contact each other, due to the coalescence, they build up microfibers comprising many starting spheres.

When Figures 4.2c and 4.12 are compared, it is seen that, the average PET microfiber diameter of the PET/HDPE/E-MA samples processed at 60 rpm and drawn with 6.2 m/min, increases in comparison with the as drawn PET/HDPE systems processed and drawn at the same conditions. The dispersed PET particles in Figure 4.11 are large and have very different dimensions from few microns to about 10 μm which tend to form microfibers with larger diameter under the influence of drawing.

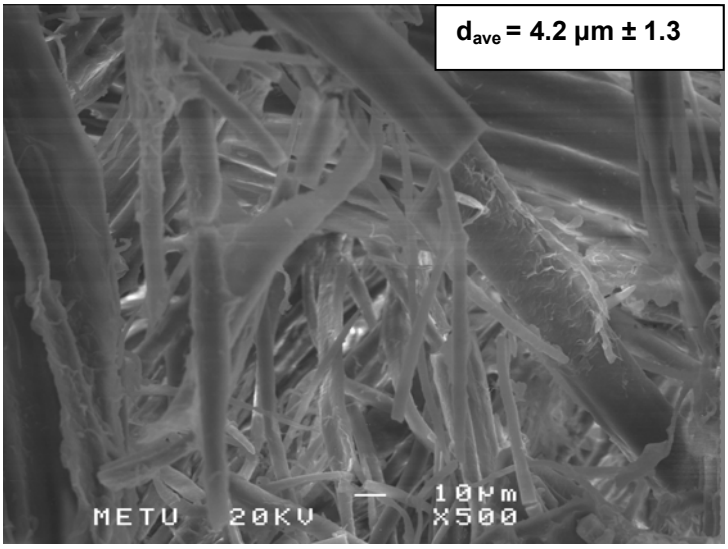

(a) 1% E-MA

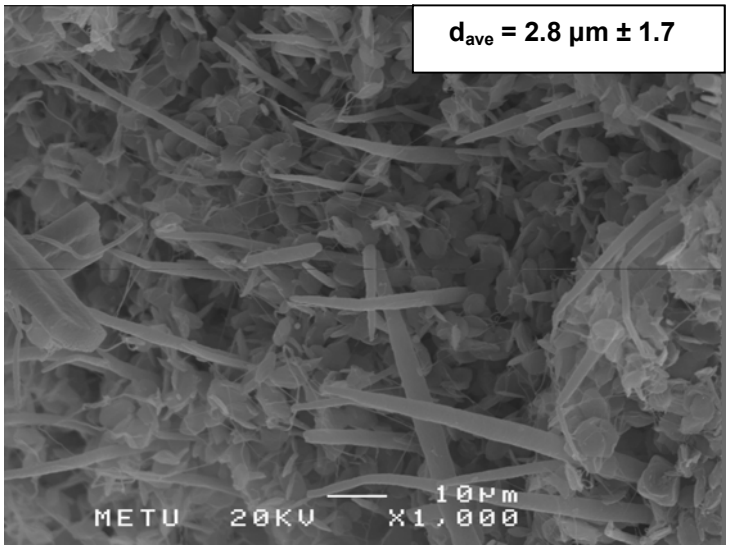

(b) 5 % E-MA

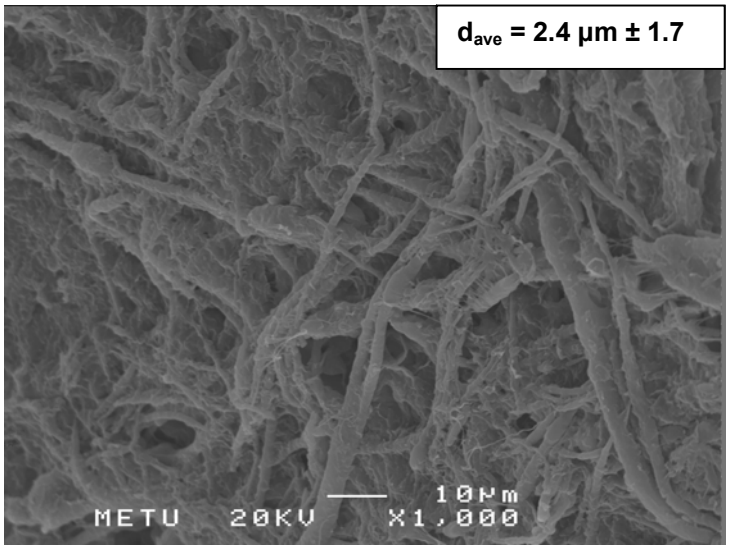

(c) 10% E-MA

Figure 4.12 SEM micrographs of drawn (a) PET/HDPE/C_2 (20/79/1), (b) PET/HDPE/C_2 (20/75/5), (c) PET/HDPE/C_2 (20/70/10) after extraction of the HDPE fraction (C_2 refers to E-MA)

Figure 4.13 shows the micrographs of injection molded MFC sample compatibilized with different contents of C_2. The fibrillar morphology is preserved after injection molding. There are non-fibrillar structures together with microfibers due to the reasons related to incomplete solvent etching as mentioned earlier. Due to the high shear and pressure conditions during injection molding, the melt temperature can be higher than the set temperature. As a result of this phenomenon, some spherical PET particles are observed.

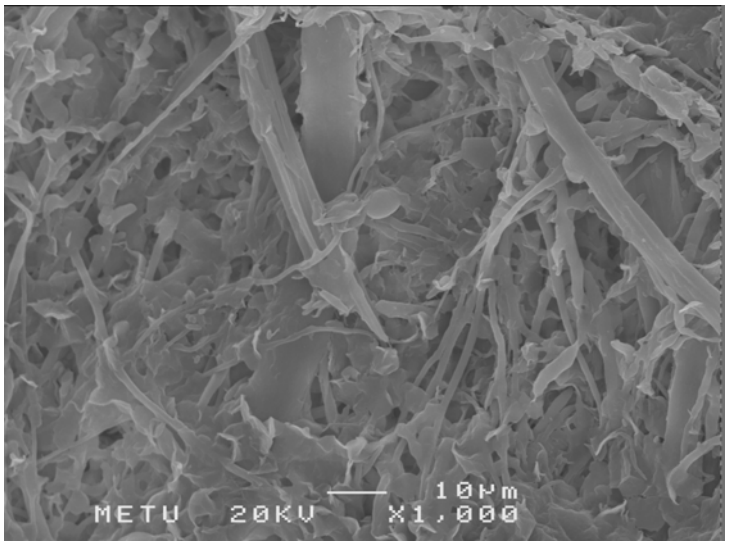

(a) 1% E-MA

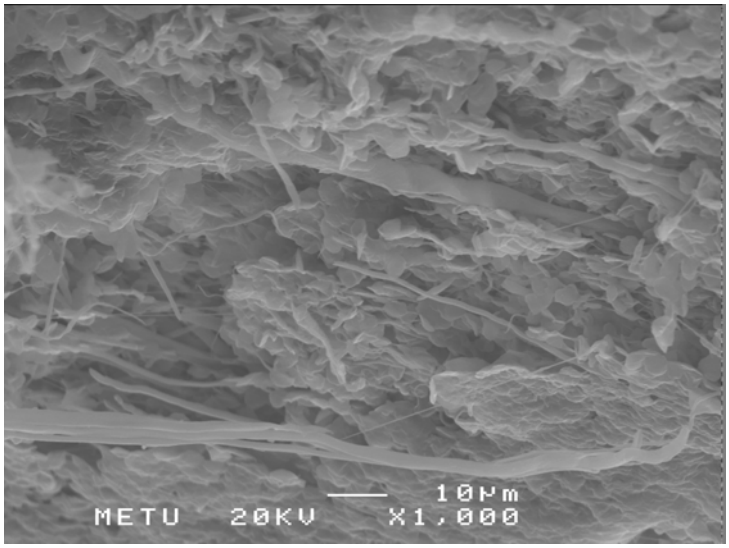

(b) 5% E-MA

Figure 4.13 SEM micrographs of fracture surfaces of injection molded MFC samples (a) PET/HDPE/C_2 (20/79/1), (b) PET/HDPE/C_2 (20/75/5) after extraction of HDPE fraction with hot xylene (C_2 refers to E-MA)

When the morphological observations are taken into account for the experimental parameters applied in this study, it can be concluded that compatibilization efficiency of E-nBA-GMA is better than E-MA. This conclusion is also supported with the mechanical test results of the study.

4.2 Mechanical Analysis

4.2.1 Tensile Properties

The representative stress-strain curves of the samples prepared are illustrated in Figure 4.14. The tensile properties will be discussed in further parts of the thesis.

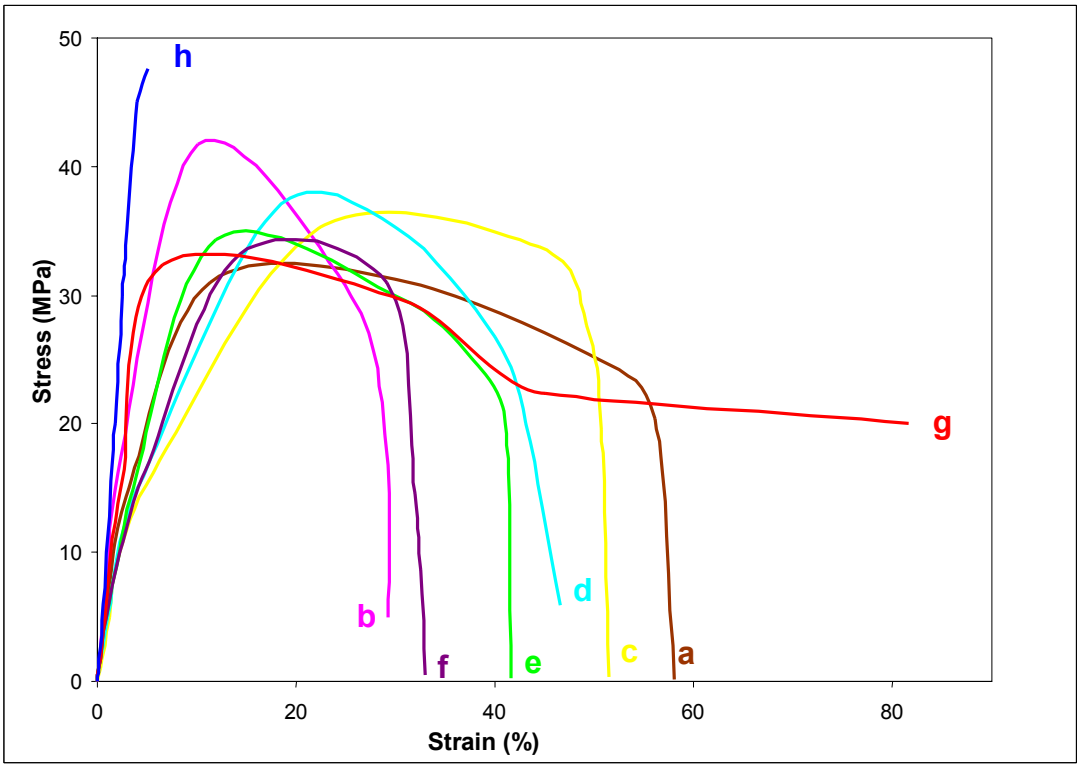

Figure 4.14 Representative stress-strain curves of samples prepared **a**: as extruded PET/HDPE sample processed at 60 rpm, **b**: PET/HDPE MFC sample processed at 60 rpm and drawn with 6.2 m/min, **c**: PET/HDPE as extruded sample compatibilized with 1% C_1, **d**: PET/HDPE as drawn sample compatibilized with 1% C_1, **e**: PET/HDPE as extruded sample compatibilized with 1% C_2, **f**: PET/HDPE as drawn sample compatibilized with 1 % C_2, **g**:pure HDPE sample processed at 60 rpm, **h**: pure PET sample processed at 60 rpm (C_1 and C_2 refers to E-nBA-GMA and E-MA, respectively.)

4.2.1.1 Effect of screw speed on tensile properties of injection molded MFC samples at different drawing speeds

Figure 4.15 represents the tensile strength of injection molded MFC samples with respect to screw speed. The average values of the results and standard deviations are given in Table C.1. It can be seen that, tensile strength value of the pure HDPE is characterized by the lowest one for the selected screw speed. The tensile strength of the as extruded PET/HDPE MFC is placed between the values of pure PET and pure HDPE which is an expected result according to the rule of mixture. The tensile strength values of MFCs are higher than those of as extruded samples for all screw speeds. When the tensile stress is applied to the extruded samples, the stress concentrates at PET domains. In the case of as drawn samples, the stress is distributed along the PET microfibers which leads to better mechanical properties.

When the screw speed increases from 60 rpm to 180 rpm, there is a slight decrease in tensile strength values. The reason may be due to the increase of shear associated with the increase in screw speed. This results in higher degree of mixing and dispersion which causes a decrease in fiber size and eventually lower tensile strength values.

Since the most fibrous morphology is obtained in the samples processed at 60 rpm and drawn with 6.2 m/min, these samples have the highest tensile strength. As the drawing speed increases from 2.7 m/min to 6.2 m/min, the PET microfiber diameter decreases from 4.3 μm to 1.3 μm. In a similar manner, the tensile strength increases with increasing drawing speeds at all screw speeds due to the decrease in the diameter of the microfibers.

In this study; for 60 rpm screw speed and 205ºC injection molding temperature, the tensile strength value of the as extruded pure HDPE is found to be 29 MPa whereas that of as extruded PET/HDPE (20/80 wt %)

sample is 32.5 MPa. This value is increased to 40 MPa for the as drawn PET/HDPE MFC sample processed and injection molded at the same conditions.

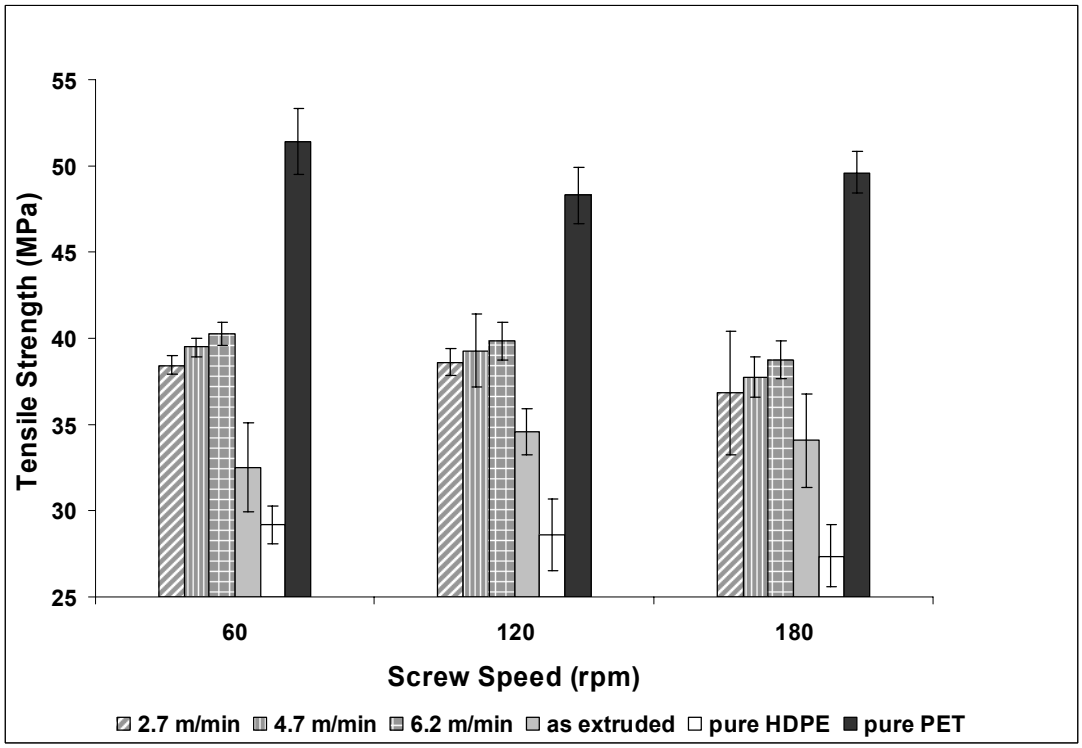

Figure 4.15 Tensile strength versus screw speed

Figure 4.16 represents the tensile modulus of the injection molded MFC samples with respect to screw speed. The average values of the results and standard deviations are given in Table C.2. As can be seen from the figure, for a given screw speed (60 rpm), as the drawing speed increases from 2.7 m/min to 6.2 m/min, the tensile modulus of the drawn samples is about 2 times higher than the modulus of as extruded samples. This result is in

accordance with the morphological observations. From Figure 4.2, it was seen that, as drawing speed increased from 2.7 m/min to 6.2 m/min, PET microfiber diameter decreased from 4.3 μm to 1.3 μm. As a result of this, the aspect ratio (L/D) increased which is responsible for the increase in tensile modulus values. In a previous study [37], from the morphological observations, it was also observed that average PET microfiber diameter decreased as the drawing speed increased which also resulted in increase in tensile modulus values.

The tensile modulus of the as extruded PET/HDPE samples is between the values of pure PET and HDPE but much closer to the values of HDPE. When the low content of PET is taken into consideration, this is an expected result according to the rule of mixture.

As the screw speed increases from 60 rpm to 180 rpm, tensile modulus values of the samples do not change significantly.

For the experimental parameters used in this study, the tensile modulus value of pure HDPE is found to be 680 MPa whereas that of the as extruded sample is 690 MPa. This value is increased to 897 MPa for the PET/HDPE MFC.

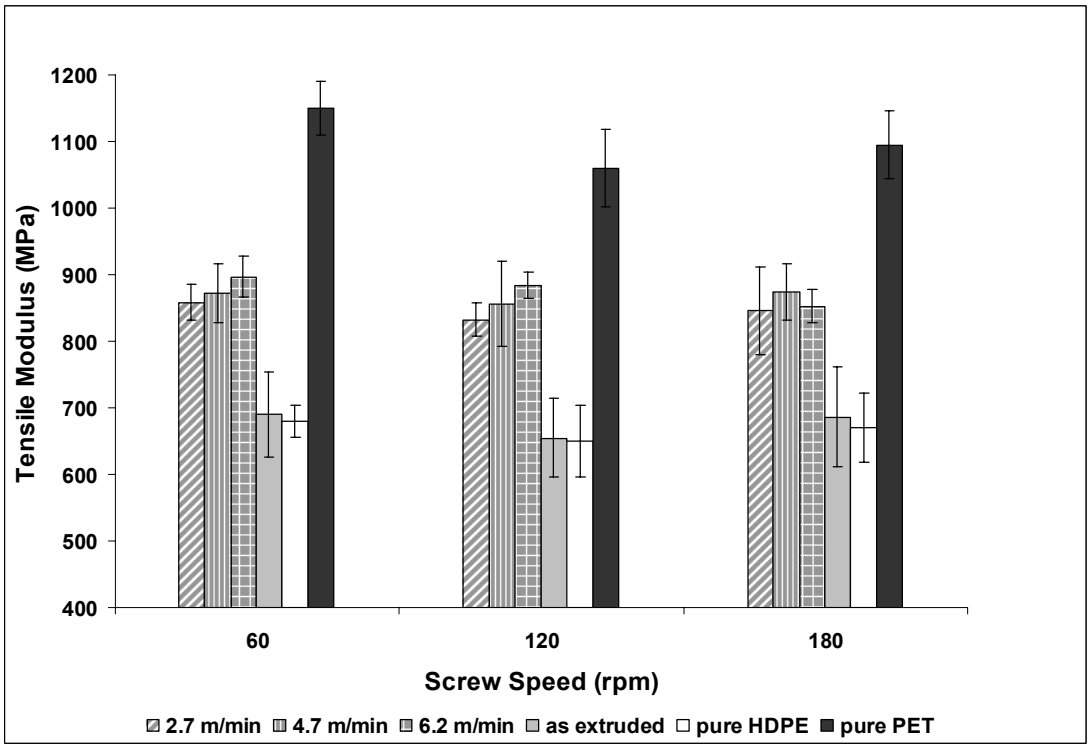

Figure 4.16 Tensile modulus versus screw speed

Figure 4.17 represents the % Elongation at break of the injection molded MFC samples with respect to screw speed. The average values of the results and standard deviations are given in Table C.3. It can be observed from the figure that, as the screw speed increases, there is a slight increase in the elongation at break values. This may be due to the increase of shear associated with the increase in screw speed. It results in higher degree of mixing and dispersion. With the increase in dispersion, voids that convert high unidirectional stresses into smaller and less effective multi-directional stresses increase and this may improve the elongation at break values.

It is also observed from the Figure 4.17 that, as extruded samples which have more spherical particles of PET, have higher elongation at break than

those of as drawn samples with PET microfibers. This may be explained by the model proposed in Figure 4.18. This model is an illustration of spherical particle and fiber leading to the elongation deformability difference. For the sample with spherical particle, when it undergoes elongation deformation influenced by tensile stress, the interface between the dispersed phase and the matrix brings out slippage due to the lack of adhesion and interactions in the incompatible interfaces. This slippage is the key to produce large elongation. The fibers have high interfacial contact with HDPE matrix as in Figure 4.2c; hence produce high frictional force to prevent the material deformation during testing. As a result of the model proposed, as the drawing speed increases, the elongation at break of the samples decreases because of the increase in the amount of the microfibers.

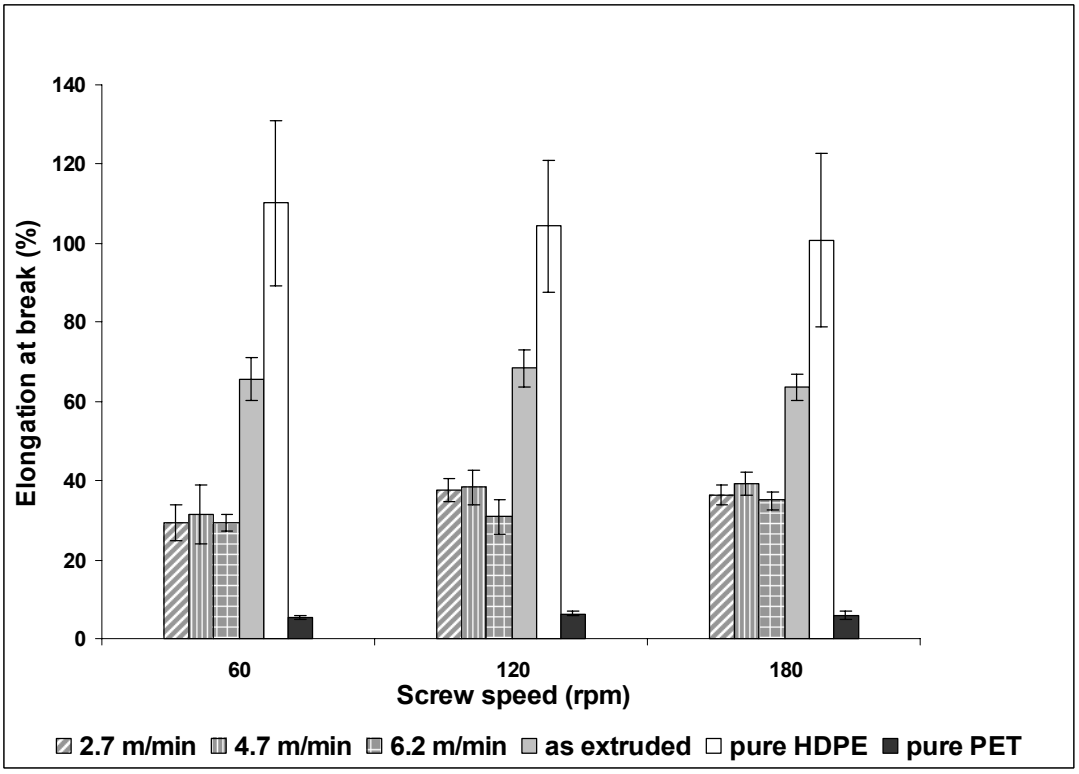

Figure 4.17 Elongation at break versus screw speed

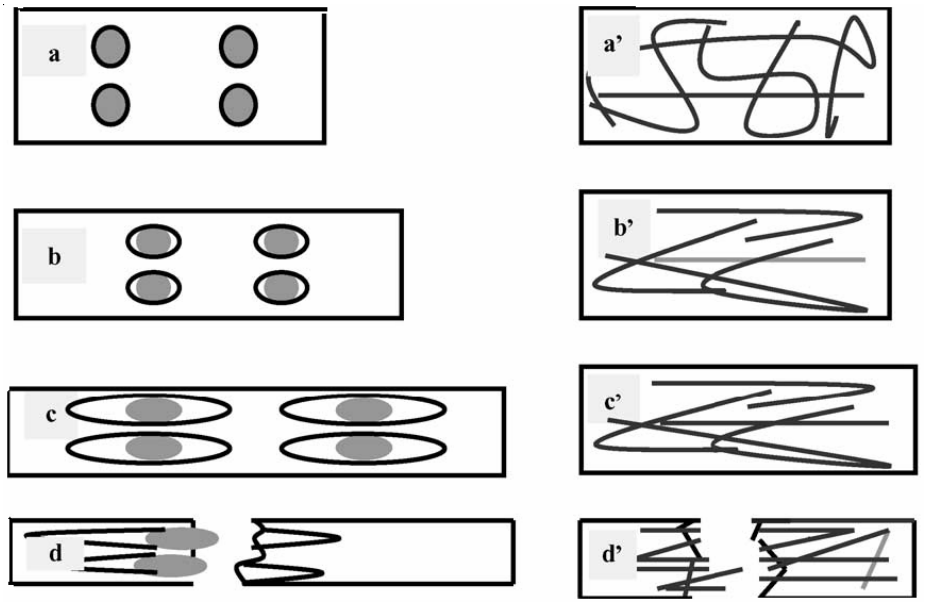

Figure 4.18 The model of tensile fracture process of the material comprised of spherical particles and microfibers [35]

4.2.1.2 Effect of compatibilizer type and content on the tensile properties of injection molded MFC samples processed at 60 rpm and drawn with 6.2 m/min

Figure 4.19 represents the tensile strength values versus compatibilizer content. The average values of the results and standard deviations are given in Table C.4. The samples without MFC structure are the as extruded ones processed at 60 rpm and injection molded at 205°C. Drawing was not applied to these samples. The tensile strength of the samples without MFC structure increases with the addition of the compatibilizers. As a result of the decrease in the interfacial tension, adhesion is improved which resulted in higher tensile strength values.

As seen in Figure 4.19, the tensile strength values of the non-compatibilized and compatibilized PET/HDPE samples with or without MFC structure are

placed between those of pure HDPE and pure PET. Regardless of the type of the compatibilizer, the tensile strength values of the samples with MFC structure first decrease with the addition of 1% compatibilizer, then increase with further increase in compatibilizer content because of the interactions between PET and the compatibilizers and exhibit an optimum at 5%. When it increases to 10%, the tensile strength values decrease which is the possible result of the elastomeric effect of the compatibilizers. These results are almost in accordance with the morphological observations in Figures 4.9 and 4.12.

From the morphological observations it is seen that C_2 is not as compatible as C_1 because of the lack of epoxy functionality. As a result of this, as seen from the figure, the tensile strength values of the samples compatibilized with C_1 are higher than those compatibilized with C_2.

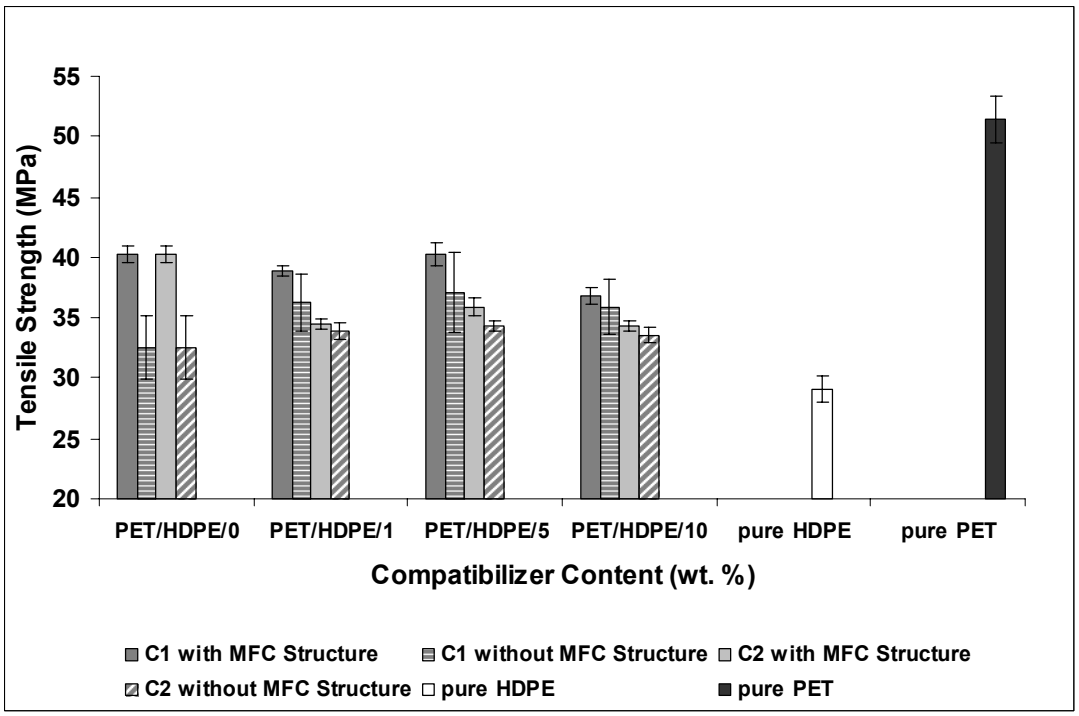

Figure 4.19 Tensile strength versus compatibilizer content

Figure 4.20 illustrates the tensile modulus values with respect to compatibilizer content. The average values of the results and standard deviations are given in Table C.5. As seen in the figure, the tensile modulus significantly decreases with the addition of the compatibilizers. This is mainly due to the addition of a rubbery material to the system. The compatibilizer produces a plasticizing effect, and this is so dominant that regardless of the structure of the composites (with or without MFC), the tensile modulus decreases. It is also discussed in a previous study [11] that, the presence of GMA leads to shorter length of microfibers and therefore reflects the aspect ratio effect in the samples with MFC structure. In the systems without compatibilizer, with the process of drawing, the matrix HDPE melt is elongated and simultaneously transfers a stress to the droplets. Under such stress, these droplets are also elongated; they become thinner but longer. When they begin to contact each other, as a result of the coalescence, they build up microfibers comprising many starting spheres. This process is impossible for the system compatibilized with C_1 because of the influence of epoxy functionality. A thin shell is formed around each PET sphere which does not allow their coalescence during drawing. As a result of this, shorter length of microfibers is obtained which causes a decrease in the aspect ratio (L/D), and eventually lower tensile modulus values.

Although the compatibilization efficiency of C_2 is much lower than that of C_1, the tensile modulus values of the samples compatibilized with C_2 is somewhat higher than those compatibilized with C_1. It has a lower T_g compared to that of C_2 as a possible result of the n-butylacrylate group in its structure. Thus, lower T_g value of E-nBA-GMA makes it a more rubbery material.

The tensile modulus of the non-compatibilized samples with and without MFC structure are both higher than that of pure HDPE, while that of the compatibilized ones, regardless of the compatibilizer content, are lower than

that of pure HDPE. Upon initial addition of the compatibilizers, the tensile modulus decreases and follows a decreasing trend with the further increase in the compatibilizer content.

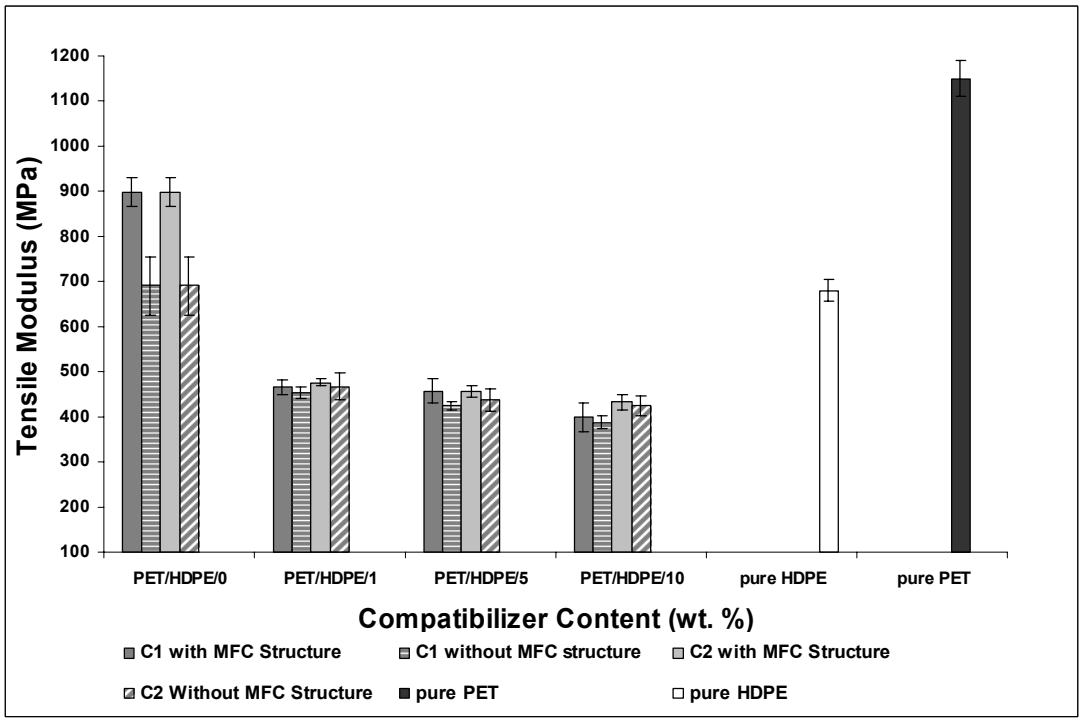

Figure 4.20 Tensile modulus versus compatibilizer content

Figure 4.21 shows the elongation at break values with respect to compatibilizer content. The average values of the results and standard deviations are given in Table C.6. According to model proposed in Figure 4.17, for the specimen with spherical particle, when it undergoes deformation, the interface between the dispersed phase and the matrix brings out slippage due to the lack of the adhesion and interactions in the incompatible interfaces. As elongation increases, the slippage can go on until the

specimen is broken. The elongation at break values of the non-compatibilized samples without MFC structure are higher than the ones with MFC structure. This resulted from the large slippage that occurs in the interfaces between the PET spheres and HDPE matrix.

With the addition of the compatibilizers, the interfacial tension is reduced and the adhesion is increased as a result of the possible reactions taking place between hydroxyl and carboxyl functional groups of PET and epoxy functional group of E-nBA-GMA or the specific polar interaction (H-bonding) between PET/E-nBA-GMA and PET/E-MA. So, slippage, which produces high elongation, does not take place between the dispersed phase and the HDPE matrix. Hence, the elongation at break values of the compatibilized samples without MFC structure is lower than those of the non-compatibilized samples without MFC structure.

Elongation at break values of the materials without MFC structure and compatibilized with C_1 are higher than those compatibilized with C_2. This is not an expected result, since the compatibilization efficiency of C_1 is better than that of C_2. Less slippage should take place between PET and HDPE phases because of the reactions taking place between PET and epoxy functional group of C_1 and this should lead to lower elongation at break values.

With the addition of the compatibilizer, the elongation at break values of the compatibilized samples with MFC structure is higher than those of the non-compatibilized samples with MFC structure. The presence of E-nBA-GMA in the blends reduces the domains of PET in the matrix and improves the interfacial adhesion between the two phases. This is a possible reason for the higher elongation at break values of the MFC structure samples compatibilized with C_1.

Upon 1% addition of C_1, the elongation at break of the samples without MFC structure decreases, and it starts to increase with the addition of 5, and 10% C_1. For the samples without MFC structure compatibilized with C_2, upon its initial addition, elongation at break of the samples decreases, and further decreases with the addition of 5% C_2, then reaches a maximum value at the C_2 content of 10%.

For both of the compatibilizers with MFC structure, the elongation at break values increases upon the 1% addition of the compatibilizers, and decreases with the addition of 5% compatibilizer, then increases and reaches a maximum value at the 10% compatibilizer content.

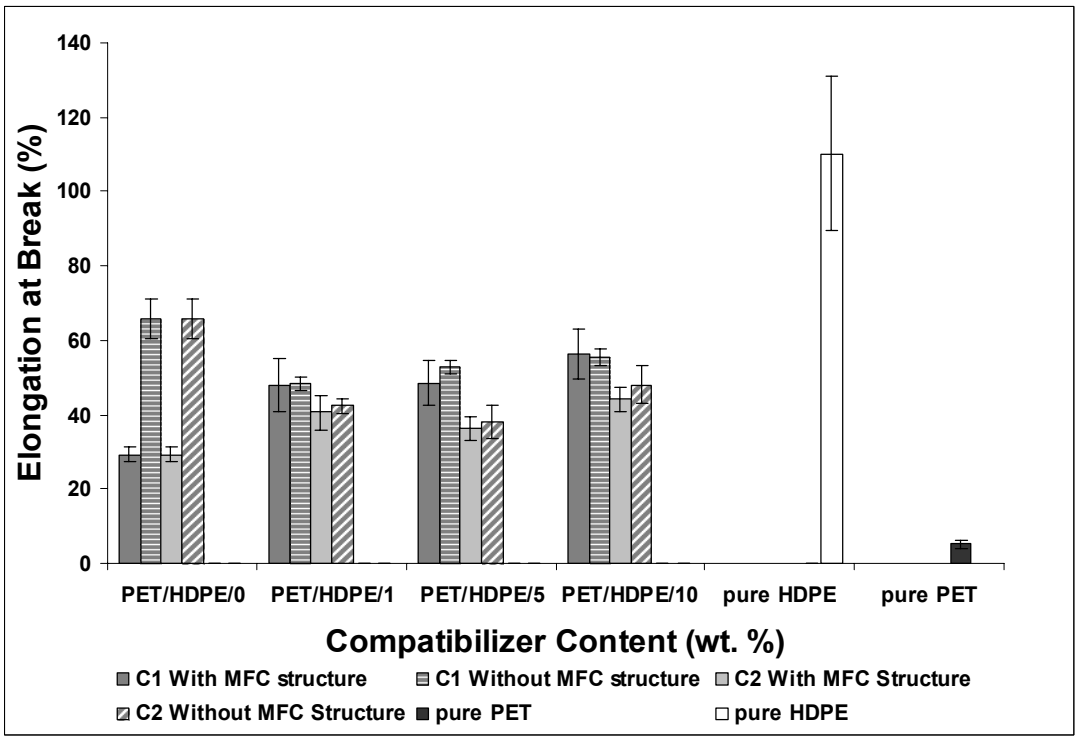

Figure 4.21 Elongation at break versus compatibilizer content

4.2.2 Impact Properties

4.2.2.1 Effect of screw speed on impact properties of PET/HDPE MFC samples at different drawing speeds

Figure 4.22 shows the values of impact strength with respect to screw speed. The average values of the results and standard deviations are given in Table C.7. Pure PET represents the lowest impact strength value because of its brittle structure. Since pure HDPE is a ductile polymer, its impact strength value is much higher. As seen in the figure, the impact strength of the as extruded PET/HDPE samples is lower than that of pure HDPE because of the incompatibility between PET and HDPE.

It is seen from the Figure 4.22 that, the minimum impact strength values are observed for the samples processed at 180 rpm. The reason may be due to the increase of shear associated with the increase in screw speed. This results in higher degree of mixing and dispersion which causes a decrease in fiber length. These results are also supported with the morphological observations as seen in Figure 4.4. As the fiber length decreases, the impact strength also decreases. The fiber ends are points of stress concentrators that weaken the composite by acting as crack initiators.

For 60 rpm screw speed, as the drawing speed increases, the impact strength values of the samples increase. From the SEM micrographs in Figure 4.2, it is seen that as the drawing speed increases, the average PET microfiber diameter decreases. The smaller diameters of PET microfibers increase the impact strength by an increase in the fracture pathway, thus absorbing more energy upon failure [48].

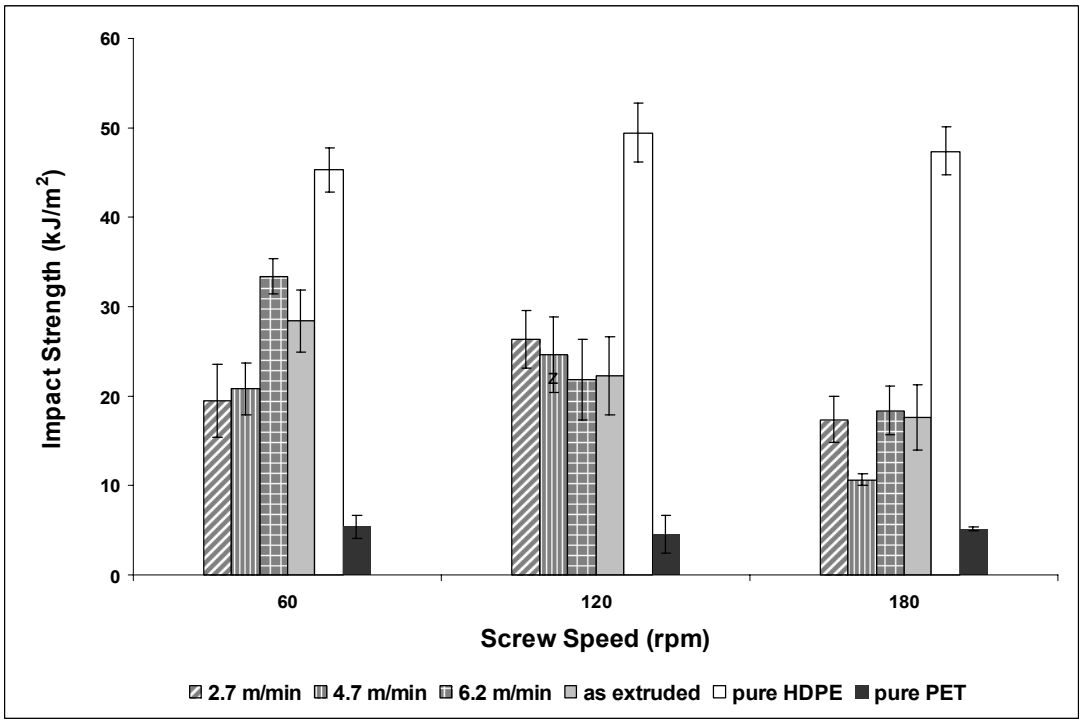

Figure 4.22 Impact strength versus screw speed

4.2.2.2 Effect of compatibilizer type and content on impact properties of injection molded MFC samples

Figure 4.23 shows the impact strength values with respect to compatibilizer content. The average values of the impact test results and standard deviations are given in Table C.8. As seen from the figure, the impact strength values of the samples with or without MFC structure compatibilized with E-nBA-GMA significantly increases with the increasing amount of C_1. This is because the rubber particles dispersed in the polymer blend, are able to initiate and control crazes growth. During impact testing, crazes are initiated due to high stress concentration, propagate almost normal to tensile stress direction and stop their growth when a neighbouring rubber particle in encountered. This resulting crazing phenomenon is able to dissipate large

amount of impact energy. Also, C_1 is known to be a reactive functional copolymer which has GMA in its structure. Due to the possible reactions that may occur between hydroxyl and carboxyl functional groups of PET and epoxy functional group of C_1, interfacial adhesion is improved. And this results in higher impact strength. Somehow, the impact strength of the samples compatibilized with C_2 exhibits smaller values with increasing amount of compatibilizer.

When the impact strength of the compatibilizers with and without MFC structure is compared, it is seen that fiber formation promotes impact strength.

For a given compatibilizer content, the samples compatibilized with C_1 have higher impact strength values than those compatibilized with C_2. The reason may be due to the difference in their compatibilizer efficiency. It may also result from the lower T_g value of C_1 which makes the sample compatibilized with C_1 a more rubbery material. The highest impact strength value is achieved for PET/HDPE sample with MFC structure compatibilized with 10% E-nBA-GMA.

It can also be concluded that, for the compatibilized materials with MFC structure, E-nBA-GMA acted as a toughening agent rather than a compatibilizer.

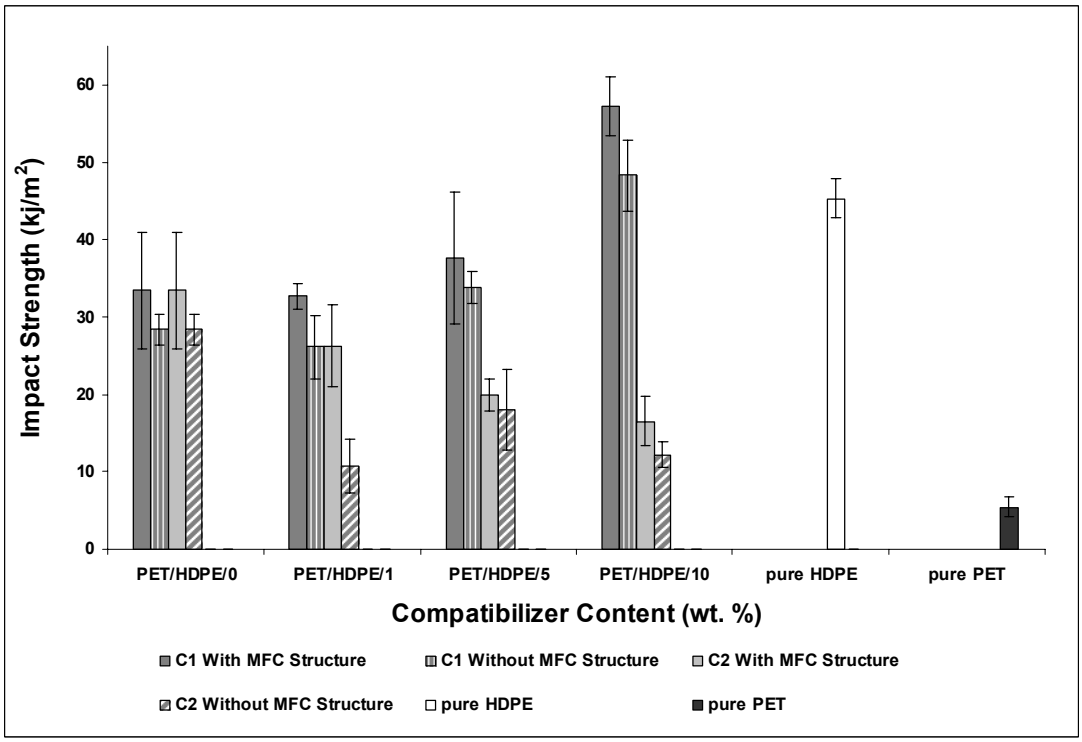

Figure 4.23 Impact strength versus compatibilizer content

4.3 Thermal Properties

The melting point, melting entalpy and the degree of crystallinity (X_c) values of as extruded, as drawn and MFC samples processed at 60 rpm and drawn with different drawing speeds are shown in Table 4.1. Crystallization temperature of PET (138ºC) could not be detected, since it is very close to the melting point of HDPE (~140ºC). Melting points of the HDPE phase do not change significantly. Therefore there is no effect of drawing speed on melting point of the samples. Processing stages of the samples (as extruded, as drawn or injection molded) has also no effect on melting point of the samples. As the drawing speed increases, X_c values of HDPE phase

decreases. Because the presence of rigid PET phase prevents the crystal growth of HDPE phase.

Melting points of PET phase do not change significantly. It is observed that, process conditions are effective on X_c. From the morphological observations, it is seen that, for the samples processed at 60 rpm, when the drawing speed increases from 2.7 m/min to 6.2 m/min, more oriented microfibers are formed. In accordance with this observation, the X_c of PET in as drawn samples increases with the increasing drawing speed. This is an expected result since orientation promotes crystallization.

X_c values of PET phase of the as extruded samples processed at 60 rpm and drawn with 6.2 m/min are lower compared to those of as drawn samples due to the increase in orientation. Also, a decrease in the X_c value of the MFC samples is observed with respect to the as drawn samples. This may be due to the high shear and pressure conditions during injection molding, the melt temperature can be higher than the set temperature. And this may cause the lack of orientation of the fibers which is supported with morphological observations as seen in Figure 4.5.

DSC thermograms of several samples are illustrated in Appendix D.

Table 4.1 Results of DSC analyses for as extruded, as drawn and MFC samples drawn at different speeds

SAMPLES		HDPE			PET		
		T_m (ºC)	ΔH_m (J/gPE)	X_c (%)	T_m (ºC)	ΔH_m (J/gPET)	X_c (%)
60 rpm screw speed – drawn with 2.7 m/min	**As extruded**	125.59	150.88	52.76	240.05	23.11	16.75
	As drawn	125.85	162.00	56.64	242.26	14.16	10.26
	MFC	125.28	151.13	52.84	240.58	18.48	13.39
60 rpm screw speed – drawn with 4.7 m/min	**As extruded**	126.77	160.25	56.03	242.43	16.26	11.78
	As drawn	125.60	147.13	51.44	240.14	23.57	17.08
	MFC	125.48	154.25	53.93	242.30	11.35	8.22
60 rpm screw speed – drawn with 6.2 m/min	**As extruded**	126.32	149.5	52.27	240.48	15.34	11.12
	As drawn	125.05	134.75	47.12	240.24	28.02	20.30
	MFC	124.64	141.38	49.43	241.39	9.59	6.95

The melting point, melting entalpy and the X_c values of as extruded, as drawn and MFC samples processed at 60 rpm and drawn with 6.2 m/min and compatibilized with E-nBA-GMA (C_1) are shown in Table 4.2. It can be seen that, for HDPE and PET phases, melting points of the samples do not change significantly with the increase in the compatibilizer content.

It is expected that crystallizable copolymer C_1 is compatible with HDPE matrix and contribute to decrease its crystallinity degree [49]. When Tables 4.1 and 4.2 are compared, it is seen that X_c value of HDPE phase of the non-compatibilized as extruded sample processed at 60 rpm and drawn with 6.2 m/min decreases from 52.27 to 30.73 with the addition of 10% C_1, whereas that of as drawn sample processed at 60 rpm and drawn with 6.2 m/min increases from 47.12 to 55.45 with the addition of 10 % C_1. This is an expected result since orientation by drawing promotes crystallinity. Also, X_c values of both the HDPE and PET phases of the MFC sample compatibilized with 5% C_1 gives the highest value which is in agreement with the tensile test results as seen in Figures 4.19 and 4.20.

Table 4.2 Results of DSC analyses for as extruded, as drawn and MFC samples processed at 60 rpm and drawn with 6.2 m/min and compatibilized with E-nBA-GMA (C_1) at different contents

SAMPLES		HDPE			PET		
		T_m (ºC)	ΔH_m (J/gPE)	X_c (%)	T_m (ºC)	ΔH_m (J/gPET)	X_c (%)
1 % C_1	**As extruded**	124.34	140.5	49.13	243.75	16.04	11.62
	As drawn	125.21	154.0	53.85	242.57	13.36	9.68
	MFC	124.57	138.88	48.56	240.79	17.12	12.41
5 % C_1	**As extruded**	126.09	154.5	54.02	240.14	26.12	18.93
	As drawn	125.71	161.0	56.29	238.46	34.72	25.16
	MFC	124.33	156.63	54.77	238.42	29.61	21.45
10% C_1	**As extruded**	124.90	87.88	30.73	239.22	25.73	18.64
	As drawn	124.78	158.5	55.45	237.57	26.93	19.51
	MFC	125.62	136.5	47.73	238.14	27.58	19.99

The melting point, melting entalpy and the X_c of as extruded, as drawn, and MFC samples compatibilized with E-MA are shown in Table 4.3. Melting points of the HDPE and PET phases do not change significantly. Therefore there is no effect of C_2 ratio on the melting point of the samples. It is seen that X_c values of HDPE phase of the non-compatibilized as extruded samples processed at 60 rpm and drawn with 6.2 m/min decreases with the addition of C_2. When Tables 4.1 and 4.3 are compared, it is seen that X_c value of the HDPE phase of the non-compatibilized as drawn samples processed at 60 rpm and drawn with 6.2 m/min increases from 47.12 to 55.47 with the addition of 10% C_2. The X_c value of the PET phase of the non-compatibilized as drawn samples processed and drawn at the same conditions decreases from 20.30 to 13.03 with the addition of 10% C_2. Also, X_c values of the MFC samples compatibilized with 5% C_2 gives the highest value which is in agreement with the tensile test results as seen from Figures 4.19 and 4.20.

Table 4.3 Results of DSC analyses for as extruded, as drawn and MFC samples processed at 60 rpm and drawn with 6.2 m/min and compatibilized with E-MA (C_2) at different contents

SAMPLES		HDPE			PET		
		T_m (ºC)	ΔH_m (J/gPE)	X_c (%)	T_m (ºC)	ΔH_m (J/gPET)	X_c (%)
1% C_2	**As extruded**	125.53	141.88	49.61	241.16	27.19	19.70
	As drawn	124.95	148.5	51.92	240.93	22.33	16.18
	MFC	124.69	135.75	48.16	241.23	14.29	10.36
5% C_2	**As extruded**	126.98	109.8	38.39	240.45	23.56	17.07
	As drawn	125.42	165.38	57.83	239.59	31.62	22.91
	MFC	124.85	155.38	54.33	241.01	19.99	14.49
10% C_2	**As extruded**	125.47	89.86	31.42	242.76	13.05	9.46
	As drawn	125.57	158.63	55.47	240.02	17.98	13.03
	MFC	125.60	137.13	47.95	241.26	13.13	9.51

CHAPTER 5

CONCLUSIONS

In this study, PET/HDPE MFC was obtained through extrusion-drawing-injection molding method. The samples at different processing stages (as extruded, as drawn and injection molded) were characterized in terms morphologies and mechanical and thermal properties. The effects of compatibilizers E-nBA-GMA and E-MA, on properties of PET/HDPE composites were also studied. For comparison purposes, conventional PET/HDPE blends with and without compatibilizer were prepared. Morphologies observed by SEM analysis indicated that fibers generated during drawing were preserved after injection molding. With the increase in drawing speed, average PET microfiber diameter decreased from 4.3 μm to 1.3 μm and a fibrous morphology was promoted which resulted in improved mechanical properties. The effect of injection molding temperature was apparently seen from the SEM micrographs. Low temperature injection molding preserved the PET microfibers generated during drawing, but during high temperature injection molding, microfibers melted again and turned into spherical shapes.

With the increase in the screw speed, size and amount of the PET microfibrils decreased. Increasing the screw speed also resulted in a slight decrease in tensile strength, and impact strength values. The most fibrous morphology was observed in the microfibers processed at 60 rpm and drawn

with 6.2 m/min drawing speed. This processing condition and drawing speed were used for the compatibilization experiments.

Tensile strength and tensile modulus values of the MFC composites were increased compared to pure HDPE and as extruded PET/HDPE samples. However, these properties decreased with the addition of the compatibilizers due to the incorporation of a rubbery material to the system. For the compatibilized systems, the highest tensile strength and tensile modulus values were achived for the samples with MFC structure compatibilized with 5% E-nBA-GMA. The samples compatibilized with E-MA represented lower tensile strength and modulus values when compared to those compatibilized with E-nBA-GMA.

Elongation at break of MFC samples was lower than that of as extruded PET/HDPE samples. As a result of the model of tensile fracture process of the material comprised of spherical particles and microfibers, as the drawing speed increased, the elongation at break of the samples decreased because of the increase in the amount of the microfibers. Also, there was a slight increase in elongation at break values because of the increase of shear associated with the increase in screw speed. It results in higher degree of mixing and dispersion. With the increase in dispersion, voids that convert high unidirectional stresses into smaller and less effective multi-directional stresses increase and this may improve the elongation at break values.

Impact strength values of MFC were lower than that of pure HDPE because of the incompatibility between PET and HDPE. Impact strength values also decreased with increasing screw speed. With the addition of the E-nBA-GMA, impact strength values increased. The highest impact strength value was achieved for the samples with MFC structure compatibilized with 10% E-nBA-GMA.

When the effect of compatibilizer type was examined, it was seen that E-nBA-GMA which is a reactive functional terpolymer is a more efficient compatibilizer than E-MA which is a non-reactive polar copolymer. In the samples compatibilized with E-nBA-GMA, the interfacial adhesion is improved with the possible reactions taking place between the hydroxyl and carboxyl functional group of PET and epoxy functional group of the compatibilizer. For the samples compatibilized with E-MA; interfacial adhesion is improved with the specific polar interactions like H-bonding. The effect of reactive functional terpolymer is more dominant than the non-reactive polar copolymer. On the other hand, for the compatibilized materials with MFC structure, E-nBA-GMA acted as a toughening agent rather than a compatibilizer.

Thermal analyses showed that melting points of HDPE phase and PET phase did not change significantly for the samples processed at 60 rpm and drawn with different drawing speeds and for the samples processed at 60 rpm and drawn with 6.2 m/min and compatibilized with different contents of compatibilizers. Processing stages (as extruded, as drawn, injection molded) also did not have an effect on the melting points of the two phases. As the drawing speed increased from 2.7 m/min to 6.2 m/min, degree of crystallinity of the samples increased because of the increase in the orientation of the microfibers. With the addition of the compatibilizers, the degree of crystallinity values of the as extruded samples decreased. The degree of crystallinity values of the MFC samples compatibilized with 5 % E-nBA-GMA and those compatibilized with 5% E-MA exhibited higher values.

The tensile strength, tensile modulus and impact strength of the samples are directly related to the properties of the reinforcing microfibers. The reinforcing effect is related to the amount of the PET microfiber, length of the microfiber, the aspect ratio, length distribution of the microfiber, direction of the microfiber, amount of entangling points of microfiber and the adhesion

between the microfiber and the matrix. If the experimental set-up and conditions used in this study can be modified, the mechanical performance of the MFCs will further be improved.

REFERENCES

[1] Harper A. C., “Modern Plastics Handbook, Mc Graw Hill, 1999

[2] Li Z. M., Yang M.B., Huang R., Yang W., and Feng J. M., “Poly(ethylene terephthalate)/Polyethylene composite based on in-situ microfiber formation”, Polymer Plastics Technology Engineering, vol.41 No.1, pg 19-32, 2002

[3] Evstatiev M., Fakirov S., Bechtold G., Friedrich K., “Structure-Property relationships of injection and compression molded microfibrillar reinforced PET/PA-6 composites”, Advances in Polymer Technology, Vol.19, No.4, pg.249-259, 2000

[4] Petermann J., “Compatibility and transesterification in binary polymer blends”, Journal of Materials Science, vol., 22, pg.1120, 1987

[5] Evstatiev M., Fakirov S., “Microfibrillar reinforcement of polymer blends”, Polymer, vol.33, pg.877-880, 1992

[6] Fakirov S., Evstatiev M., Schultz J. M., “Microfibrillar reinforced composite from drawn poly(ethylene terephthalate)/nylon 6 blend”, Polymer, Vol.34, pg 4669, 1993

[7] Fakirov S., Evstatiev M., Petrovich S., “Microfibrillar reinforced composites from binary and ternary blends of polyesters and nylon 6”, Macromolecules, Vol.26, pg 5219, 1993

[8] Fakirov S., Evstatiev M., “Microfibrillar reinforced composites – new materials from polymer blends”, Advanced Materials, Vol.6, pg 395, 1994

[9] Evstatiev M., Fakirov S., Friedrich K., In: Cunha AM, Fakirov S., editors, “Structure development during polymer processing”, Dordrecht, Boston, London, U.K., Kluwer Academic Publisher, 2000

[10] Fakirov S., Evstatiev M., Friedrich K., “Handbook of Thermoplastic Polyesters”, Wiley-VCH, Weinheim, pp.1093-1132, 2002

[11] Friedrich K., Evstatiev M., Fakirov S., Evstatiev O., Ishii M., Harrass M., “Microfibrillar reinforced composites from PET/PP blends: processing, morphology and mechanical properties”, Composites Science and Technology, vol. 65, pgs. 107-116, 2005

[12] Fakirov S., Evstatiev M., Friedrich K., “From Polymer Blends to Microfibrillar Reinforced Composites“ in: D. R Paul, C. B. Bucknall (eds) “Polymer Blends”, Vol. 2, chap. 33, Wiley, New York, 2000

[13] Fakirov S., Manufacturing of MFC, Centre for Advanced Composite Materials and Department of Mechanical Engineering, The University of Auckland, New Zealand, 2002

[14] Fakirov S., Bhattacharyya D., “Polymer – Polymer Nano – and Microfibrillar Composites: Manufacturing, Properties and Applications”, Centre for Advanced Composite Materials and Department of Mechanical Engineering, The university of Auckland, New Zealand, 2000

[15] Deanin R.D., “The Relationship between Structures, Properties, and Applications in Polymer”, Cahners Publishing Company Inc., York, Pennsylvania, 1972

[16] Evstatiev M., Fakirov S., Krasteva B., Friedrich K., Covas J. A., and Cunha A. M., “Recycling of poly(ethylene terephthalate) as polymer-polymer Composites”, Polymer Engineering and Science, Vol.42, No.4, 2002

[17] Billmeyer W. F.,Jr., “ Textbook of Polymer Science”, 3rd edition, John Wiley & Sons, Toronto, Canada, 1984

[18] Moad G., “The synthesis of polyolefin graft copolymers by reactive extrusion”, Progress in Polymer Science, vol. 24, pg. 81, 1999

[19] Datta S., Lohse D. J., “ Polymeric Compatibilizers”, Hanser Publications, Munich, chapter B4, p.196, 1996

[20] Sambaru P., Jabarin S. A., “Properties and morphology of oriented ternary blends of poly(ethylene terephthalate), high density polyethylene, and compatibilizing agent”, Polymer Engineering Science, vol.33, pg 827, 1993

[21] Carte T. L., Moet A., “Morphological origin of super toughness in poly(ethylene terephthalate)/polyethylene blends”, Journal of Applied Polymer Science, vol.48, pg 611, 1993

[22] Fakirov S., “Handbook of Thermoplastic Polyesters”, Wiley-VCH, Weinheim, 2002

[23] Tsiourvas D., Tsartolia E., Stassinopoulos A., Barrell M., Bontemps J., “A new approach to reclaimed PET utilization – blends of recycled PET suitable for extrusion blow-molding technology”, Advanced Polymer Technology, vol.14, 227, 2003

[24] Loyens W., Groeninckx G., “Phase morphology development in reactively compatibilized poly(ethylene terephthalate)/Elastomer Blends”, Macromolecular Chemistry and Physics, Vol.203, pgs 1702-1714, 2002

[25] Kroschwitz J. I., “Concise Encyclopedia of Polymer Science and Engineering”, Wiley, New York, 1990

[26] Tadmor Z., Gogos G. Co., “Principles of Polymer Processing”, John Wiley & Sons, 2nd edition, 2006

[27] Simon G. P., “Polymer Characterization Techniques and their Applications to Blends”, Oxford University Press, 2003

[28] Strong A. B., “Plastics, Materials & Processing”, Prentice Hall, New York, 2000

[29] Bikales N. M., “Molding of Plastics”, Wiley Interscience, New York, 1971

[30] www.mete.metu.edu.tr/facilities/service/ sem/semlb.htm, Middle East Technical University Department of Metallurgical and Materials Engineering, (the last day accessed 12/1/2007)

[31] www.pslc.ws/mactest/mech.htm, Polymer Science Learning Center, (the last day accessed 12/1/2007)

[32] http://en.wikipedia.org/wiki/Differential_Scanning_Calorimetry, Wikipedia Free Encyclopedia, (the last day accessed 12/1/2007)

[33] Sarkissova M., Harrats C., Groeninckx G., Thomas S., “Design and characterization of microfibrillar reinforced composite materials based on PET/PA12 blends”, Composites. Part A, Applied science and Manufacturing, Vol.35, No.4, 489-499, 2004

[34] Lin X. D., Cheung W. L., “Study on poly(ethylene terephthalate)/polypropylene microfibrillar composites. I. Morphological development in melt extrusion”, Journal of Applied Polymer Science, Vol.89, 1743-1752, 2003

[35] Li. Z.M., Yang M.B., Lu A., Feng J. M., Huang R., “Tensile properties of poly(ethylene terephthalate) and polyethylene in-situ microfiber reinforced composite formed via slit die extrusion and hot-stretching”, Materials Letters, 56, 756-762, 2002

[36] Monticciolo A., Cassagnau P., and Michel A., “Fibrillar morphology development of PE/PBT blends: rheology and solvent permeability”, Polymer Engineering Science, Vol.38, pg 1882, 1998

[37] Li. Z.M., Yang M.B., Feng J. M., Yang W., Huang R., “Morphology of in situ poly(ethylene terephthalate)/polyethylene microfiber reinforced composite formed via slit-die extrusion and hot-stretching”, Materials Research Bulletin, 37, 2185-2197, 2002

[38] Quan H., Zhong G. J., Li, Z.M., Yang M.B., “Morphology and mechanical properties of poly(phenylene sulfide)isotactic polypropylene in situ microfibrillar blends”, Polymer Engineering and Science, Vol.45, Iss.9. 1303-1312, 2005

[39] Kroschwitz J. I., “Concise Encyclopedia of Polymer Science and Engineering”, Wiley, New York, 1990

[40] Kılınç M., “Processing and Characterization of Poly(ethylene terephthalate) Based Composites, MS Thesis, Middle East Technical University, Ankara, 2004

[41] http://www.dupont.com/industrial-polymers/plastics, Dupont Polymer Modifiers, (the last day accessed 12/1/2007)

[42] http://www.specialchem4polymers.com/tc/Adhesion-Promoters, SpecialChem S.A, ((the last day accessed 2/3/2007)

[43] Lubin G., “Handbook of Fiberglass and Advanced Plastic Composites, New York, 1969

[44] Wunderlich B., “Macromolecules Physics”, Vol.3, Academic Press, New York, p.58, 1980

[45] Karger-Kocsis J., “Composites (structure, properties and manufacturing), Polymeric Materials Encyclopedia, J.C. Salamone, ed., CRC Press, Boca Raton, Vol. 2, p.1378, 1996

[46] Hull D., “An Introduction to Composite Materials”, Cambridge University Press, U.K., 1978

[47] Flory P.J., “On the morphology of the crystalline state in polymers”, Journal of the American Society, Vol.34, pg 2857-2867, 1962

[48] Taepaiboon P., Junkasem J., Dangtungee R., Amornsakchai T., Supaphol P., “In situ microfibrillar reinforced composites of isotactic polypropylene/recycled poly(ethylene terephthalate) system and effect of compatibilizer”, Journal of Applied Polymer Science, Vol.102, pg 1173-1181, 2006

[49] Pracella M., Rolla L., Chionna D., Galeski A., “Compatibilization and properties of poly(ethylene terephthalate)/polyethylene blends based on recycled materials”, Macromolecular Chemistry and Physics, Vol.203, pg 1473-1485, 2002

APPENDIX A

Drawing Speed versus Draw Ratio Graphs

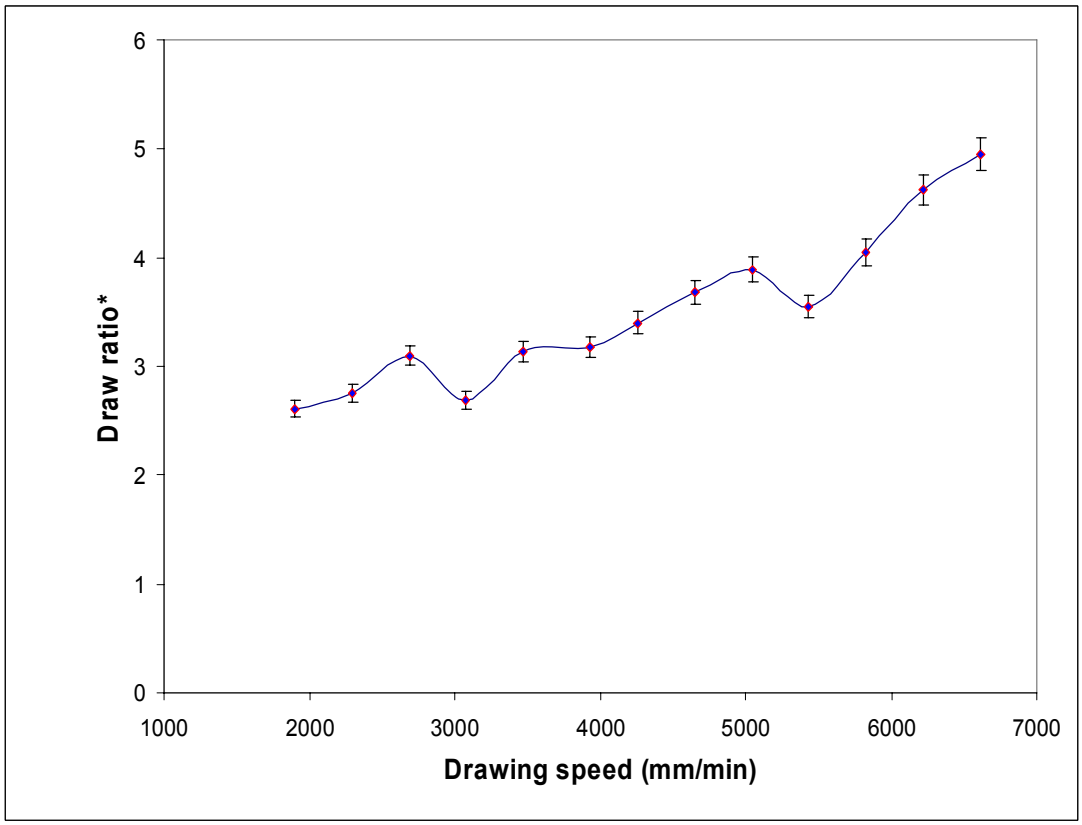

Figure A.1. Effect of drawing speed on draw ratio of PET/HDPE sample processed at 60 rpm and drawn at room temperature (~20ºC)

* : draw ratio = diameter of the as extruded sample/diameter of the drawn sample at take-up device

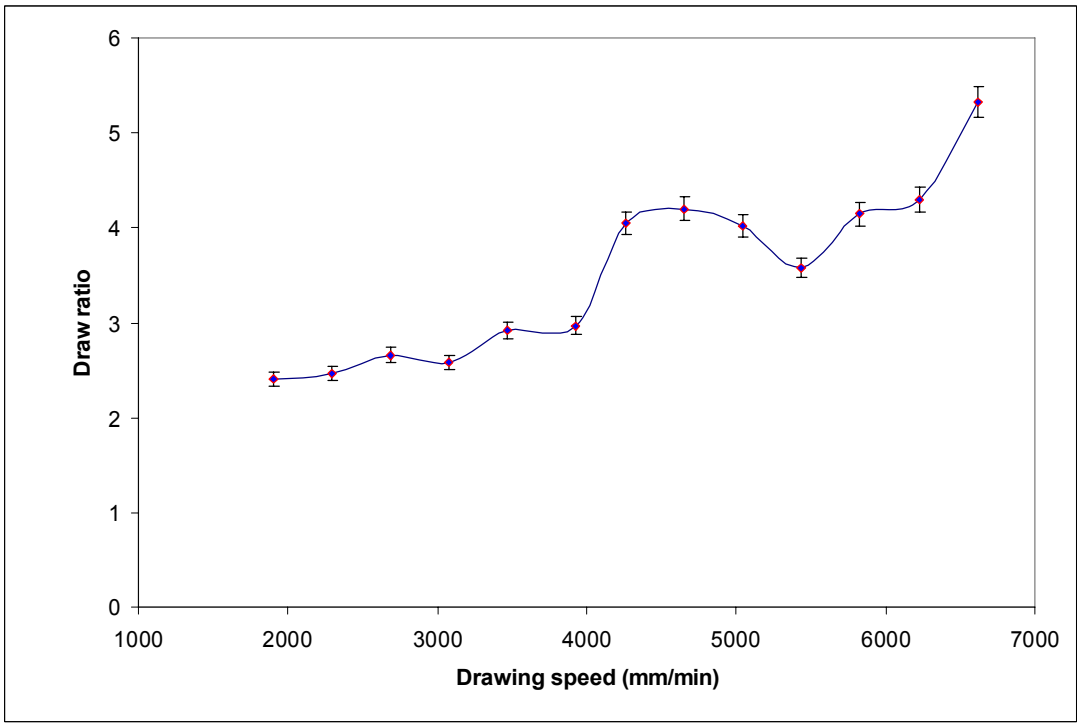

Figure A.2. Effect of drawing speed on draw ratio of PET/HDPE sample processed at 120 rpm and drawn at room temperature (~20ºC)

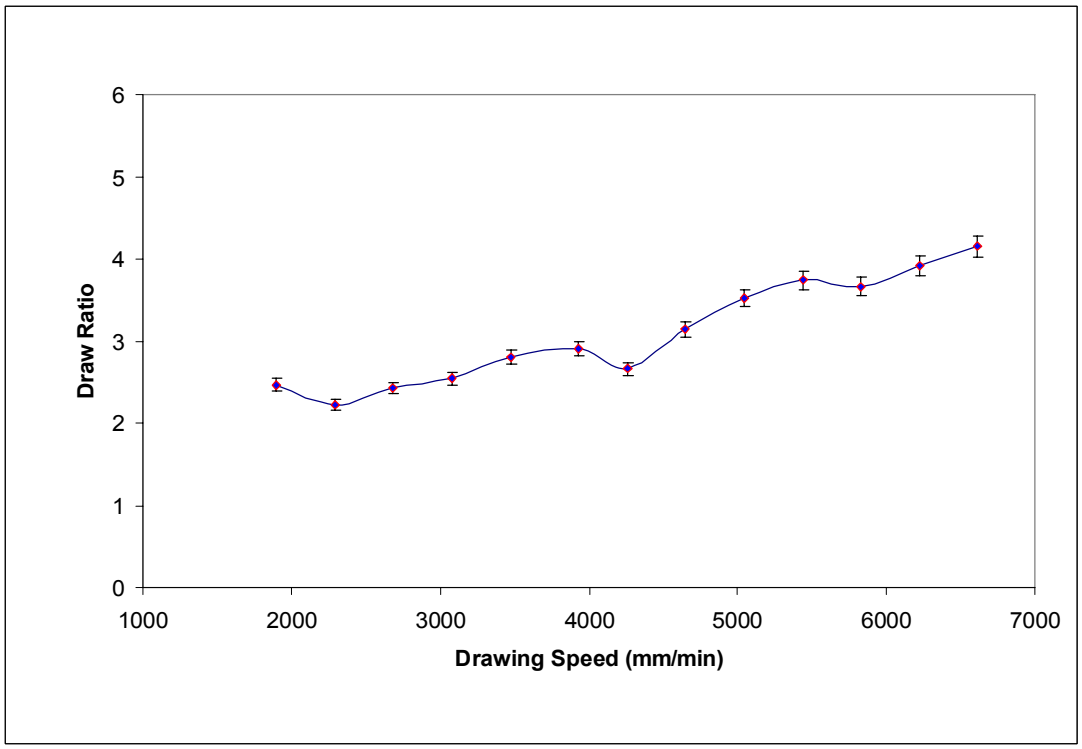

Figure A.3. Effect of drawing speed on draw ratio of PET/HDPE sample processed at 180 rpm and drawn at room temperature (~20ºC)

APPENDIX B

PET Microfiber Diameter

Table B. Minimum, maximum and average PET microfiber diameters for drawn samples

Samples	Minimum/maximum PET microfiber diameter (μm)	Average diameter (μm)
60 rpm-2.7 m/min	2.5-8.0	4.3
60 rpm-4.7 m/min	1.9-9.2	4.0
60 rpm-6.2 m/min	0.5-1.5	1.3
120 rpm-2.7 m/min	1.8-10.8	5.0
120 rpm-4.7 m/min	1.4-2.7	2.0
120 rpm-6.2 m/min	0.7-3.5	1.5
180 rpm-2.7 m/min	1.0-4.0	2.0
180 rpm-4.7 m/min	1.0-2.9	2.0
180 rpm-6.2 m/min	1.1-3.4	1.8
PET/HDPE/1%E-nBA-GMA	0.4-2.0	1.1
PET/HDPE/5%E-nBA-GMA	0.4-1.5	1.0
PET/HDPE/10%E-nBA-GMA	0.6-2.1	0.9
PET/HDPE/1%E-MA	2.0-7.5	4.2
PET/HDPE/5%E-MA	1.4-3.5	2.8
PET/HDPE/10%E-MA	1.2-4.3	2.4

APPENDIX C

Mechanical Test Results

Table C.1. Tensile strength and standard deviation data for injection molded samples

Samples	Tensile strength (MPa)
Pure HDPE-60 rpm	29.15 ± 1.10
Pure HDPE-120 rpm	28.60 ± 2.10
Pure HDPE-180 rpm	27.36 ± 1.80
Pure PET-60 rpm	51.40 ± 1.90
Pure PET-120 rpm	48.30 ± 1.60
Pure PET-180 rpm	49.60 ± 1.20
As extruded-60 rpm	32.49 ± 2.60
As extruded-20 rpm	34.59 ± 1.30
As extruded-180 rpm	34.07 ± 2.70
60 rpm-2.7 m/min	38.45 ± 0.57
60 rpm-4.7 m/min	39.46 ± 0.51
60 rpm-6.2 m/min	40.25 ± 0.68
120 rpm-2.7 m/min	38.61 ± 0.77
120 rpm-4.7 m/min	39.29 ± 2.10
120 rpm-6.2 m/min	39.81 ± 1.07
180 rpm-2.7 m/min	36.83 ± 3.56
180 rpm-4.7 m/min	37.75 ± 1.20
180 rpm-6.2 m/min	38.75 ± 1.06

Table C.2. Tensile modulus and standard deviation data for injection molded samples

Samples	Tensile modulus (MPa)
Pure HDPE-60 rpm	680 ± 23.40
Pure HDPE-120 rpm	650 ± 53.80
Pure HDPE-180 rpm	670 ± 51.80
Pure PET-60 rpm	1150 ± 39.60
Pure PET-120 rpm	1060 ± 57.90
Pure PET-180 rpm	1095 ± 51.60
As extruded-60 rpm	690 ± 64.30
As extruded-120 rpm	655 ± 58.60
As extruded-180 rpm	670 ± 74.30
60 rpm-2.7 m/min	859 ± 26.30
60 rpm-4.7 m/min	872 ± 44.70
60 rpm-6.2 m/min	897 ± 31.70
120 rpm-2.7 m/min	833 ± 24.60
120 rpm-4.7 m/min	856 ± 64.70
120 rpm-6.2 m/min	884 ± 19.60
180 rpm-2.7 m/min	846 ± 65.50
180 rpm-4.7 m/min	874 ± 41.80
180 rpm-6.2 m/min	853 ± 24.30

Table C.3. % Elongation at break and standard deviation data for injection molded samples

Samples	% Elongation at break
Pure HDPE-60 rpm	110.23 ± 20.80
Pure HDPE-120 rpm	104.29 ± 16.80
Pure HDPE-180 rpm	100.79 ± 21.80
Pure PET-60 rpm	5.30 ± 0.54
Pure PET-120 rpm	6.40 ± 0.74
Pure PET-180 rpm	5.90 ± 1.10
As extruded-60 rpm	65.70 ± 25.30
As extruded-120 rpm	68.46 ± 4.80
As extruded-180 rpm	63.78 ± 3.30
60 rpm-2.7 m/min	29.36 ± 4.70
60 rpm-4.7 m/min	31.24 ± 7.40
60 rpm-6.2 m/min	29.22 ± 2.00
120 rpm-2.7 m/min	37.71 ± 12.90
120 rpm-4.7 m/min	38.31 ± 14.30
120 rpm-6.2 m/min	30.82 ± 4.20
180 rpm-2.7 m/min	36.43 ± 2.40
180 rpm-4.7 m/min	39.22 ± 3.00
180 rpm-6.2 m/min	34.98 ± 2.30

Table C.4. Tensile strength and standard deviation data for compatibilized injection molded samples (C_1 and C_2 refers to E-nBA-GMA and E-MA, respectively)

Samples	Tensile strength (MPa)
Pure HDPE	29.15 ± 1.10
Pure PET	51.40 ± 1.90
60 rpm PET/HDPE (without MFC structure)	32.49 ± 0.68
60 rpm-6.2 m/min (with MFC structure)	40.25 ± 2.60
1% C_2 (without MFC structure)	33.91 ± 0.71
1% C_2 (with MFC structure)	34.48 ± 0.41
5% C_2 (without MFC structure)	34.32 ± 0.45
5% C_2 (with MFC structure)	35.87 ± 0.77
10% C_2 (without MFC structure)	33.52 ± 0.62
10% C_2 (with MFC structure)	34.31 ± 0.45
1% C_1 (without MFC structure)	36.25 ± 0.42
1% C_1 (with MFC structure)	38.89 ± 2.33
5% C_1 (without MFC structure)	37.11 ± 0.98
5% C_1 (with MFC structure)	40.30 ± 3.31
10% C_1 (without MFC structure)	35.88 ± 0.68
10% C_1 (with MFC structure)	36.78 ± 2.29

Table C.5. Tensile modulus and standard deviation data for compatibilized injection molded samples (C_1 and C_2 refers to E-nBA-GMA and E-MA, respectively)

Samples	Tensile modulus (MPa)
Pure HDPE	680 ± 23.40
Pure PET	1150 ± 39.60
60 rpm PET/HDPE (without MFC structure)	690 ± 64.30
60 rpm-6.2 m/min (with MFC structure)	897 ± 31.70
1% C_2 (without MFC structure)	466 ± 29.86
1% C_2 (with MFC structure)	476 ± 7.18
5% C_2 (without MFC structure)	437 ± 25.02
5% C_2 (with MFC structure)	456 ± 11.73
10% C_2 (without MFC structure)	425 ± 21.68
10% C_2 (with MFC structure)	433 ± 18.28
1% C_1 (without MFC structure)	453 ± 11.90
1% C_1 (with MFC structure)	467 ± 15.80
5% C_1 (without MFC structure)	425 ± 10.20
5% C_1 (with MFC structure)	457 ± 27.50
10% C_1 (without MFC structure)	387 ± 14.60
10% C_1 (with MFC structure)	400 ± 31.40

Table C.6. % Elongation at break and standard deviation data for compatibilized injection molded samples (C_1 and C_2 refers to E-nBA-GMA and E-MA, respectively)

Samples	% Elongation at break
Pure HDPE	110.23 ± 20.82
Pure PET	5.30 ± 0.54
60 rpm PET/HDPE (without MFC structure)	65.72 ± 5.30
60 rpm-6.2 m/min (with MFC structure)	29.22 ± 2.00
1% C_2 (without MFC structure)	42.33 ± 2.05
1% C_2 (with MFC structure)	40.51 ± 4.65
5% C_2 (without MFC structure)	38.11 ± 4.55
5% C_2 (with MFC structure)	36.28 ± 3.30
10% C_2 (without MFC structure)	48.51 ± 2.00
10% C_2 (with MFC structure)	44.08 ± 3.24
1% C_1 (without MFC structure)	48.30 ± 1.65
1% C_1 (with MFC structure)	47.96 ± 7.12
5% C_1 (without MFC structure)	52.70 ± 1.72
5% C_1 (with MFC structure)	48.49 ± 6.04
10% C_1 (without MFC structure)	55.50 ± 2.41
10% C_1 (with MFC structure)	56.28 ± 6.59

Table C.7. Impact strength and standard deviation data for injection molded samples

Samples	Impact strength (kJ/m^2)
Pure HDPE-60 rpm	45.30 ± 2.50
Pure HDPE-120 rpm	49.40 ± 3.30
Pure HDPE-180 rpm	47.40 ± 2.70
Pure PET-60 rpm	5.40 ± 1.30
Pure PET-120 rpm	4.60 ± 2.10
Pure PET-180 rpm	5.10 ± 0.20
As extruded-60 rpm	28.40 ± 3.50
As extruded-120 rpm	22.30 ± 4.40
As extruded-180 rpm	17.60 ± 3.60
60 rpm-2.7 m/min	19.50 ± 4.10
60 rpm-4.7 m/min	20.80 ± 2.90
60 rpm-6.2 m/min	33.40 ± 2.00
120 rpm-2.7 m/min	26.30 ± 4.50
120 rpm-4.7 m/min	24.60 ± 4.20
120 rpm-6.2 m/min	21.80 ± 3.20
180 rpm-2.7 m/min	17.40 ± 2.50
180 rpm-4.7 m/min	10.70 ± 0.60
180 rpm-6.2 m/min	18.40 ± 3.60

Table C.8. Impact strength and standard deviation data for compatibilized injection molded samples (C_1 and C_2 refers to E-nBA-GMA and E-MA, respectively)

Samples	Impact strength (kJ/m^2)
Pure HDPE	45.30 ± 2.50
Pure PET	5.40 ± 1.30
60 rpm PET/HDPE (without MFC structure)	28.40 ± 3.50
60 rpm- 6.2 m/min (with MFC structure)	33.40 ± 2.00
1% C_2 (without MFC structure)	10.70 ± 4.00
1% C_2 (with MFC structure)	26.20 ± 1.60
5% C_2 (without MFC structure)	18.00 ± 2.10
5% C_2 (with MFC structure)	20.00 ± 8.50
10% C_2 (without MFC structure)	12.20 ± 4.60
10% C_2 (with MFC structure)	16.50 ± 3.80
1% C_1 (without MFC structure)	26.10 ± 3.50
1% C_1 (with MFC structure)	32.70 ± 5.30
5% C_1 (without MFC structure)	33.80 ± 8.50
5% C_1 (with MFC structure)	37.60 ± 2.10
10% C_1 (without MFC structure)	48.30 ± 1.60
10% C_1 (with MFC structure)	57.20 ± 5.10

APPENDIX D

DSC Thermograms

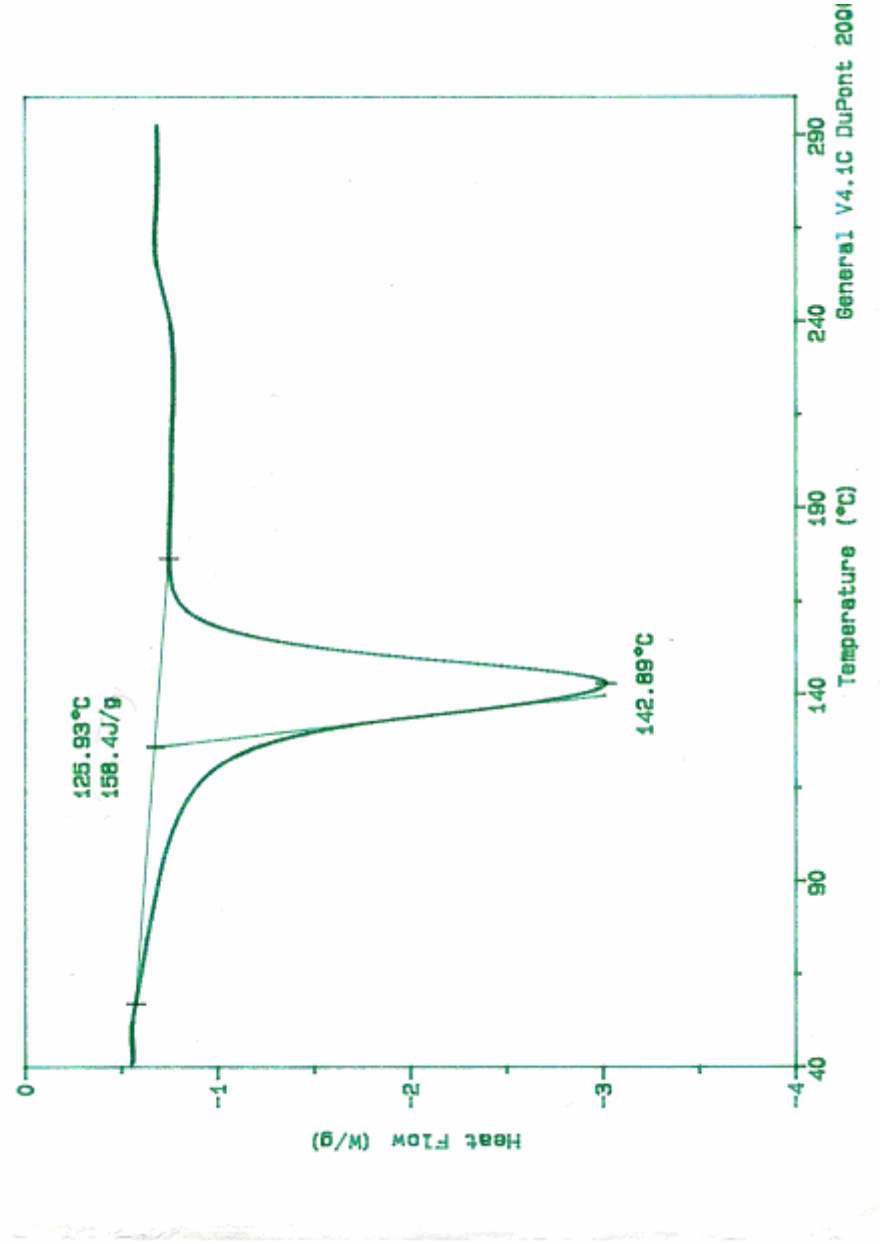

Figure D.1. DSC thermogram of pure HDPE

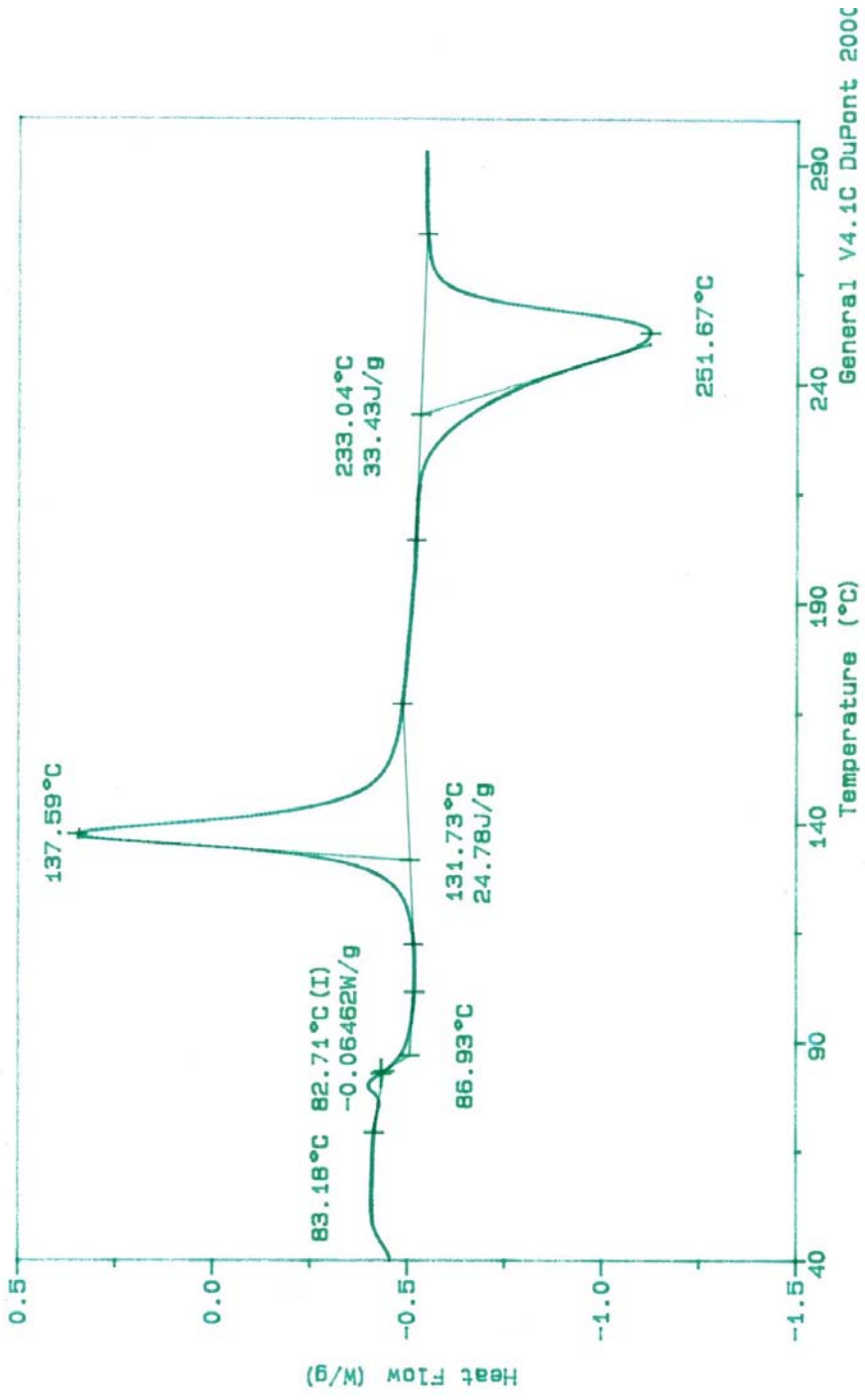

Figure D.2. DSC thermogram of pure PET

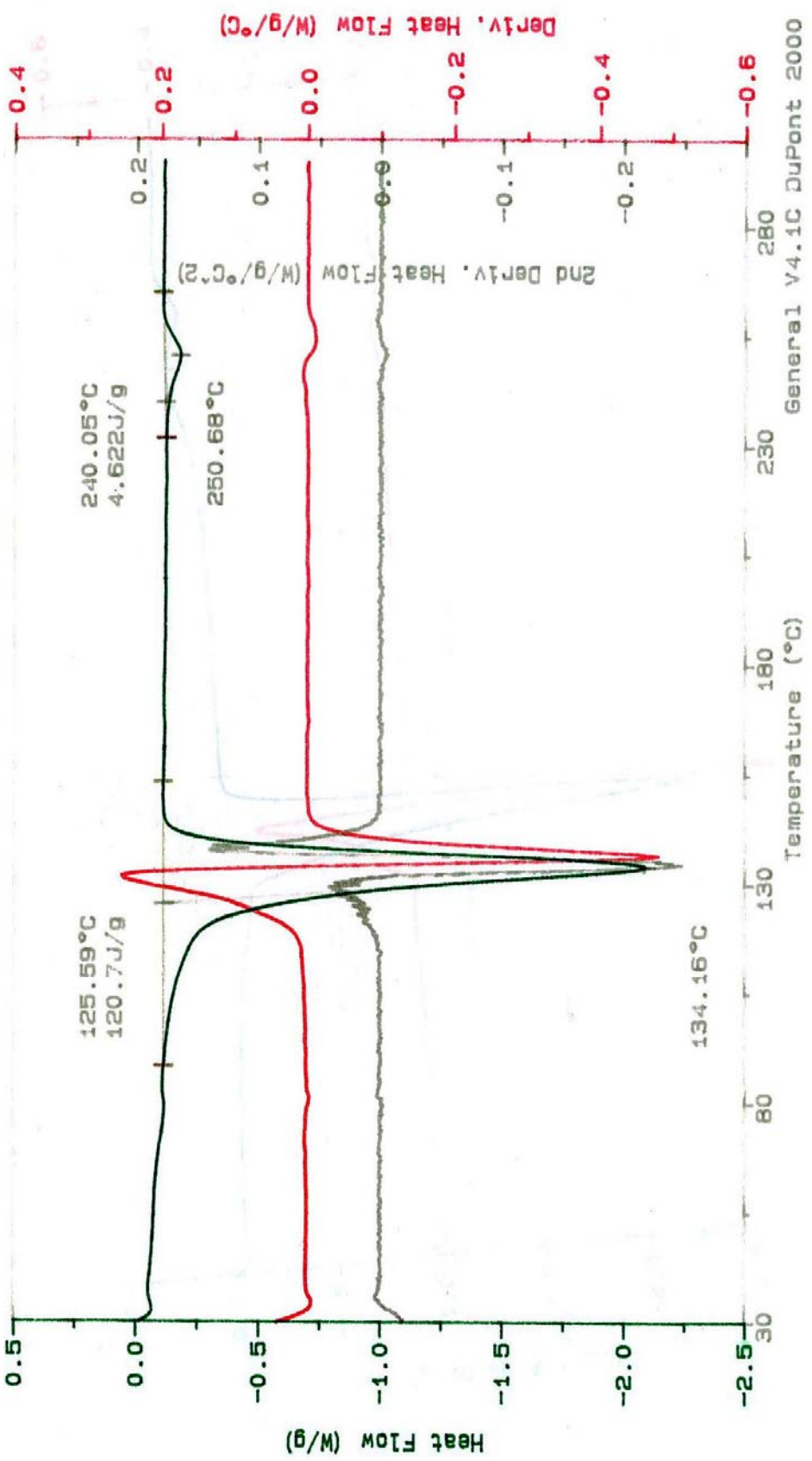

Figure D.3. DSC thermogram of PET/HDPE as extruded sample processed at 60 rpm and drawn with 2.7 m/min

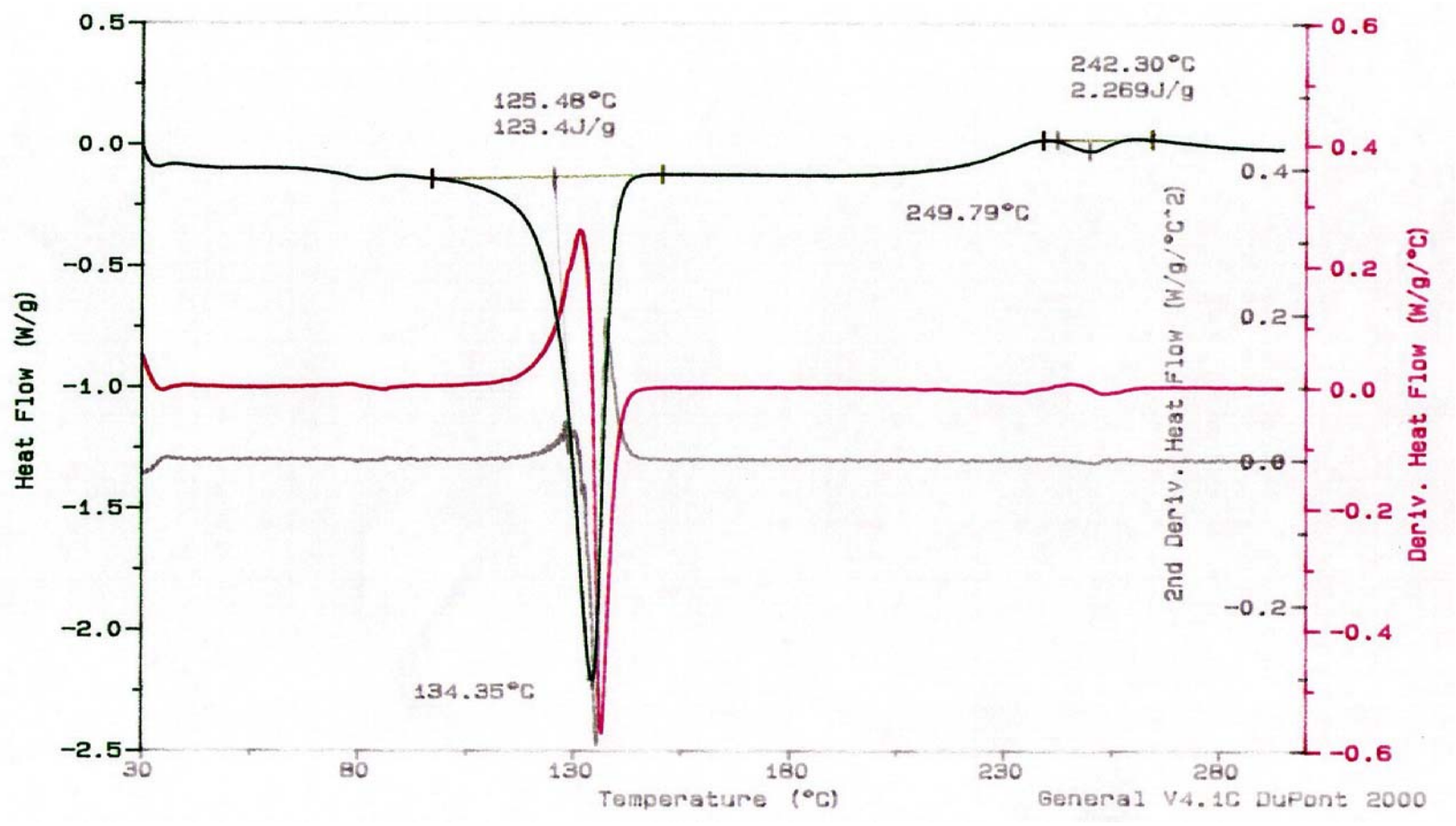

Figure D.4. DSC Thermogram of PET/HDPE MFC sample processed at 60 rpm and drawn with 4.7 m/min

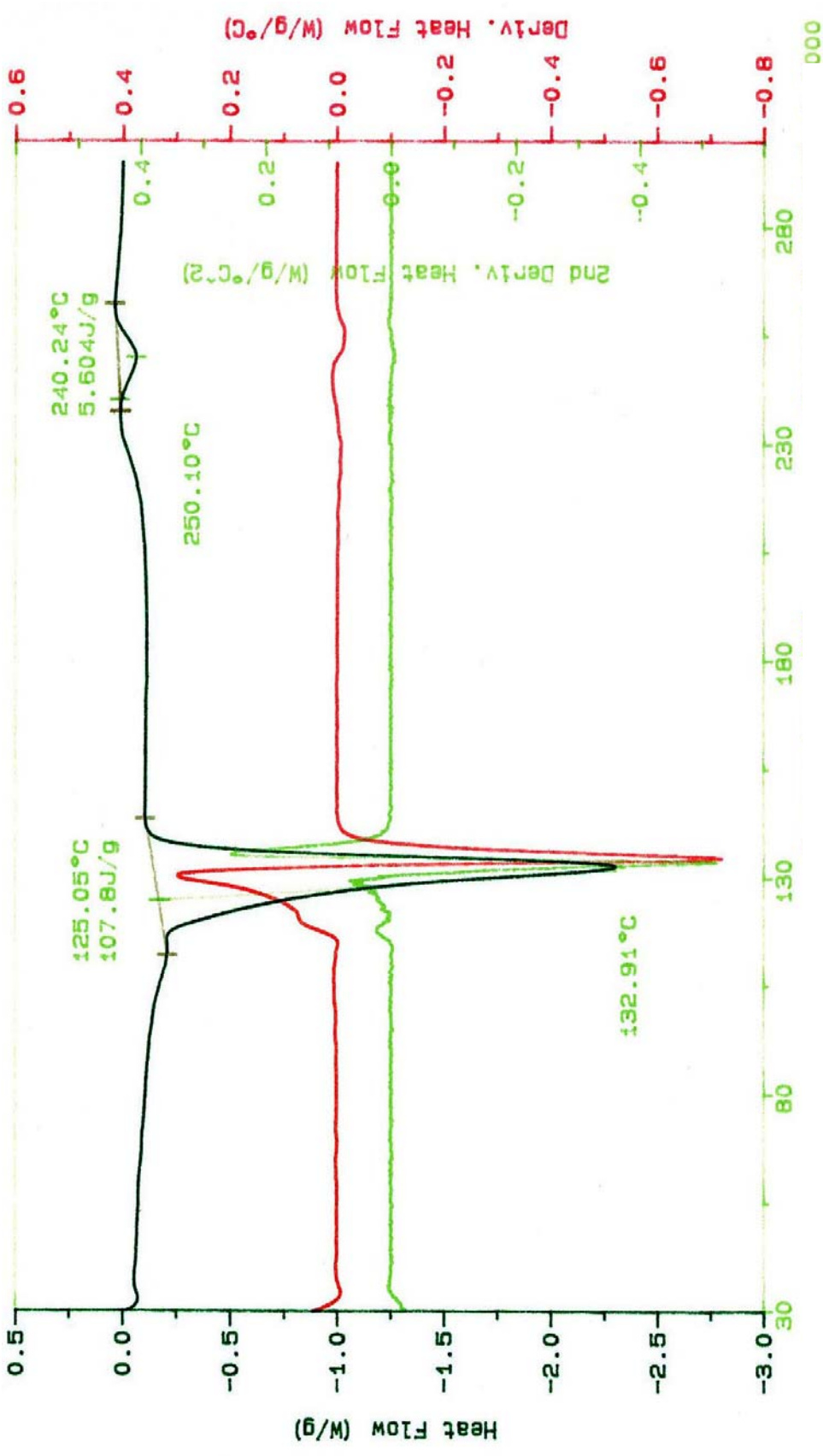

Figure D.5. DSC Thermogram of PET/HDPE as drawn sample processed at 60 rpm and drawn with 6.2 m/min

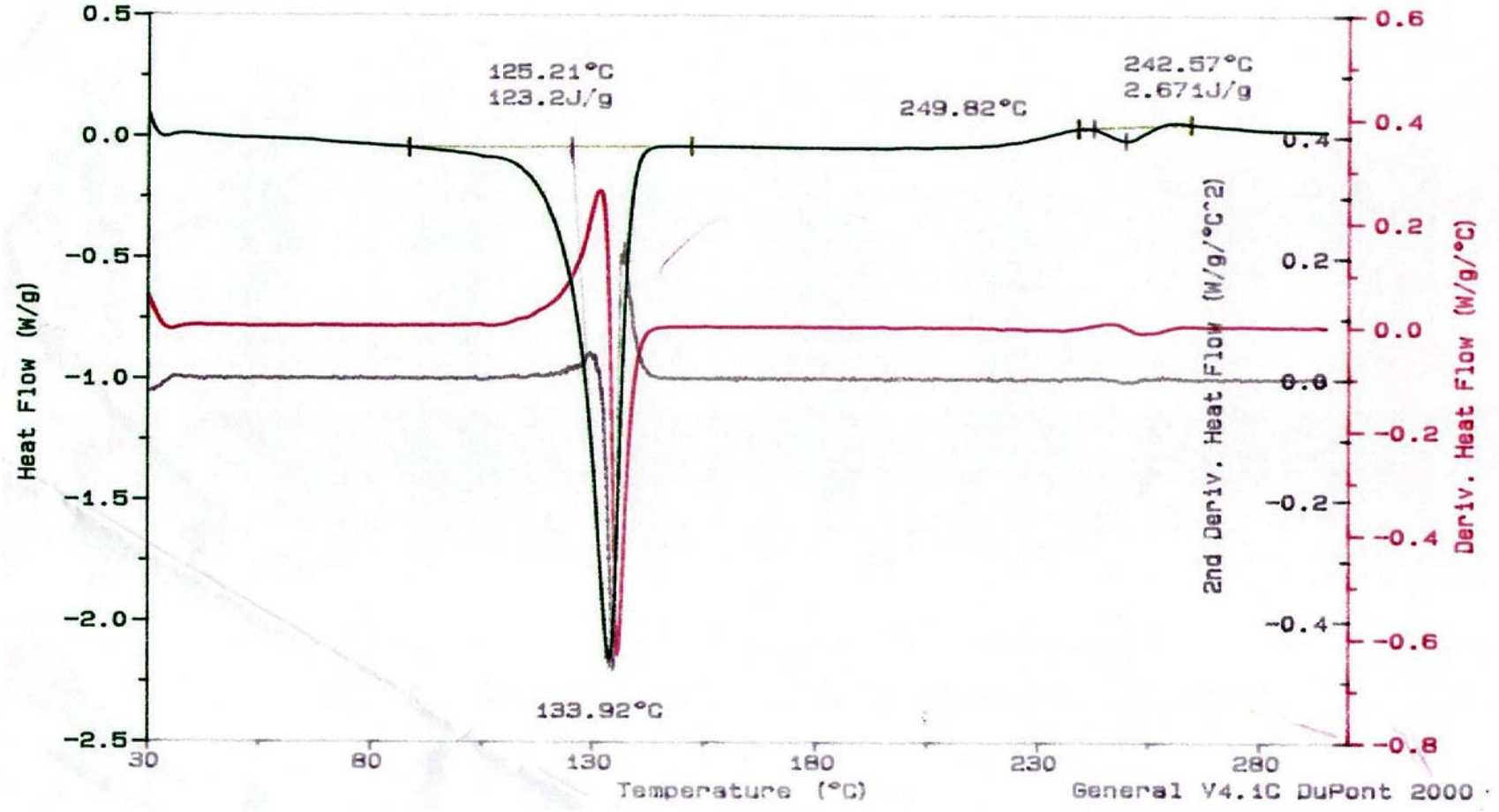

Figure D.6. DSC Thermogram of PET/HDPE as drawn sample compatibilized with 1% C_1 (C_1 refers to E-nBA- GMA)

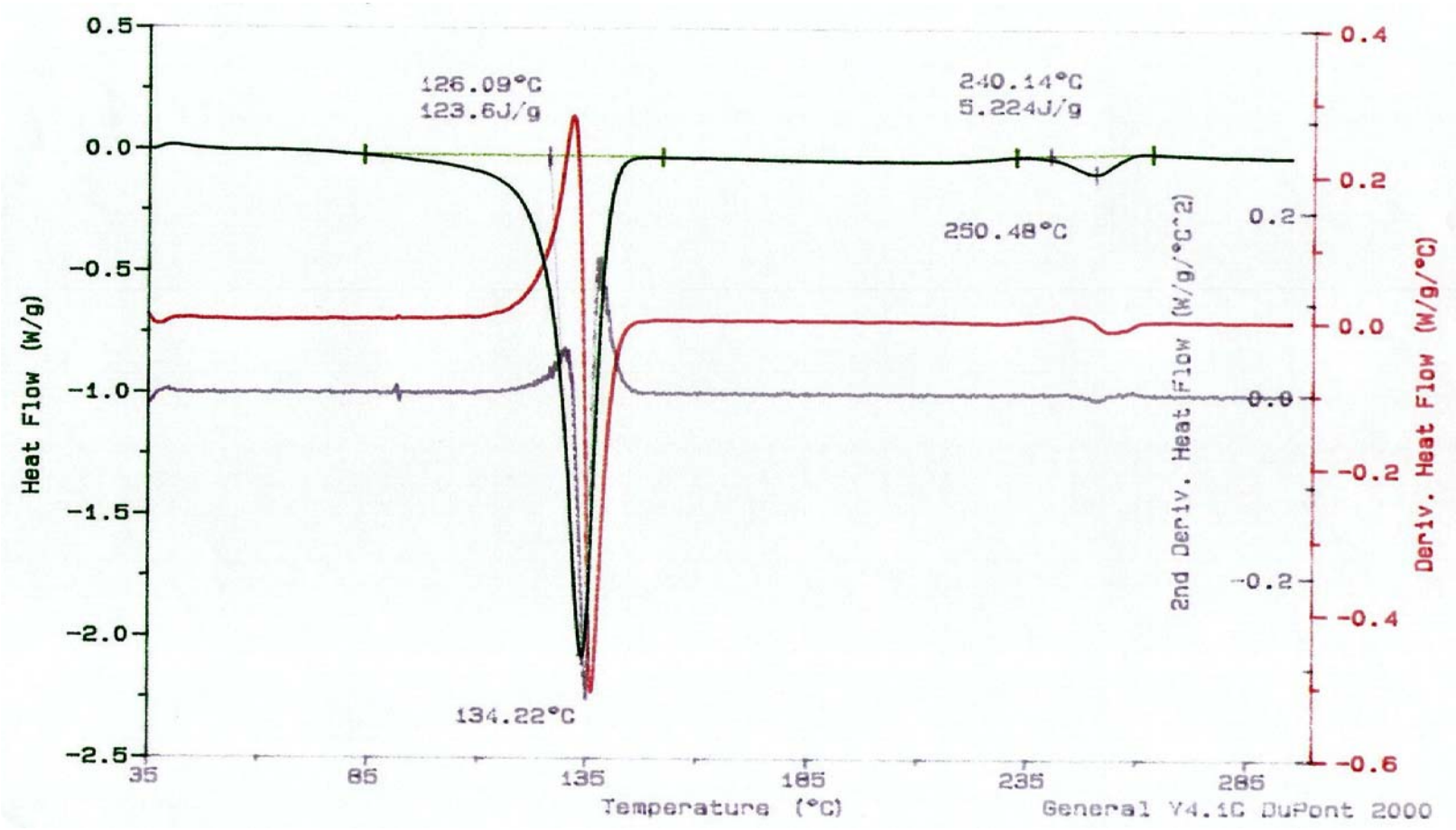

Figure D.7. DSC Thermogram of PET/HDPE as extruded sample compatibilized with 5% C_1 (C_1 refers to E-nBA-GMA)

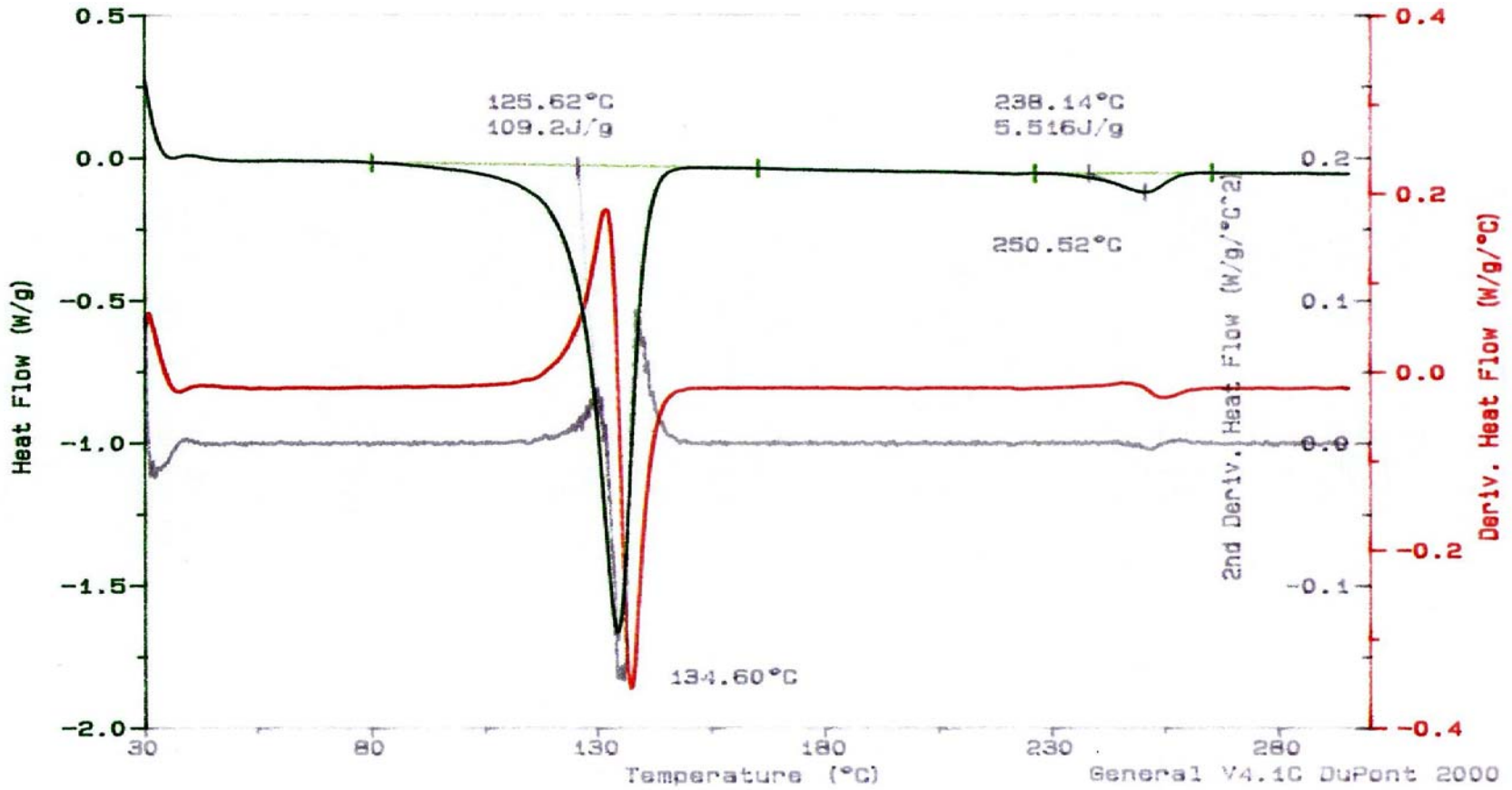

Figure D.8. DSC Thermogram of PET/HDPE MFC sample compatibilized with 10% C_1 (C_1 refers to E-nBA-GMA)

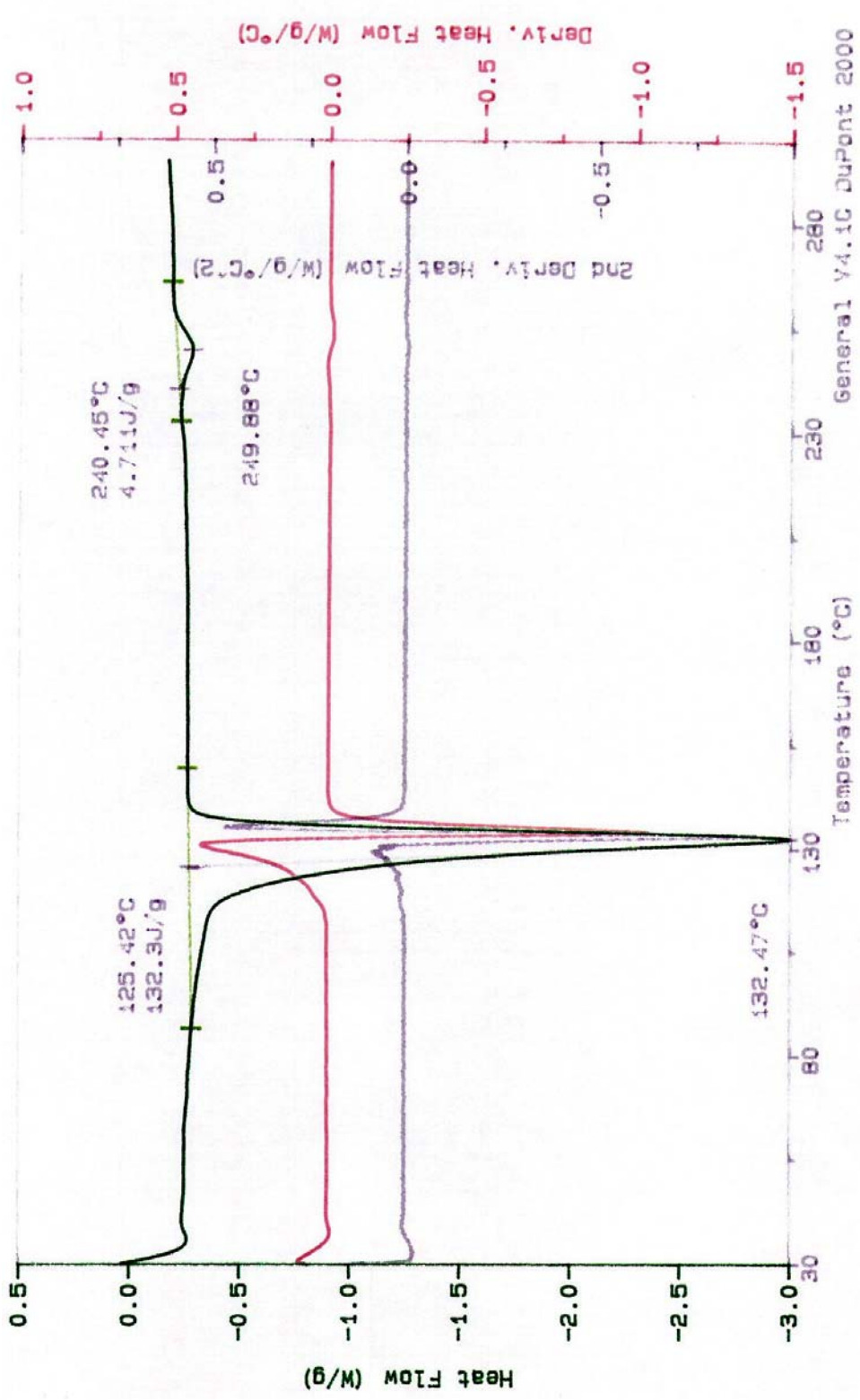

Figure D.9. DSC Thermogram of PET/HDPE as extruded sample compatibilized with 5 % C_2 (C_2 refers to E-MA)

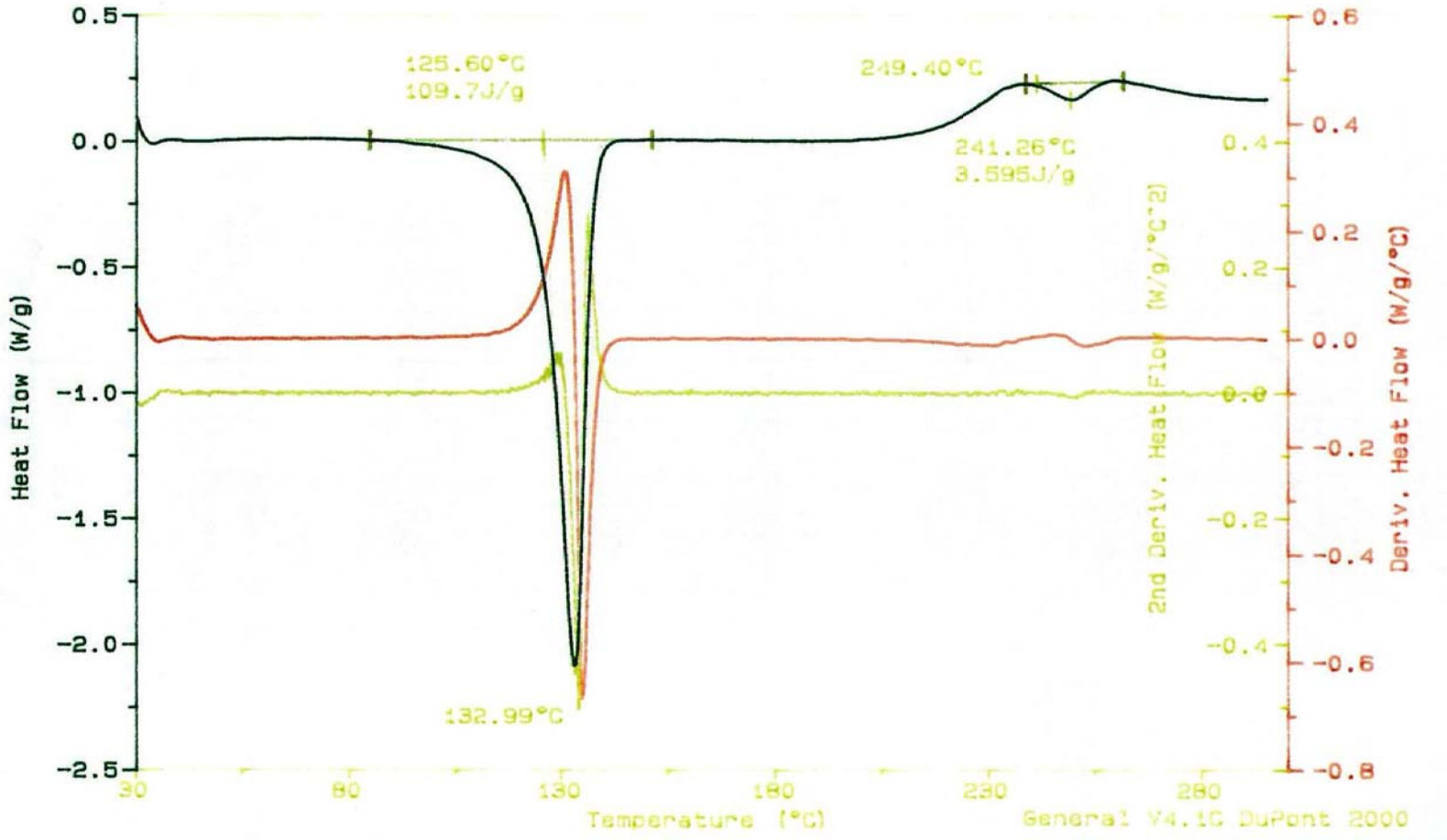

Figure D.10. DSC Thermogram of PET/HDPE MFC samplecompatibilized with 10% C_2 (C_2 refers to E-MA)